Inflationary Cosmology, phase transitions and primordial power spectra

A thesis
submitted in partial fulfilment
of the requirements for the Degree
of
Doctor of Philosophy in Physics
in the
University of Canterbury

by

Bevan Cresswell

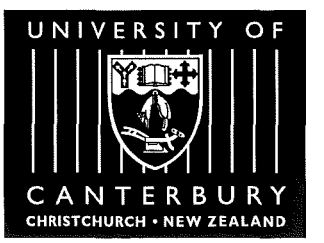

University of Canterbury
May 20, 2004

Abstract

We present the results of research into inflationary cosmology. This consists firstly of a basic overview of the inflationary scenario, including the currently accepted model of inflation as being driven by a weakly interacting scalar field with a slowly varying effective potential energy function. We then consider the theory of density perturbations, their quantum origins in the inflaton scalar field, and evolution in a rapidly expanding universe. This all acts as background material for the research carried out, which involves the generation of density perturbations by a non-standard effective potential for the inflaton field, and how their evolution is effected by features in the potential. The potentials are motivated by phase transitions in fields weakly coupled to the inflaton. These potentials violate the normally assumed slow roll conditions and the resulting power spectra do not have the scale independence characteristic of slow roll. Instead they exhibit scale dependent oscillations, whose nature depend on the details of the potential being considered. We finally consider the effect such power spectra would have on the Cosmic Microwave Background and compare this to the current observational data.

Acknowledgements

There are many people who deserve thanks for helping me throughout the course of my thesis. I am eternally grateful to my supervisor, Jenni Adams, for being so understanding, helpful and supportive. Thanks are also due to my colleagues, in particular Bryn, Hamish, Pauline, Ewan and Sonia for their constant stream of intelligent advice, empathy and the odd much needed distraction. This thesis would not have been possible without the support of my friends from during my time at Canterbury, and from my family. And finally my thanks go to Bridget for her belief in me and encouragement to finish.

Contents

Figures

Tables

Chapter 1

Introduction

1.1 Summary of the content of this thesis

This thesis deals with the seeding of structure in the early universe by inflation. We look at the idea that a field coupled to the field driving inflation undergoes a phase transition. We find that such a transition can cause a rapid change in the energy density, that is otherwise changing very slowly as the universe is inflating. This leads to the amplitude of metric perturbations no longer being scale invariant and instead we find features in the perturbation spectrum. If the characteristic length scale of such a feature is within a certain range, these features in the perturbation spectrum are observable today in the large scale structure and cosmic microwave radiation. The overall content of this thesis is shown graphically in Figure 1.1. We calculate the primordial power spectrum from particular inflaton potentials containing a step transition, analytically and/or numerically. This is then compared to known CMB anisotropy results.

We are concerned primarily with the formation of structure in the universe on large scales. Here large scale structure corresponds to the size of galaxies or clusters of galaxies. The seeds for the large scale structure we observe today originate in the early universe, at a time when the universe is dominated by a scalar field. This scalar field leads to an extremely rapid period of expansion in the universe known as inflation. Due to this period of rapid expansion, quantum fluctuations in the scalar field evolve to form the observed structure. The amplitude of these

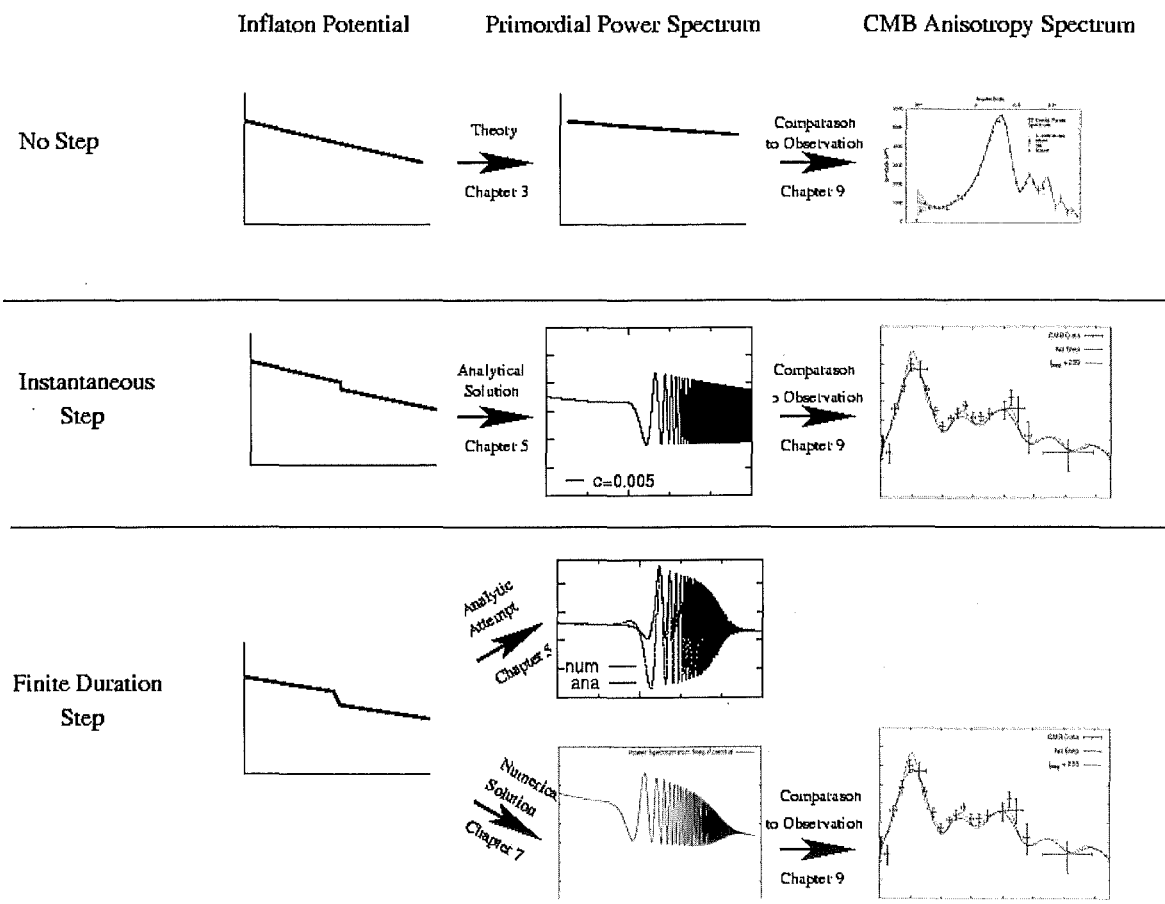

Figure 1.1: The major accomplishments of this thesis. We calculate for various forms of the inflaton effective potential the resulting primordial power spectrum. This is done analytically and/or numerically in different sections for the cases of an instantaneous step and for a finite duration step. We are able to predict the CMB anisotropy spectrum resulting from these primordial power spectra, and this is compared to observation.

fluctuations is largely independent of scale size, which leads to perturbations on all scales having approximately the same amplitude.

In the rest of this chapter I give a brief summary of some of the more important results in cosmology. This is followed by an outline of the failings of the original big bang cosmology, dominated initially by radiation and then matter. Then I shall explain how the period of accelerating expansion associated with the inflationary big bang model can solve these problems. Chapter 2 discusses the basics of inflation based on the evolution of a single scalar field. We then look at the concept of slow roll inflation, and how this simplifies the inflationary dynamics, as well as some of the general classes of inflation. In Chapter 3 we go into the theory of linear density perturbations and specifically how this can be applied to the inflationary scenario. Chapter 4 discusses the particle physics ideas that could be relevant at the inflationary epoch and how phase transitions could occur in these fields which would affect the inflationary effective potential. We also mention the observational evidence for such a transition in terms of large scale structure measurements.

The effect of a phase transition on the density perturbation spectrum is treated analytically in Chapter 5, during which we make some assumptions about the potential being in the slow roll regime. This is found to cause problems in the resulting power spectrum. In Chapter 6 we present a numerical solution to the background evolution of the universe and the evolution of the density perturbations. We show such a treatment is consistent with accepted slow roll solutions and look at some other inflationary models. In Chapter 7 we calculate the numerical solution in the case that we have a sudden change in the inflation potential, motivated by a phase transition in a field coupled to the inflaton. We then compare this numerical solution to the solutions from Chapter 5 in Chapter 8. In Chapter 9 we look at the CMB anisotropy spectrum and how results from Chapter 6 for the primordial power spectrum can be incorporated to give very different anisotropy spectra from the standard ΛCDM results. Then finally in

Chapter 10 we repeat the work of Chapters 5 - 9 for a different inflationary potential, the Broken Scale Invariance potential, where instead of having a step in the inflaton potential we have a sudden change in the slope of the potential. This corresponds to a step in the derivative of the potential.

1.2 Standard Big Bang Model

We are going to derive some of the basic results of relativistic cosmology. We begin with Einstein's equation relating the curvature of space with the matter content, which is

$$R_{\mu\nu} - \frac{1}{2} g_{\mu\nu} R = 8\pi G T_{\mu\nu}. \tag{1.1}$$

Here $R_{\mu\nu}$ is the Ricci tensor, R is the Ricci scalar, $g_{\mu\nu}$ is the spacetime metric and $T_{\mu\nu}$ is the stress energy tensor. We also have the continuity constraint

$$T^{\mu\nu}{}_{;\mu} = 0. \tag{1.2}$$

We follow the Copernican Assumption that on large scales the universe appears the same in all directions, and that this is true when observing from all spatial locations. In other words that the universe is homogeneous and isotropic. This assumption is clearly not true locally, or on the scale of galaxies or even that of clusters of galaxies. It is however observed to be true on extremely large scales. This is demonstrated by the galaxy correlation measurements observed by the Sloan Digital Sky Survey [5] and the 2 Micron All Sky Survey [47]. It can also be verified from the temperature uniformity of the CMBR.

It was Friedmann [28] in 1922 who first showed that Einstein's equations had dynamical solutions. Then in 1927 Lemaître [40] showed that in order to correctly solve for dynamical universe models pressure must be taken into account. The most simple way to formulate these dynamical solutions was first discovered independently by Robertson [56, 57] in 1935 and Walker [66] in 1936.

This Robertson-Walker line element and metric for a spatially homogeneous and isotropic universe was found to be

$$\mathrm{d}s^2 = \mathrm{d}t^2 - a(t)^2 \left(\frac{1}{1-kr^2} \mathrm{d}r^2 + r^2 \mathrm{d}\theta^2 + r^2 \sin^2(\theta)\, \mathrm{d}\psi^2 \right). \tag{1.3}$$

Here the constant k is normalized to take on the values of $+1$, -1 or 0, and the $a(t)$ term is required by generality.

The energy momentum tensor T^{μ}_{ν} is given by the matter content of any particular model. For a perfect cosmological fluid of energy density ρ and pressure p the energy momentum tensor takes the simple block diagonal form

$$T^{\mu}_{\nu} = \begin{pmatrix} \rho & & & \\ & -p & & \\ & & -p & \\ & & & -p \end{pmatrix}. \tag{1.4}$$

We can use this in Einstein's equations to describe how the behaviour of the parameter $a(t)$ (often just denoted a) is related to the content of the universe. Doing this we find

$$H^2 + \frac{k}{a^2} = \frac{8\pi G}{3}\rho \qquad \text{and} \tag{1.5}$$

$$\frac{\ddot{a}}{a} = -\frac{4\pi G}{3}(\rho + 3p), \tag{1.6}$$

where H is the Hubble parameter defined by $H \equiv \dot{a}/a$. From the continuity equation we find that

$$\dot{p}a^3 = \frac{\mathrm{d}}{\mathrm{d}t}\left(a^3(\rho + p)\right). \tag{1.7}$$

Combining these equations with an equation relating pressure to energy density, we can solve for the evolution of the parameter $a(t)$.

We find that for realistic models the scale factor of the universe evolves with time. Matching this with observational data originally due to Hubble [34] we conclude that the universe is expanding. We can describe this expansion solely in terms of the scale factor $a(t)$, which is conventionally normalized to 1 at the

present time. The coordinates r, θ and ψ are comoving. They are coordinates on a non-expanding $3D$ space, with the expansion of the $3D$ surface entirely incorporated in the $a(t)$ term. The physical distance is related to the co-moving co-ordinate distance by

$$\text{physical distance} = a(t) \times \text{comoving coordinate distance.} \tag{1.8}$$

The other quantity in our metric, k can take values -1, 0 or $+1$. This quantity tells us the topology of the metric describing the universe, with $k = -1$ for a negatively curved metric, $k = 0$ for a spatially flat metric and $k = +1$ for a positively curved metric.

We note that throughout this thesis we make use of natural units, where $\hbar = c = 1$. Also to simplify the equations governing inflation later on, the Planck mass is taken to be $M_p = \sqrt{8\pi}$ which means that Newton's gravitational constant is given by $G = 1/M_p^2 = 1/8\pi$.

For a universe which is dominated by hot (relativistic) matter and/or radiation we can relate pressure to energy density by

$$p = \frac{\rho}{3}. \tag{1.9}$$

Substituting this into the continuity equation we find that

$$\frac{\dot{a}}{a} = -\frac{1}{4}\frac{\dot{\rho}}{\rho} \tag{1.10}$$

and hence we can relate the energy density to the expansion of the universe by

$$\rho \propto \frac{1}{a^4}. \tag{1.11}$$

Using this result in Equation (1.5) we find that the scale factor increases with time according to

$$a(t) \propto t^{1/2}. \tag{1.12}$$

Alternatively when the universe is matter dominated we have negligible pressure and hence by the continuity equation we have that $a^3\rho$ is constant, or

$$\rho \propto \frac{1}{a^3}. \tag{1.13}$$

Again using Equation (1.5) we find the scale factor evolves with time according to

$$a(t) \propto t^{2/3}. \tag{1.14}$$

The standard model of cosmology before inflation was that the universe was initially dominated by radiation. We can understand this by noting that the radiation energy density scales as $a(t)^{-4}$ whereas that of matter scales as $a(t)^{-3}$. So for an expanding universe ($\dot{a}(t) > 0$) the relative energy contribution from radiation reduces with time. We currently observe our universe in which matter dominates radiation. Extrapolating the current matter and radiation densities backwards radiation density becomes a larger and larger contribution to the total density. Eventually we come to a stage at which radiation is the dominant form of energy in the universe. We call the time at which we have equal contributions to the total energy density from matter and radiation to be the time of radiation-matter equality. We have in this argument ignored the cosmological constant or dark energy portion of the density of the universe. This can easily be included into the calculations.

1.3 The Cosmic Microwave Background

The earlier in time we consider, the higher the average particle energies. Before some specific time we find that the energy of the average particle is higher than the ionization energy of hydrogen. At this time instead of a universe where the baryonic matter is primarily in the form of atoms we have the baryonic matter in the form of completely ionized plasma. When the universe is in this state it is opaque to radiation as photons are unable to travel very far without Compton scattering off the bare electrons. This constant scattering leads to all particles being in thermal equilibrium. We consider for simplicity only the reaction

$$p + e^- \rightleftharpoons H + \gamma \tag{1.15}$$

to be taking place. Hydrogen has a binding energy of $B_H \approx 13.6\text{eV}$ (corresponding to a temperature of $T_H \approx 1.6\times10^5\text{K}$). The matter particles are non-relativistic at around these temperatures (electrons are the lightest of the particles and have a mass energy of $m_e c^2 = 0.511\text{MeV} \gg 13.6\text{eV}$). We define the ionization fraction as

$$x = \frac{n_e}{n_H + n_p}, \tag{1.16}$$

which is the proportion of total particles present which are electrons. We can apply Boltzmann statistics to the plasma, using the fact that by total charge neutrality we have $n_e = n_p$ to find that

$$\frac{x^2}{1-x} = \frac{1}{n_{tot}}\left(\frac{m_e k_B T}{2\pi\hbar}\right)^{3/2} \exp\left(\frac{-B_H}{k_B T}\right). \tag{1.17}$$

Most hydrogen recombination does not occur at T_H because of the large numerical factor in front of the exponential in Equation (1.17). However as temperature decreases we find that the ionization fraction falls sharply, and by $T \approx 3500\text{K}$ we find that the vast majority of the electrons present have combined to form neutral hydrogen. Because there are no longer significant numbers of bare electrons for the photons to interact with, photons travel undeflected (save for some slight gravitational interactions), and these photons can be observed today. The observation of this radiation, which has been highly red shifted but retains its characteristic blackbody spectrum, gives a very useful picture of the universe at the time of recombination.

The existence of this Cosmic Microwave Background Radiation (CMB) was initially predicted in a paper by Gamow [29] in 1946. He said there should be a uniform radiation left over from the big bang, and that this radiation would be at a temperature of around 6 K. It was not until almost 20 years later when in 1965, Arno Penzais and Robert Wilson [51] observed a uniform microwave radiation present regardless of which direction a sensitive microwave receiver was pointed. They initially thought this was due to instrument failure, specifically the presence of pigeon droppings in the antenna. The presence of the CMB has since been confirmed by various experiments. It is observed to very high precision

to be a blackbody spectrum with temperature of $2.7K$. This temperature is found to have a dipole deviation of the order of 10^{-3} resulting from our motion relative to the rest frame of the background. Removing this dipole we find small perturbations about the mean temperature of the order of 10^{-5}.

Any inhomogeneities in the matter distribution at the time of decoupling will still be present in the current CMB temperature spectrum. This means that the inhomogeneities in the CMB are a valuable tool for studying both the configuration of the universe at the time of recombination and the evolution of the universe between the time of recombination and the current time. We will discuss these inhomogeneities more in Chapter 9.

The remainder of this chapter deals with the failings of the standard big bang model, and how a period of accelerating expansion early in the evolution of the universe can solve these problems.

1.4 The problems with the pre-inflationary big bang model

The big bang model before inflation answered many questions about the origin of features observed in the universe. However it also left many questions unanswered, which we will now discuss further:

- *Spatial flatness*
  We currently observe Ω, the ratio of the current density of the universe to the critical density required to close the universe, to be $\Omega_0 = 1.02 \pm 0.02$. [17]. Ω is known to evolve with time in a way that makes $|\Omega(t) - 1|$ increase according to

$$\Omega(t) = \frac{1}{1 - x(t)}, \qquad \text{where} \qquad x(t) \propto \begin{cases} a(t)^2 & (t \lesssim t_{EQ}) \\ a(t) & (t \gtrsim t_{EQ}) \end{cases} \tag{1.18}$$

and where t_{EQ} is the time of radiation and matter equality. This means that for Ω to be within the current observational bounds, at earlier times Ω must have been extremely close to one. For instance

$$|\Omega(10^{-43}\,\text{sec}) - 1| \lesssim \mathcal{O}(10^{-60}) \tag{1.19}$$

$$|\Omega(1\,\text{sec}) - 1| \lesssim \mathcal{O}(10^{-16}). \tag{1.20}$$

This amounts to extraordinary fine tuning. It is seen as unnatural to assume as an initial condition for the big bang model that Ω in the early universe is very close to one, without imposing this as a requirement of the model. Another way of thinking about this is to say that the natural timescale that can be constructed from the various numerical constants of the universe $(c, G, \hbar)$ is the Planck time of roughly 5×10^{-44} seconds. The universe has been around for about 4×10^{17} seconds, which is a factor of 10^{61} larger than this with no explanation as to why these numbers should be so different.

- *Large scale smoothness*

  The CMB is observed to be uniform in all directions, with perturbations in temperature of the order of 10^{-5}. This means that to a good approximation we live in a universe which is homogeneous and isotropic on large scales. In the standard big bang model this is a problem as the CMB consists of 10^5 causally disconnected regions, that is regions that could never have had any effect on one another, and hence could not have reached thermal equilibrium. This is like asking 100 000 people to all choose a random number and having them all pick the same one, the logical conclusion being that they had somehow communicated with one another beforehand. Such communication is not possible according to relativity, and so the fact that the CMB is so smooth must be inserted into the standard big bang model as an initial condition.

- *Relic particles*

  Theory predicts the existence of many exotic particles, such as magnetic monopoles. These particles would be present in large quantities the early

universe. Such particles would become non-relativistic much earlier than the observed matter, and hence would evolve with scale factor as $\rho \equiv a^{-3}$ instead of $\rho \equiv a^{-4}$. This early change in evolution from the universe being radiation dominated to matter dominated would cause the universe to recollapse before structure had time to form [52, 68].

- *Density perturbation formation*
  The standard big bang model has no obvious way of generating the inhomogeneities which evolve to form the large scale structure we now observe in the universe. The density perturbations instead have to be inserted arbitrarily at some stage after the big bang, without any explanation of their cosmological origins. The perturbations in the universe are observed to be scale invariant. By this we mean that the amplitude of the perturbations is approximately constant regardless of the scale size of the perturbation. This is a very interesting result, and one that merits some logical physical explanation.

1.5 Resolving the problems with the standard big bang model

Inflation was first proposed by Guth [31] as a solution to the problems of the standard model. The theory involves the universe going through a period of rapidly accelerating expansion, where

$$\ddot{a} > 0. \tag{1.21}$$

During such an expansion, a small patch of space can expand by enormous amounts to encompass the entire currently observable universe. Inflation occurs at energies of $\approx 10^{14}$ GeV, when a non-zero vacuum energy density in the form of a scalar field is the dominant form of energy density in the universe. A scalar field with a non-zero vacuum energy can have an equation of state with $\rho \approx -p$. From Friedmann's Equation (1.6) we find that any occurrence of constant pressure and

constant density with $3p < -\rho$ would result in the right hand side of equation being positive. This would result in an equation of the form

$$\frac{\ddot{a}}{a} = K, \tag{1.22}$$

where $K > 0$. This has the simple solution

$$a(t) = a_0(e^{\sqrt{K}t} + e^{-\sqrt{K}t}). \tag{1.23}$$

Over time the second term in the equation becomes negligible and we are left with the scale factor growing exponentially. This is a simplification as the evolution of the state of the scalar field will lead to p and ρ being functions of time, but the general idea behind the derivation still stands, with a negative pressure leading to a positive RHS and hence $\ddot{a} > 0$.

Inflation solves the problems of the standard big bang model in the following ways :-

- *Spatial flatness problem*
  Inflation solves the spatial flatness problem by having the curvature radius of the universe grow exponentially while the energy density remains constant. This has the effect of decreasing the difference between Ω and 1, which explains why the current value of Ω is observed to be so close to one. The value of Ω before inflation occurs is not observable as during inflation it has evolved to be so close to 1 that we would still observe it to be effectively 1 now.

- *Large scale smoothness*
  Before inflation occurred the size of the patch that evolved to become the observable universe is as small as 0.3 meters across or smaller (depending on the model of inflation). This is much smaller than the size of the patch required in a model without inflation. This means that the entire observable universe can be in causal contact before inflation, and has time to reach thermal equilibrium.

- *Relic particles*

  Because of the exponential expansion of the universe, any relic particles are diluted to an extent that their presence would not have a significant effect on the final energy density of the universe. The matter that we observe today originates from the decay of the quantum field that drives the inflation. This means that there is still a possibility that relic particles are created in large numbers by the decay of the inflaton field, something that must be considered in models of the end of the inflationary period.

- *Density perturbation formation*

  The presence of structure in the universe hinges on a means for generating the initial inhomogeneities that evolve to form the currently observed structure. Inflation provides this by causing very small quantum fluctuations in the scalar field to grow to macroscopic size. Because of the nature of the quantum fluctuations, this will result in a perturbation spectrum that is (nearly) scale invariant.

Chapter 2

Inflation

Inflation occurs because the energy density of the universe is dominated by the potential energy of a scalar field. We will show that from Einstein's equations for the evolution of the scale factor, a universe dominated by such an energy potential will undergo a period of rapid expansion. We then make some assumptions about the scalar field, namely that the field is assumed to be weakly interacting so that the effective potential is slowly varying with time. This allows inflation to occur for long enough to fix the problems associated with the non-inflationary big bang model. This set of assumptions, referred to as slow roll, allow the equations governing the evolution of the scale factor to be simplified.

2.1 The currently accepted model of Inflation

We begin by looking at the evolution of a universe dominated by a scalar field ϕ, known as the inflaton. It has been suggested that this scalar field could be the Higgs field, however this has proven hard to model theoretically as the energy level of this field and the Higgs are so different. It is more likely that ϕ is a scalar field derived from supersymmetric theory, the formulation of which involves multiple scalar fields. The particular details of this field are not important to modeling inflation and we will not delve further into them in this thesis.

The energy density of this universe is given by the effective potential $V(\phi)$.

This effective potential incorporates all the couplings of the field ϕ to the other fields present, as well as possible self coupling terms, such as $m^2\phi^2$ and $\lambda\phi^4$. The exact form of this potential is not important in the formulation of the theory as long as the potential satisfies certain criteria. We formulate our evolution as a function of this potential. We can construct a Lagrangian from the effective potential to give

$$\mathcal{L} = \frac{1}{2}\partial_\mu\phi\partial^\mu\phi - V(\phi). \tag{2.1}$$

From this we calculate the stress energy tensor

$$T^{\mu\nu} = \partial_\mu\phi\partial^\mu\phi - \mathcal{L}. \tag{2.2}$$

We can ignore the spatial derivatives[1] which means the density and pressure are given by

$$\rho = T^0_0 = \frac{1}{2}\dot{\phi}^2 + V(\phi) \quad \text{and} \tag{2.3}$$

$$p = T^i_i = \frac{1}{2}\dot{\phi}^2 - V(\phi). \tag{2.4}$$

This illustrates the key difference between the evolution of a universe dominated by a scalar field and one dominated by matter or radiation. If the effective potential term $V(\phi)$ is larger than the term involving the rate of change of the field, $\phi^2/2$, then we have a negative pressure. In the case that the pressure is so negative that $3p < -\rho$ then from Equation (1.6) the scale factor has the required positive acceleration $\ddot{a} > 0$ for inflation.

Using Equations (2.3) and (2.4), for the energy density and pressure, in Equations (1.5) and (1.6), we find two equations relating the evolution of the universe to the effective potential and the derivative of the scalar field,

$$H^2 = \frac{8\pi G}{3}\left(\frac{1}{2}\dot{\phi}^2 + V(\phi)\right) \quad \text{and} \tag{2.5}$$

$$\frac{\ddot{a}}{a} = \frac{8\pi G}{3}(V(\phi) - \dot{\phi}^2). \tag{2.6}$$

[1]We assume the field is uniform in space as before inflation begins it is in causal contact and is able to reach thermal equilibrium on the scale of the observable universe.

We have dropped the term involving k from the first of these equations because after a short period of inflation the value of a has increased enough to make the k/a term negligible.

The equation of motion of the ϕ field can be derived from Equation (1.7)

$$\ddot{\phi} + 3H\dot{\phi} + \frac{\mathrm{d}V(\phi)}{\mathrm{d}\phi} = 0. \tag{2.7}$$

This equation has the same form as that of an object sliding down a hill with a friction term proportional to the velocity of the sliding object

$$\ddot{x} + \mu\dot{x} + \frac{\mathrm{d}y}{\mathrm{d}x} = 0. \tag{2.8}$$

This leads us to the idea of terminal speed at which the acceleration term $\ddot{\phi}$ is negligible and the other two terms are equal in magnitude. This is the condition of slow roll.

2.2 Slow roll

The majority of the inflation in the universe occurs under the conditions of slow roll. Slow roll makes some assumptions which are required so that enough inflation occurs to explain the observed universe. In making these assumptions, slow roll simplifies the dynamics of inflation field. Most models of inflation are formulated in terms of these slow roll parameters.

For slow roll we require that the potential is slowly changing with time, so that the energy density is dominated by the effective potential $V(\phi)$ and not the kinetic energy $\dot{\phi}/2$, so

$$V(\phi) \gg \frac{1}{2}\dot{\phi}^2. \tag{2.9}$$

Furthermore we require that this condition remains valid for a significant time, and so we restrict $\ddot{\phi}$ by

$$\ddot{\phi} \ll 3H\dot{\phi}. \tag{2.10}$$

These two conditions are equivalent to the slow roll parameters ϵ and η both being much less than one, where

$$\epsilon \equiv -\frac{1}{2}\left(\frac{\dot{\phi}}{H}\right)^2 = -\frac{\dot{H}}{H^2} = 2M_P^2\left(\frac{H'}{H}\right)^2 \qquad \text{and} \tag{2.11}$$

$$\eta \equiv \frac{\ddot{\phi}}{H\dot{\phi}} = 2M_P^2\frac{H''}{H}. \tag{2.12}$$

We can further define slow roll parameters to any order in the time derivatives of the field ϕ. For $n \geq 1$ we have

$$\eta_n = \frac{1}{H^n\dot{\phi}}\frac{\mathrm{d}^{n+1}\phi}{\mathrm{d}t^{n+1}}. \tag{2.13}$$

Making the slow roll assumptions allows several simplifications to the cosmological equations to be made. Equation (2.7) becomes

$$\dot{\phi} = -\frac{1}{3H}V'(\phi), \tag{2.14}$$

and Equation (2.5) becomes

$$H^2 = \frac{8\pi G}{3}V(\phi). \tag{2.15}$$

These equations can be combined to give the exponential expansion characteristic of inflation, by solving the equation

$$H = \frac{\dot{a}}{a} \quad \Longrightarrow \quad a(t) = a_0 \exp\left(\int_0^t H(t)\mathrm{d}t\right). \tag{2.16}$$

Under the slow roll approximation this becomes

$$a_{(\phi=\phi_1)} = a_{(\phi=\phi_0)} \exp\left(\frac{-8\pi}{M_P^2}\int_{\phi_0}^{\phi_1}\frac{V(\phi)}{V'(\phi)}\right). \tag{2.17}$$

There are other definitions of the slow roll parameters. One choice of slow roll parameters is to write them in terms of the inflaton potential and its derivatives

up to nth order. We label slow roll parameters defined in this way with the subscript V, the first two being

$$\epsilon_V = \frac{M_P^2}{2}\left(\frac{V'(\phi)}{V(\phi)}\right)^2 \qquad \text{and} \qquad \eta_V = M_P^2\frac{V''(\phi)}{V(\phi)}. \tag{2.18}$$

Again more generally to nth order in the derivatives we can define a slow roll parameter

$$\eta_n = M_P^{2n}V'^{n-1}\frac{\mathrm{d}^{n+1}V}{\mathrm{d}\phi^{n+1}}. \tag{2.19}$$

This definition for the slow roll parameters can be related to the slow roll parameters defined in Equations (2.11) and (2.12). We find to first order in the slow roll parameters that $\epsilon_V = \epsilon$ and $\eta_V = \eta - \epsilon$. The definition of the slow roll parameters in terms of the potential has the advantage that the slow roll parameters can immediately be calculated given a potential $V(\phi)$. This makes it easy to evaluate the validity of slow roll. For instance for a potential of the form

$$V(\phi) = \frac{1}{2}m^2\phi^2, \tag{2.20}$$

we have that

$$\epsilon = \eta = \frac{2}{\phi^2} \tag{2.21}$$

and so we have slow roll for $\phi \gg 2$.

It is also possible to define slow roll parameters in terms of time derivatives of the Hubble parameter. In some ways this is the most general and most easily applicable definition because it does not depend on the inflationary potential being formulated in terms of a single scalar field ϕ. This allows single field models to be compared with more complicated models of inflation, such as inflationary models involving the coupling of multiple scalar fields.

2.3 How much inflation do we need?

In order to solve the flatness problem we require $|\Omega - 1| \lesssim 10^{-60}$ at the end of inflation. Now assuming H is approximately constant during inflation, the ratio

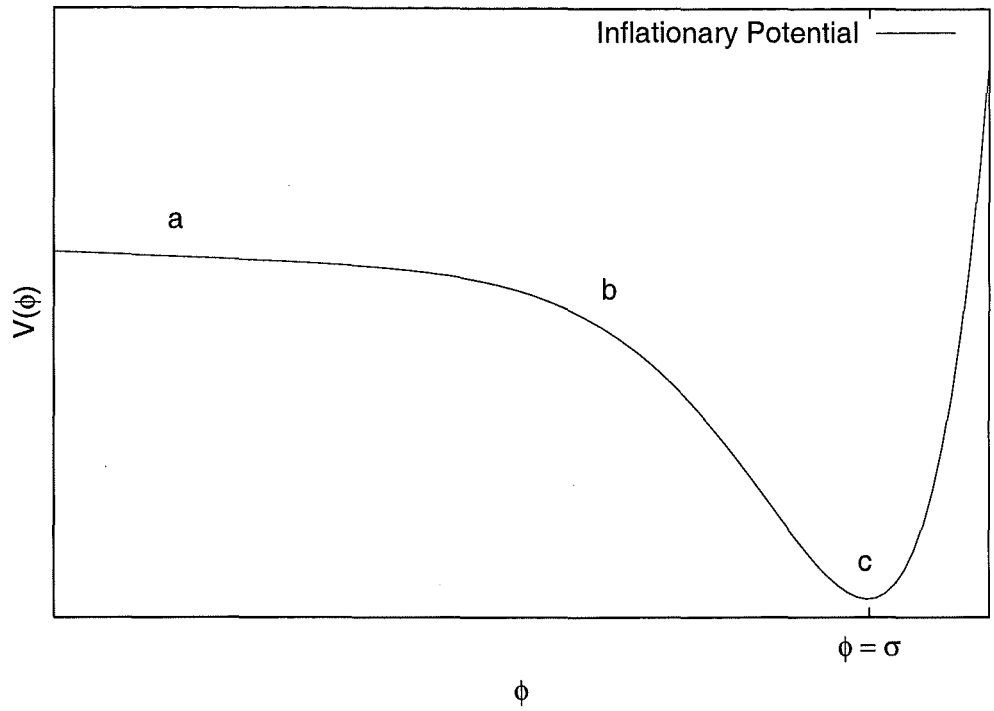

Figure 2.1: A typical Inflationary potential. We can see this comprises three sections, a) showing when ϕ is undergoing slow roll, b) showing the transition from slow roll, and c) the phase in which the field undergoes approximately simple harmonic oscillations about the minimum of the potential σ.

of $|\Omega - 1|$ changes during inflation by a factor

$$\frac{|\Omega_f - 1|}{|\Omega_i - 1|} \simeq \left(\frac{a_f}{a_i}\right)^2 = e^{-2N}. \tag{2.22}$$

Where N is the number of e-folds of inflation. Thus if $|\Omega_i - 1|$ is of the order of unity before inflation, to drive Ω close enough to unity by the end of inflation so that we currently observe $\Omega \approx 1$, we require at least 70 efolds of inflation.

2.4 Models of Inflation

Many different models of inflation have been suggested, which we can classify by particular characteristics into various classes. Most models of inflation are

one field models, where the evolution of the inflaton alone dictates the course of inflation.

Following the treatment of Tsujikawa [65], we class single scalar field models of inflation into three categories. Firstly large field models where the field begins at a large value and rolls downward towards a potential minimum at lower values of the field. An example of this is Chaotic Inflation where the potential is of a simple polynomial form $V(\phi) = \frac{1}{2}m^2\phi^2$ or $V(\phi) = \lambda\phi^4$. These are the models we will largely be dealing with throughout the course of this thesis.

The second class, "small field" models, have the potential initially small and evolving to larger values. The main difference between this and large field models is that this type more readily allows for $V''(\phi)$ to change sign. An example of this type is Natural Inflation which has an effective potential of the form

$$V(\phi) = m^4\left[1 + \cos\left(\frac{\phi}{f}\right)\right]. \tag{2.23}$$

This equation is motivated by a particular class of supergravity theories.

The third type is Hybrid inflationary models which are generally formulated in terms of two interacting scalar fields. In these models the field which drives inflation is coupled to another field in the effective potential. As the second field evolves it causes a change in the effective potential relative to the first field. So the location of a local minimum can be shifted or the minimum can be erased altogether, resulting in evolution of the inflaton from its initial location. This evolution eventually halts of inflation. An example is Linde's Hybrid inflation model [45]

$$V(\phi,\xi) = \frac{\lambda}{4}\left(\chi^2 + \frac{M^2}{\lambda}\right)^2 + \frac{1}{2}g^2\phi^2\chi^2 + \frac{1}{2}m^2\phi^2, \tag{2.24}$$

where the inflaton ϕ is coupled to a second scalar field ξ.

Chapter 3

Density Perturbations

In this chapter I will discuss the theory of density perturbations. I begin with a brief outline of the general treatment of perturbations before focusing on how fluctuations in the inflaton field lead to macroscopic density perturbations. I will discuss slow roll results for the perturbation spectrum as well as derive the exact equation which needs to be solved to calculate the spectrum. I will also compare this to the tensor modes, which are shown to follow a very similar evolution equation.

3.1 Formalism for describing density perturbations

To begin we seek a means of describing how the contents of the universe are distributed spatially. Cosmological perturbations at early epochs are best described as deviations from the average value of the variable. At these early epochs, the deviation from the average value is usually small, and so one can often neglect terms greater than first order in the perturbations. The relevant variables we are considering are the density $\rho(x,t)$, the pressure $p(x,t)$ and the Hubble parameter $H(x,t)$. A small perturbation in each of these can be described in terms of the average values (denoted by ${}^{(0)}X$) by

$$\rho(x,t) = {}^{(0)}\rho(t) + \delta\rho(x,t), \tag{3.1}$$

$$p(x,t) = {}^{(0)}p(t) + \delta p(x,t) \qquad \text{and} \tag{3.2}$$

$$H(x,t) = {}^{(0)}H(t) + \delta H(x,t). \tag{3.3}$$

It proves useful to consider the Fourier transforms of the variables we are considering. A given variable $\xi(\mathbf{x})$ can be expanded into Fourier components by

$$\xi_{\mathbf{k}} = \frac{1}{(2\pi)^3} \int \mathrm{d}^3\mathbf{x}\, \xi(\mathbf{x}) e^{-i\mathbf{k}\cdot\mathbf{x}}, \tag{3.4}$$

with the volume term suppressed. Here $\mathbf{x}$ and $\mathbf{k}$ are comoving variables which can be related to the physical values of distance and wavenumber by the relations

$$\mathbf{x}_{phys} = a(t)\mathbf{x} \qquad \text{and} \qquad \mathbf{k}_{phys} = \mathbf{k}/a(t). \tag{3.5}$$

The value of $a(t)$ is normalized so that $a_0 \equiv a(t = \text{now}) = 1$ so that at the current time the physical values of the variables is equal to their comoving values. Making the assumption of large scale isotropy, we can assume that there is no directional dependence on $\mathbf{k}$. This means we are free to only consider the magnitude of $\mathbf{k}$, which we denote by $k = |\mathbf{k}|$.

The evolution of density inhomogeneities was first described by Jeans [35] who wrote a description of how the inhomogeneities of a fluid in a Newtonian gravity field would evolve with time. When the perturbation amplitudes are much less than one, we are said to be in the linear regime. This is because terms involving the square of the perturbations, and larger powers, are much smaller than the linear terms and hence can be ignored. During this time the size of the density perturbation grows at the same rate as the expansion of the universe ($\lambda_{phys} = a(t)\lambda$). After a density perturbation grows to a certain size, it decouples from the expansion of the universe and behaves in terms of general relativity in a similar way to a closed Robertson Walker universe, expanding as a closed universe until a maximum size and then recollapsing to form a closed system such as a galaxy or cluster of galaxies. The nonlinear portion of density perturbation evolution can be considered by doing n-body simulations. This portion of the density perturbation theory is not relevant to our work. The portion of the theory relevant to the inflationary scenario is when the perturbations are small

and hence they scale linearly with the expansion of the universe. For further information on the Jeans mechanism, either Kolb and Turner [37] or the article by Liddle and Lyth [43] are recommended.

3.2 Inflationary perturbations

In this section we are going to focus on the evolution of perturbations during inflation. We begin with a more qualitative approach, explaining how the length scale of the perturbations increases during and after inflation. We then discuss the generation and evolution of perturbations from a quantum mechanical and general relativistic viewpoint. Finally we consider the small and large length scale limits, and how the slow roll approximation can be used to simplify the calculation of the primordial power spectrum.

3.2.1 The qualitative evolution of Inflationary perturbations

To deal with inflationary perturbations we must account for the fact that the scale size of an inflationary perturbation evolves to be larger than the Hubble size. We begin by considering a perturbation with scale size much smaller than the Hubble size (or the distance of the event horizon in de Sitter space). During inflation the scale size of a perturbation increases at a much faster rate than the horizon distance, and because of this the scale of perturbations can evolve to be larger than the horizon. When this happens the perturbation is no longer able to evolve, and freezes in as a classical metric perturbation. After inflation ends the size of the perturbation scales with the expansion of the universe, undergoing a radiation and then matter dominated stage. During this time the horizon distance increases much more rapidly than the increase in scale of the perturbations. So the perturbations evolve to again be smaller than the horizon. It is this "goodbye" and "hello again" feature of the inflationary scenario that makes it possible for the

scalar field to imprint density perturbations on scales that are now cosmologically interesting. This feature is described graphically in Figure 3.1.

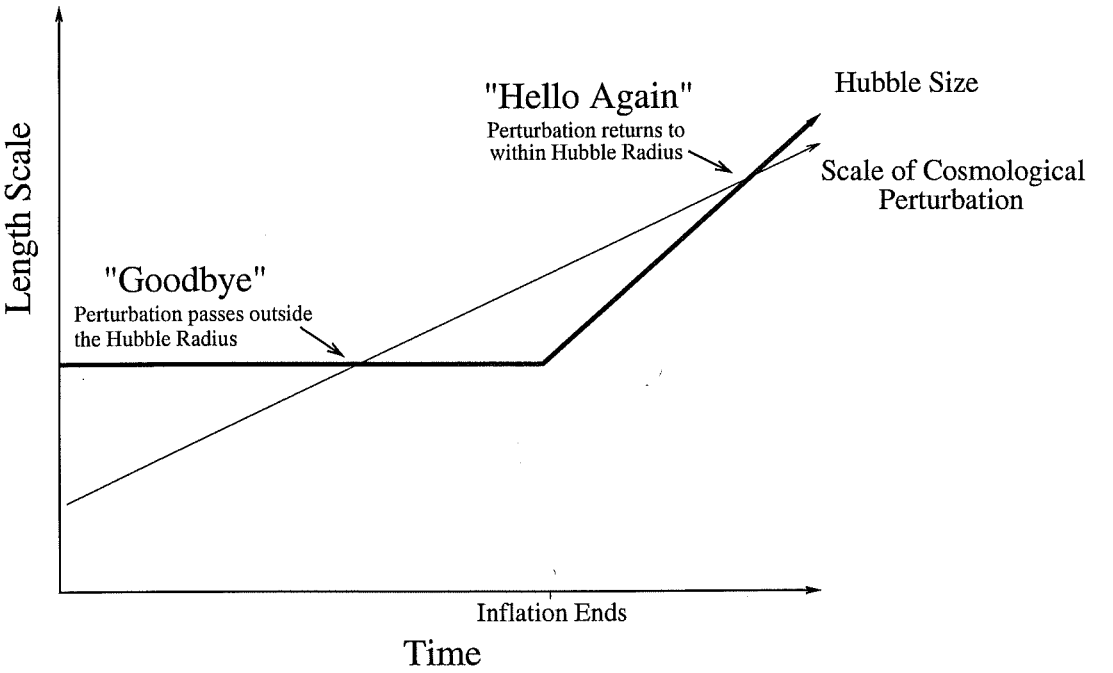

Figure 3.1: The evolution of the scale size of cosmological perturbations and Hubble size. During inflation the perturbation increases in length scale until it is larger than the Hubble size, where it freezes in as a classical perturbation of the metric and ceases to evolve. After inflation the Hubble size increases in scale until eventually it is again larger than the scale size of the perturbation. At this point the perturbation begins evolving again. This diagram is pedagogical in nature and is not drawn to scale

3.2.2 Gauge invariant metric perturbations

In the context of inflation, where the perturbations are small compared to the average values[1], the relevant equations can be written to first order in the perturbation terms. The theory of cosmological density perturbations must be formu-

[1]The deviation from the average temperature at the time of last scattering of photons is only a factor of 10^{-5}, as measured from the CMB anisotropy. This occurs approximately 300 000 years after the big bang, when the deviations have had a long time to evolve from their inflationary values.

lated in terms of general relativity, which has the property of general covariance. Because of this principle we find that *only gauge invariant quantities have any inherent physical meaning* [3]. This means that any perturbation variables should be considered in gauge invariant combinations. Here we follow the treatment of Mukanov *et. al.* [49], with some changes in notation for consistency with the rest of our work.

The Friedmann-Robertson-Walker background metric is described by the line element

$$\mathrm{d}s^2 = {}^{(0)}g_{\mu\nu}\mathrm{d}x^\mu\,\mathrm{d}x^\nu = \mathrm{d}t^2 - a^2(t)\gamma_{ij}\mathrm{d}x^i\,\mathrm{d}x^j \tag{3.6}$$

with

$$\gamma_{ij} = \delta_{ij}\left[1 + \frac{1}{4}q(x^2+y^2+z^2)\right]^{-2}, \tag{3.7}$$

where $q = -1, 0, 1$ for a closed, critical and open universe, respectively. We wish to decompose the full metric into its background and perturbation parts $g_{\mu\nu} = {}^{(0)}g_{\mu\nu} + \delta g_{\mu\nu}$.

Here we are going to consider only scalar perturbations. There are two ways of introducing scalar quantities into $g_{\mu\nu}$, either multiplying the tensor γ_{ij} by a scalar or by taking the covariant derivative of a scalar function. This means that the scalar metric perturbation can then be written as a function of four scalar quantities ψ, A, B and E as

$$\delta g_{\mu\nu} = a^2(\tau)\begin{pmatrix} 2A & -B_{|i} \\ -B_{|i} & 2(\psi\gamma_{ij} - E_{|ij}) \end{pmatrix}, \tag{3.8}$$

where $X_{|i}$ is the covariant derivative of X with respect to the coordinate i. This leads to the line element

$$\mathrm{d}s^2 = a^2(\tau)\{(1+2A)\mathrm{d}\tau^2 - 2B_{|i}\mathrm{d}x^i\,\mathrm{d}\tau - [(1-2\psi)\gamma_{ij} + 2E_{|ij}]\mathrm{d}x^i\,\mathrm{d}x^j\}. \tag{3.9}$$

From this we must find the gauge independent metric variables. By considering an arbitrary coordinate transform of the form

$$x^\alpha \to \tilde{x}^\alpha = x^\alpha + \xi^\alpha, \tag{3.10}$$

and writing the spatial part of this four vector as

$$\xi^i = \xi^i_{tr} + \gamma^{ij}\xi_{|j}, \tag{3.11}$$

where the function ξ solves the equation $\xi^{|i}_{|i} = \xi^i_{|i}$ and the "transverse" vector satisfies $\xi^i_{tr|i} = 0$. Then the most general diffeomorphism that preserves the scalar nature of metric fluctuations can be described by the coordinate transformation

$$\tau \to \tilde{\tau} = \tau + \xi^0(\tau, x), \qquad x^i \to \tilde{x}^i = x^i + \gamma^{ij}\xi_{|j}(\tau, x). \tag{3.12}$$

The metric perturbation is not invariant under this change, but is changed by

$$\delta g_{\alpha\beta} \to \delta\tilde{g}_{\alpha\beta} = \delta g_{\alpha\beta} + \Delta g_{\alpha\beta}, \tag{3.13}$$

which may be written in terms of the variables A, B, ψ and E to give their change into the new coordinate system to be

$$\tilde{A} = A - \frac{a'}{a}\xi^0 - \xi^{0\prime}, \quad \tilde{\psi} = \psi + \frac{a'}{a}\xi^0, \quad \tilde{B} = B + \xi^0 - \xi', \quad \tilde{E} = E - \xi, \tag{3.14}$$

where $X' \equiv \mathrm{d}X/\mathrm{d}\tau$. By taking invariant combinations of these we can construct gauge invariant variables. Two such variables which span the 2-dimensional space of invariant variables are found to be [3]

$$\Phi = A + \frac{1}{a}[(B - E')a]', \qquad \Psi = \psi + \frac{a'}{a}(B - E'). \tag{3.15}$$

This means that when considering metric perturbations these variables should be used, as otherwise the calculations will not be gauge invariant and hence lose physical meaning.

We are free to choose a gauge to remove three unnecessary degrees of freedom from this set of equations. The simplest example of this is the longitudinal gauge in which we have $B = E = 0$. This then means that the metric becomes

$$\mathrm{d}s^2 = a^2(\tau)\left[(1 + 2\Phi)\mathrm{d}\tau^2 - (1 + 2\Psi)\delta_{ij}\mathrm{d}x^i\,\mathrm{d}x^j\right]. \tag{3.16}$$

This provides a physical interpretation of the gauge invariants Φ and Ψ.

We can now use the gauge invariant variables Φ and Ψ to generate the left hand side of the linearized Einstein equation. For the rest of this chapter we will use the notation that X' is the conformal time derivative $\mathrm{d}X/\mathrm{d}\tau$. Also we define the variable $\mathcal{H} = a'/a$. This is not to be confused with the Hubble parameter $H = \dot{a}/a$. The perturbed Einstein tensor then becomes

$$\delta G_0^0 = 2a^{-2}\left(-3\mathcal{H}(\mathcal{H}\Phi - \Psi') + \nabla^2\Psi\right) \tag{3.17}$$

$$\delta G_i^0 = 2a^{-2}(\mathcal{H}\Phi - \Psi')_{,i} \tag{3.18}$$

$$\delta G_j^i = -2a^{-2}\left[\left((2\mathcal{H}' - \mathcal{H}^2)\Phi + \mathcal{H}\Phi' + \Psi'' + 2\mathcal{H}\Psi' + \frac{1}{2}\nabla^2 D\right)\delta_j^i - \gamma^{ik}D_{,kj}\right] \tag{3.19}$$

Here subscripts after commas denote differentiation with respect to that variable, and $D = \Phi - \Psi$.

We are now going to compare this metric perturbation to the perturbations in the stress energy tensor. Here we choose to look at perturbations during inflation, and so we consider a universe where the stress energy tensor is dominated by a scalar field ϕ. We can equate the background parts of the stress energy tensor and metric tensor according to Einstein's equations, which gives us for the perturbed part of the equations that

$$\delta G_\nu^\mu = 8\pi G \delta T_\nu^\mu. \tag{3.20}$$

δT_ν^μ can be evaluated in terms of the perturbations in the scalar field ϕ. We do this by inserting $\phi = \phi_0 + \delta\phi$ into our expression for T_ν^μ. This decomposition of the energy momentum tensor into background and perturbation terms gives us

$$\delta T_0^0 = a^{-2}\left[-\phi_0'^2\Phi + \phi_0'\delta\phi' + V'(\phi)a^2\delta\phi\right] \tag{3.21}$$

$$\delta T_i^0 = a^{-2}\phi_0'\delta\phi_{,i} \tag{3.22}$$

$$\delta T_j^i = a^{-2}\left[+\phi_0'^2\Phi - \phi_0'\delta\phi' + V'(\phi)a^2\delta\phi\right]\delta_j^i. \tag{3.23}$$

Comparing these equations to the metric perturbations and specifically the ij component one can see that $D = \Phi - \Psi = 0$, which greatly simplifies the equations. We can combine this with Equations (2.5) and (2.6) which describe

the evolution of the background. Doing this we obtain a set of equations relating the curvature of space with the distribution of the scalar field

$$\nabla^2\Phi - 3\mathcal{H}\Phi' - (\mathcal{H}' + 2\mathcal{H}^2)\Phi = \frac{(8\pi G)^2}{2}(\phi_0'\delta\phi + V'(\phi)a^2\delta\phi), \tag{3.24}$$

$$\Phi' + \mathcal{H}\Phi = \frac{(8\pi G)^2}{2}\phi_0'\delta\phi, \tag{3.25}$$

$$\Phi'' + 3\mathcal{H}\Phi' + (\mathcal{H}' + 2\mathcal{H}^2)\Phi = \frac{(8\pi G)^2}{2}(\phi_0'\delta\phi - V'(\phi)a^2\delta\phi). \tag{3.26}$$

Eliminating the scalar field perturbation $\delta\phi$ from this set of equations the gives the differential equation for the gauge invariant cosmological perturbation

$$\Phi'' + 2(a/\phi_0')'(a/\phi_0')^{-1}\Phi' - \nabla^2\Phi + 2\phi_0'(\mathcal{H}/\phi_0')'\Phi = 0. \tag{3.27}$$

Introducing the new variables

$$u \equiv (a/\phi_0')\Phi \qquad \text{and} \qquad z \equiv \phi_0'/(a\mathcal{H}) = a\dot{\phi}/H \tag{3.28}$$

we can reduce this expression to give

$$u'' - \nabla^2 u - (z''/z)u = 0. \tag{3.29}$$

Finally we take the Fourier transformation of this to get an equation for the evolution of the mode u_k (with wave number k) to be

$$u_k'' + \left(k^2 - \frac{z''}{z}\right)u_k = 0. \tag{3.30}$$

Equation (3.30) is valid to first order in the perturbations $\delta\phi$ and can be assumed to be accurate for the period from when the perturbations are formed to when they pass outside the horizon. This equation has two obvious solutions in the small and large wavelength limits, which we discuss in the following sections.

3.2.3 Inflationary perturbations in the short wavelength limit

We begin by looking at the short wavelength limit, by which we mean at early times during inflation when $k^2 \gg z''/z$. Looking at Equation (3.30) we see that

we can ignore the z''/z term entirely to get the solution as a linear combination of sine and cosine. We choose the particular combination that corresponds to the free field solution,

$$u_k \rightarrow \frac{1}{\sqrt{2k}} e^{-ik\tau} \tag{3.31}$$

with normalization determined by the quantum origin of the perturbations (see [44] for a more detailed discussion).

3.2.4 Inflationary perturbations in the long wavelength limit

We now consider the solution to Equation (3.30) in the long wavelength limit, where $k^2 \ll z''/z$. The mode can be related to z by

$$u_k = z\left[c_1 + c_2 \int \frac{\mathrm{d}\tau}{z^2}\right], \tag{3.32}$$

with integration constants c_1 and c_2.

This leads to a gauge invariant quantity first introduced by Bardeen called the curvature perturbation, which we define as

$$\mathcal{R}_k \equiv |u_k/z|. \tag{3.33}$$

Using this we define the perturbation spectrum (or power spectrum) to be given by the formula

$$\mathcal{P}_\mathcal{R} \equiv \frac{k^3}{2\pi^2}\langle|\mathcal{R}|^2\rangle. \tag{3.34}$$

Hence we see

$$\mathcal{P}_\mathcal{R}{}^{1/2}(k) = \sqrt{\frac{k^3}{2\pi^2}}\left|\frac{u_k}{z}\right|. \tag{3.35}$$

We define the spectral index by

$$n_\mathcal{R} \equiv 1 + \frac{\mathrm{d}\ln\mathcal{P}_\mathcal{R}}{\mathrm{d}k}. \tag{3.36}$$

In the scale invariant case where the power spectrum is independent of scale size, we have a spectral index of 1.

3.2.5 Solution in the slow roll scenario

Exact analytic solutions to Equation (3.30) only exist for very specific and often unphysical forms of the inflationary potential. One approach to simplifying the equations is to consider slow roll inflation. By simply assuming the slow roll parameters are small, we find that the power spectrum is given by

$$\mathcal{P}_{\mathcal{R}}{}^{1/2}(k) \approx \left.\frac{H^2}{2\pi\dot{\phi}}\right|_{k=aH}. \tag{3.37}$$

This is valid to first order in the slow roll parameters. We can evaluate Equation (3.35) to arbitrary order in the slow roll parameters, however as one gets beyond second order the equations become increasingly complicated. Evaluating the spectral index to second order in the slow roll parameters gives [63]

$$\begin{aligned} n_{\mathcal{R}}^{\mathcal{O}(2)}(k) = 1 - 4\epsilon - 2\eta - 2(1+c)\epsilon^2 + \frac{1}{2}(3-5c)\epsilon\eta \\ -\frac{1}{2}(3-5c)\eta^2 + \frac{1}{2}(3-c)\frac{\dddot{\phi}}{3H\ddot{\phi}}\eta, \end{aligned} \tag{3.38}$$

where $c = 4(\ln(2)+\gamma) - 5 \simeq 0.08145$ and $\gamma \simeq 0.57721$ is the Euler-Mascheroni constant.

Another assumption which can be made, though now we are dealing with much more specific cases of inflation, is to assume that the parameter ϵ is not only small, but constant. If ϵ is constant then the Equation (3.30) can be solved analytically. This can then be inserted into Equation (3.35) to give

$$\mathcal{P}_{\mathcal{R}}{}^{1/2}(k) = 2^{(\nu-3/2)}\frac{\Gamma(\nu)}{\Gamma(3/2)}(1-\epsilon)^{(\nu-1/2)}\left.\frac{H^2}{2\pi|\dot{\phi}|}\right|_{aH=k}, \tag{3.39}$$

where

$$\nu = \frac{1+\eta+\epsilon}{1-\epsilon} + \frac{1}{2}. \tag{3.40}$$

3.2.6 Tensorial modes

Throughout this work on perturbations we have assumed we are in the linear regime. This means we have been able to treat the scalar and tensor modes independently of one another. The tensor perturbations are found to evolve according to a differential equation very similar to Equation (3.30) which describes the scalar mode perturbations. We find that behaviour of the tensor modes is somewhat simpler than that of the scalar perturbations. The tensor modes are found to obey [49]

$$v_k'' + \left(k^2 - \frac{a''}{a}\right) v_k = 0. \tag{3.41}$$

Here $v_k = a\psi_k$ describes the amplitude of the tensor perturbation. We also find very similar boundary conditions for the behaviour of v_k to those of u_k, again being dependent on whether the mode is inside or outside the horizon. So

$$v_k \to \frac{1}{\sqrt{2k}} e^{-ik\tau} \qquad \text{for} \qquad k \gg aH \tag{3.42}$$

$$v_k \propto a \qquad \text{for} \qquad k \ll aH. \tag{3.43}$$

The power spectrum for gravitational waves is then given by the formula

$$\mathcal{P}_\psi{}^{1/2}(k) = \sqrt{\frac{k^3}{2\pi^2}} \left|\frac{v_k}{a}\right|. \tag{3.44}$$

We can again consider the analytic solution in the limit of slow roll, and that the parameter ϵ is constant. Using this we find that

$$\mathcal{P}_\psi{}^{1/2}(k) = \sqrt{\frac{k^3}{2\pi^2}} \left|\frac{v_k}{a}\right| = 2^{(\mu-3/2)} \frac{\Gamma(\mu)}{\Gamma(3/2)} (1-\epsilon)^{(\mu-1/2)} \left.\frac{H}{2\pi}\right|_{aH=k} \tag{3.45}$$

where $\mu = \frac{1}{1-\epsilon} + \frac{1}{2}$. The assumption that ϵ is constant is not a good one as one nears a sudden change in the potential, but away from such a feature it is accurate.

These equations are not particularly useful in the case of an inflationary potential which does not obey the slow roll restrictions. In the case where there

is a period of non-slow roll expansion, we must use equations that are valid to all orders in the parameters ϵ and η. So in the situation of a phase transition the equations that are exact to all orders in the slow roll terms, Equation (3.30) and Equation (3.35), must be solved.

Chapter 4

Non standard effective potentials

In this chapter we examine the motivation for looking at effective potentials which include a period of non-slow roll inflation. We work in the context of supergravity, where models of inflation contain the inflaton potential. This potential is in a "hidden" sector, so termed because it is coupled only gravitationally to the visible sector containing the quarks and leptons. Our motivation for features in the inflaton potential comes from considering phase transitions in the visible sector, which can have significant effects on the inflaton potential through the inevitable gravitational interactions. Section 4.1 details this, following the work of Adams *et. al.* [1].

We also detail the observational evidence for a non-scale invariant primordial power spectrum. Such a power spectrum is contrary to the predictions for slow roll inflation outlined in Section 3.2.5, and so could be evidence of a non-slow roll period during inflation.

4.1 Phase transitions in the visible sector

Inflation is believed to take place at energies of $\approx 10^{-4} M_p$ because at such energies the resulting amplitude of quantum fluctuations corresponds to the temperature fluctuations we observe in the CMB. At such energies the applicable effective field theory is believed to be that of supergravity, the local version of supersymme-

try. Supergravity originates from an underlying unified "Theory of Everything", the most likely candidate of which is the superstring. The only scale present in superstring theory is the string tension, and other scales are generated by spontaneous symmetry breaking. The first requirement is a source of symmetry breaking. The origin of this is not firmly established but the most promising mechanism is through a stage of dynamical symmetry breaking in which there is a strongly coupled hidden sector. In analogy with QCD it is then reasonable to assume that the strongly interacting fermions - the gaugino partners of the gauge bosons of the strong group - form a condensate which necessarily breaks the local supersymmetry. The scale of supersymmetry breaking is the scale at which the coupling becomes strong and hence can be far from the Planck scale. In supersymmetric theories there are many "flat" directions, even amongst fields with other large gauge (or other) couplings. Before inflation gauge interactions will ensure the field is in thermal equilibrium with temperature dependent terms ensuring the symmetry is unbroken. However when the temperature drops to the supersymmetry breaking scale the field will make a transition to its true vacuum expectation value which can be very large, and close to the Planck scale.

The idea that such a symmetry breaking phase transition would have an effect on the inflationary power spectrum was suggested by Adams *et. al.* [1]. Many such transitions would take place, which means it is reasonable to expect one to occur within the observable inflationary era without having to resort to fine tuning of the model. The calculations in Adams *et. al.* [1] state that a phase transition could be expected to occur every 10-15 efolds of inflation.

We consider inflation to be driven by the evolution of a scalar field ϕ. We can write the effective potential of this field about the value of the field at which the quantum perturbations of interest are produced ϕ^*. Writing the field as $\phi = \phi^* + \tilde{\phi}$ we can expand the inflaton potential as

$$V_I(\phi) = \Lambda^4(1 + c_1\tilde{\phi} + c_2\tilde{\phi}^2 + c_3\tilde{\phi}^3 + c_4\tilde{\phi}^4 + \ldots). \tag{4.1}$$

Here we have used $V_I(\phi)$ to indicate that this is the inflationary portion of the

overall potential. This will dominate the overall potential during the inflationary era. The parameter Λ indicates the scale of inflation at the time when the quantum perturbations which grew to become large scale structure were produced, which as we have stated will be around $10^{-4}M_P$ by observation.

One can easily verify that the slow roll constraints on such a potential take the form

$$c_1 \ll 1, \qquad c_2 \ll 1, \qquad c_3\tilde{\phi} \ll 1 \qquad \text{and} \qquad c_4\tilde{\phi}^2 \ll 1. \tag{4.2}$$

We focus our attention on inflationary models where the variable ϕ is slowly changing and hence we have that $\tilde{\phi} \ll 1$. This means that only the parameters c_1 and c_2 are strongly constrained.

We now add another field ρ, which we assume to be real. This field undergoes a stage of supersymmetry breaking. The full scalar potential describing the inflaton field ϕ and the field ρ then becomes

$$V(\phi,\rho) = V_I(\phi) + m^2\left(\frac{\rho}{M}\right)\rho^2\left[1+\mathcal{O}\left(\frac{\rho}{M}\right)\right]. \tag{4.3}$$

Here we have included the possibility that radiative corrections allow the SUSY breaking mass m to run. We consider the case that m^2 is positive at the Planck scale but changes sign at some intermediate scale Σ. This scale will be very large and can be close to the Planck scale. We also introduce a thermal coupling term which means that the potential becomes

$$V(\phi,\rho,T) = V_I(\phi) + \left[-|m|^2\left(\frac{\rho}{M}\right)+\alpha T^2\right]\rho^2\left[1+\mathcal{O}\left(\frac{\rho}{M}\right)\right]. \tag{4.4}$$

This form of the potential maintains the field ρ at small values where there is a minimum present until the temperature drops below $T^2 = |m|^2/\alpha$. The temperature decreases rapidly during inflation and hence once below this scale the temperature term may be safely ignored.

After the temperature drops, the field ρ will evolve to the new minima in the potential at a scale close to the value Σ. The evolution of ρ is equivalent to the

corresponding evolution of ϕ given by Equation (2.7), that is

$$\ddot{\rho} + 3H\dot{\rho} + \frac{\mathrm{d}V}{\mathrm{d}\rho} = 0. \tag{4.5}$$

Initially $\rho \ll \Sigma$ and so assuming that m and H are constant we have the evolution of ρ given by

$$\rho = \rho_0 \exp\left[\frac{3Ht}{2}\left(\sqrt{1+\frac{8m^2}{9H^2}} - 1\right)\right] \tag{4.6}$$

Note here that this solution is very different to that gained from assuming that the field is in slow roll. The total effective potential is still dominated by the field ϕ and it is this that is driving the inflation of the universe. This evolution of ρ occurs for a number of e-folds but due to the fact the growth is exponentially fast, most of the change in the potential occurs during the last 1-2 e-folds of the exponential region.

Now when ρ reaches the minimum in the potential at $\rho = \Sigma$ its evolution slows and stops, depending on how the potential varies above $\rho = \Sigma$. For instance if $-|m|^2$ suddenly jumps to zero, then we have $\mathrm{d}V/\mathrm{d}\rho = 0$. Equation (4.5) then gives the evolution of ρ to be

$$\rho = \rho_0 - |B|e^{-3Ht}. \tag{4.7}$$

for constants ρ_0 and B. However the exact details of how the evolution of the field slows and stops at the minimum near Σ are not important. The important thing to note is that once $\rho \approx \Sigma$ the effective potential has been reduced, and has a new scale

$$V_I(\phi) \to V_I(\phi)\left[1 - \left(\frac{\Sigma^2}{M^2}\right)\right]. \tag{4.8}$$

This means in simple terms that there has been a sudden dip in the overall effective potential, the majority of which takes place in less than 1 e-fold.

There is another way in which the change in ρ can influence the inflationary effective potential, by the presence of a term $\beta\phi^\dagger\phi\rho^2/M^2$ in the potential. A

term of this form could be allowed by the symmetries of the theory. Such a term effectively changes the inflaton mass by an amount

$$\delta m_\phi^2 \approx \beta \frac{\Sigma^2}{M^2} \tag{4.9}$$

as ρ evolves from 0 to Σ. Again the majority of the change in the inflaton mass occurs during the last 1-2 e-folds of the exponential growth of the field. If this term is of the order of the initial inflaton mass then this can have a significant effect on the inflaton potential.

We have seen that both of these effects are proportional to a numerical constant multiplied by the change in the value of the field ρ^2. We have also shown that the evolution of ρ is approximately exponential and so in the last e-fold of exponential expansion the majority of the change will take place.

4.2 Observational evidence

We can compare predictions about the structure, content and evolution of the universe to observable properties of the universe. The large scale clustering of matter is related to the perturbations present in the early universe.

We know from Chapter 3 that slow roll inflation predicts a flat nearly scale invariant primordial power spectrum. This result has been fitted to the observational data successfully, but there have also been suggestions of peculiarities in the matter spectrum which could better be explained by a feature in the primordial power spectrum. Examples include the spatial distribution of Abell-ACO clusters [12, 54], and the power spectrum derived from the deep pencil beam survey of Broadhurst *et. al.* [6]. The paper by Barriga *et. al.* [4] suggests that a primordial power spectrum with two flat sections joined smoothly gives a better fit to the CMB data of Boomerang and Maxima, combined with the APM power spectrum data.

There are two recent experiments into the structure of the universe which will offer more precise measurement of the matter power spectrum. Both measure the spatial distribution and redshift of galaxies and from these we can construct the power spectrum of galactic clustering. The 2 degree Field Galaxy Redshift Survey (2dFGRS) surveys two strips of the northern and southern galactic plane. This survey now encompasses over 230 000 galaxies with medial redshift of $z = 0.1$. [7] [50] Also the Sloan Digital Sky survey (SDSS) experiment intends to image one quarter of the celestial sphere, and to obtain spectra from the galaxies and quasars in this region. [19], [25]

One of the more recent suggestions is that the observational data is fitted better by a model including the idea of Trans-Planckian physics effects [11]. Because of the exponential increase in the size of perturbations during inflation, it is suggested that perturbations of size around or even smaller than the Planck scale could become physically significant. This has an effect on the primordial power spectrum [10], introducing oscillations with scale size. Such a primordial power spectrum is found to provide a better fit the the CMB anisotropy data of WMAP [48] with a $\chi^2/d.o.f.$ of 1415/1340 compared to 1432/1342 for the best fit model not including trans-Planckian physics (for details on the WMAP experiment and their data, see Section 9.2.3).

Chapter 5

Analytic solution

5.1 Solution for perturbation spectrum

We seek an expression for the primordial power spectrum that results from a given inflationary potential. In this chapter we solve Equation (3.30) in an analytic way by making some assumptions about the form of the inflationary potential. We note that in doing this we are only offering an extension of the slow roll solution. This solution while insightful is by no means an exact solution. The technique used in this chapter however is a lot more relevant to the work we are considering than the slow roll result of Chapter 3, as in our current work the slow roll approximation is not applicable.

We follow the formalism of Stewart [62]. We make a change of variables in Equation (3.30). Defining

$$y \equiv \sqrt{2k}u_k \qquad \text{and} \qquad x \equiv -k\tau \tag{5.1}$$

we see that Equation (3.30) describing the evolution of the perturbation becomes

$$\frac{\mathrm{d}^2 y}{\mathrm{d}x^2} + \left(1 - \frac{1}{z}\frac{\mathrm{d}^2 z}{\mathrm{d}x^2}\right) y = 0. \tag{5.2}$$

The boundary conditions for y in terms of x can be calculated from our previous conditions (Equations (3.31) and (3.32)) to give

$$y = \begin{cases} e^{ix} & x \to \infty \\ \sqrt{2k}A_k z & x \to 0. \end{cases} \tag{5.3}$$

Our approach from here is to assume that the z variable can be written as a function of x, of the form

$$z = \frac{1}{x} f(\ln(x)), \tag{5.4}$$

for some function f. With this assumption we find that

$$\frac{1}{z}\frac{\mathrm{d}^2 z}{\mathrm{d}x^2} = \frac{2}{x^2} + \frac{1}{x^2} g(\ln(x)), \tag{5.5}$$

where the function g is related to f by

$$g = \frac{f'' - 3f'}{f}. \tag{5.6}$$

Combining all these results Equation (5.2) becomes

$$\frac{\mathrm{d}^2 y}{\mathrm{d}x^2} + \left(1 - \frac{2}{x^2}\right) y = \frac{1}{x^2} g(\ln x) y. \tag{5.7}$$

The homogeneous solution to this equation which has the correct behaviour as $x \to \infty$ is

$$y_0(x) = \left(1 + \frac{i}{x}\right) e^{ix}. \tag{5.8}$$

Using Green's Function method, the solution to Equation (5.7) with the boundary conditions given by Equation (5.3) can be written as the integral equation

$$y(x) = y_0(x) + \frac{i}{2}\int_x^\infty \mathrm{d}u \, \frac{1}{u^2} g(\ln u) y_0(u) \left[y_0^*(u) y_0(x) - y_0^*(x) y_0(u)\right]. \tag{5.9}$$

The power spectrum is then given by

$$\mathcal{P}_\mathcal{R}(k) = \left(\frac{k}{2\pi}\right)^2 \lim_{x\to 0} \left|\frac{xy}{f}\right|^2. \tag{5.10}$$

Following the method of Stewart [61] we can solve this equation by expanding $f(\ln x)$ and $g(\ln x)$ about some convenient time around horizon crossing. At this time we set $x = x_\star$. Expanding as a Taylor series about this point gives

$$f(\ln x) = \sum_{n=0}^{\infty} \frac{f_n(x_\star)}{n!} \left[\ln\left(\frac{x}{x_\star}\right)\right]^n \tag{5.11}$$

and

$$g(\ln x) = \sum_{n=0}^{\infty} \frac{g_{n+1}(x_\star)}{n!} \left[\ln\left(\frac{x}{x_\star}\right)\right]^n. \tag{5.12}$$

It is at this point that we make assumptions about the parameters f_n and g_n. Specifically we assume that values of $f(\ln x) - f(\ln x_\star)$ and $g(\ln x)$ are both small around the time when the mode k leaves the horizon. This means that we require

$$\frac{f_n}{f_0} \ll 1 \qquad \text{and} \qquad g_n \ll 1. \tag{5.13}$$

It can be shown that these conditions are equivalent to the slow roll conditions mentioned previously (Equations (2.11), (2.12) and (2.13)). We solve for the power spectrum in terms of the inflationary potential, to first order in the small quantities defined in Equation (5.13). We see that

$$\mathcal{P}_\mathcal{R}(k) = \left(\frac{k}{2\pi}\right)^2 \lim_{x\to 0} \frac{1}{f^2} \left|1 + \frac{1}{2}x \int_x^\infty \frac{\mathrm{d}u}{u^2} g(\ln u) y_0(u) \left[y_0^*(u) y_0(x) - y_0^*(x) y_0(u)\right]\right|^2. \tag{5.14}$$

After a considerable amount of mathematical manipulation (see [61] for details) it can be shown that to first order in the slow roll parameters we have

$$\mathcal{P}_\mathcal{R}(k) = \frac{V_\star^3}{12\pi^2 V_\star'^2} \left\{1 + \left(3\alpha - \frac{7}{6}\right)\frac{V_\star''}{V_\star^2} + 2\int_0^\infty \mathrm{d}u\, W'(u) \ln\left(\frac{V'}{V_\star'}\right)\bigg|_{u=\frac{k}{aH}}\right\}. \tag{5.15}$$

Here α is a numerical constant defined to be $\alpha = 2 - \ln 2 - b \approx 0.7296$ with b the Euler-Mascheroni constant. We use the notation that $\star$ denotes that the function in question is being evaluated at the time $x = x_\star$ as mentioned previously. This means that the variable is question is being evaluated at some time close to horizon crossing. The function $W(x)$ is given by

$$W(x) = \frac{3\sin(2x)}{2x^3} - \frac{9\cos(2x)}{x^2} - \frac{3\sin(2x)}{2x} \tag{5.16}$$

and hence

$$W'(x) = -\frac{9\sin(2x)}{2x^4} + \frac{9\cos(2x)}{x^3} + \frac{15\sin(2x)}{2x^2} - \frac{3\cos(2x)}{x}. \tag{5.17}$$

The function $xW'(x)$ is shown in Figure 5.1. This function arises by considering the real part of Equation (5.14), using the fact that e^{ix} introduces cosine and sine terms. The imaginary part of Equation (5.14) is found to be second order in the function g and so can be ignored. This $W'(x)$ function introduces oscillations into

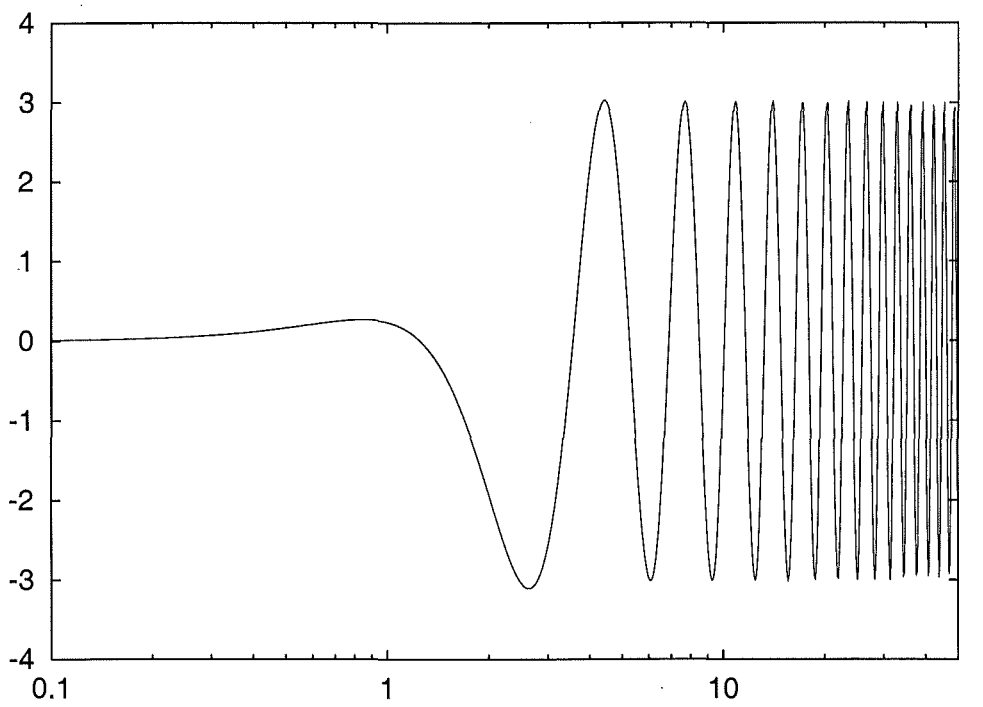

Figure 5.1: The evolution of the parameter $xW'(x)$. We can see that as x tends to zero, $xW'(x)$ tends to zero, and as x tends to infinity we find that $xW'(x)$ tends to $3\cos(2x)$

a power spectrum if there is some form of sudden change in the evolution of the inflationary potential. In standard inflationary scenarios the function $\ln(V'/V'_\star)$ will be proportional to u and hence the integral term here will be some constant related to this proportionality times the integral of $uW'(u)$. Evaluating the integral gives

$$\int_0^\infty uW'(u)\mathrm{d}u = 1. \tag{5.18}$$

This means in standard inflationary scenarios there is no oscillatory component to the power spectrum. In the case of a sudden change in the behaviour of the potential (such as a jump or a sudden derivative change) our integral term will

be able to be split into two parts, one for before the change and one for after the change. This means that we are not integrating simply from zero to infinity the function $uW'(u)$. The nature of the change will effect this integration which will be looked at in further detail in the following sections.

We consider Equation (5.15) term by term and then combine these terms to get the resultant power spectra. We split the equation into three terms as follows.

$$\begin{aligned} \textit{Power spectrum} = \ & \textit{Amplitude} \quad \times \\ & (1 + \textit{Slow roll correction} + \textit{Non-slow roll correction}), \end{aligned} \tag{5.19}$$

with

$$\begin{aligned} \textit{Amplitude} &= \frac{V_\star^3}{12\pi^2 V_\star'^2}, \\ \textit{Slow roll correction} &= \left(3\alpha - \frac{7}{6}\right)\frac{V_\star'^2}{V_\star^2}, \\ \textit{Non-slow roll correction} &= 2\int_0^\infty \mathrm{d}u\, W'(u) \ln\left(\frac{V'}{V_\star'}\right)\bigg|_{u=\frac{k}{aH}}. \end{aligned} \tag{5.20}$$

The *amplitude* term is just the standard inflationary result for the power spectrum given in Equation (3.37). The *slow roll correction* is a commonly used adjustment to take into account deviations in the power spectrum to first order in the slow roll parameters. The third term, the *non-slow roll correction* is only significant when slow roll is violated. This will be highly relevant to our later work when we consider discontinuities and breaks in slow roll. If the power spectrum obeys the slow roll conditions then the third term can safely be ignored.

It should be noted here that Equation (5.15) is not an exact solution. The assumptions of Equation (5.13) must be made to arrive at Equation (5.15), and so the assumptions are to first order equivalent to the slow roll assumptions made previously. Our solution is only valid to first order in these parameters. Some of the results from Equation (5.15) are not present in the other results for the power spectrum based on the slow roll approximation. Specifically the presence of the oscillatory term $W'(u)$ in the solution is of great importance. We will show

in Chapter 7 that oscillations in the primordial power spectrum can occur in the numerical solution to Equation (3.30), particularly when the inflaton potential has a sharp change in value or derivative.

5.2 Step potential

In Chapter 4 we mentioned the possibility of having a step in the inflationary effective potential. We will detail two ways of modelling such a step, and use the results from the previous section to obtain the primordial power spectrum in each case. For our potential we can firstly use an instantaneous step, which is a piecewise function with two slow roll periods which is discontinuous at one point. As we explained in Chapter 4 we do not expect an instantaneous change in potential. Instead we expect any drop in the potential to occurs over some finite but small range of the potential $\Delta\phi$. This results in a short period during which the slow roll conditions potentially do not apply, but remain continuous and finite.

5.2.1 Instantaneous Drop in Potential

We will calculate a solution to Equation (5.15) for the power spectrum in the case that we have an instantaneous drop in the inflaton potential. We are making the assumption that away from the point at which the step occurs, the potential is a well behaved slowly rolling potential. The form of potential we consider in this case is

$$V(\phi) = \begin{cases} V_0(\phi) + c & \phi > \phi_{step} \\ V_0(\phi) & \phi \leq \phi_{step} \end{cases} . \tag{5.21}$$

Here we have chosen the function $V_0(\phi)$ as some underlying slow roll potential such as $V_0(\phi) = \frac{1}{2}m^2\phi^2$ and c is the size of the drop in the potential. We will see that while the specific details of the function $V(\phi)$ are important, how exactly they

arise in the equations is generally in terms of the slow roll parameter $\epsilon_V = V_0'/V_0$. The equation for the potential can be rewritten in terms of the Heaviside Step function (a step function $S(x)$ being 0 when $x \leq 0$ and 1 when $x > 0$). We can also make a redefinition of the field $\phi \rightarrow \phi - \phi_{step}$, and correspondingly the potential $V_0(\phi) \rightarrow V_0(\phi + \phi_{step})$, so that the step occurs at the point $\phi = 0$. Doing this our potential becomes

$$V(\phi) = V_0(\phi) + cS(\phi). \tag{5.22}$$

Differentiating this equation we find that

$$V'(\phi) = V_0'(\phi) + c\delta(\phi). \tag{5.23}$$

Here $\delta(x)$ is the Dirac delta function defined as being zero at all points besides at the point $x = 0$. At $x = 0$ the Dirac delta function effectively has an infinitely large spike such that the integral

$$\int_{-\infty}^{\infty} \delta(x)\mathrm{d}x = \lim_{\theta \to 0} \int_{-\theta}^{\theta} \delta(x)\mathrm{d}x = 1. \tag{5.24}$$

This implies the derivative of the potential is exactly what we would expect for a slow roll potential $V_0(\phi)$ away from the point $\phi = 0$, and is poorly behaved at $\phi = 0$.

We can insert this result into Equation (5.15). We consider the three terms detailed in Equation (5.20) separately. To do this we must choose a value of x for which the power spectrum is being calculated. We choose here to evaluate the power spectrum about the point when $x_\star = 1$. Given our definition that $x = -k\tau$ we find that evaluation at $x_\star = 1$ implies that we are evaluating at the moment that the mode crosses the horizon, so when $k = aH$. We now have to calculate the value of ϕ at the time when the mode crosses the horizon. According to slow roll

$$\frac{\mathrm{d}\phi}{\mathrm{d}\ln(aH)} \approx \frac{\dot{\phi}}{H} \approx \frac{V_0'}{V_0}. \tag{5.25}$$

We know at the time of the step that $\phi|_{step} = 0$. At this time we denote that $aH|_{step} = k_{step}$. Physically this is the value of k which at is the point of horizon

crossing when the step takes place. Then Equation (5.25) gives us that

$$\phi_\star = \frac{V_0'(0)}{V_0(0)} \ln \frac{k_{step}}{k} = -\frac{V_0'(0)}{V_0(0)} \ln \kappa, \tag{5.26}$$

where we have introduced the notation $\kappa = k/k_{step}$. We have made the assumption here that the term $V_0'(\phi)/V_0(\phi)$ is roughly constant between $\phi = 0$ and $\phi = \phi_\star$. We can also relate u to ϕ using Equation (5.25)to give

$$\phi|_{aH=k/u} = \frac{V_0'(0)}{V_0(0)} \ln \kappa + \frac{V_0'(0)}{V_0(0)} \ln(u). \tag{5.27}$$

For the *amplitude* term we ignore the other two terms completely and just evaluate the *amplitude* as though our potential is just the smooth function $V_0(\phi)$. This gives us

$$Amplitude = \frac{V_{0\star}(\phi)^3}{12\pi^2 V_{0\star}'(\phi)^2} = \frac{V_0(\phi_\star)^3}{12\pi^2 V_0'(\phi_\star)^2}. \tag{5.28}$$

Here $\phi_\star$ is given by Equation (5.26). Similarly for the *slow roll correction* (which is proportional to the parameter ϵ) we are able to ignore the step part of the potential. This gives us that

$$Slow\ roll\ correction = \frac{V_{0\star}'(\phi)^2}{V_{0\star}(\phi)^2} = \frac{V_0'(\phi_\star)^2}{V_0(\phi_\star)^2}. \tag{5.29}$$

The *non-slow roll correction* is the one where the effect of the step will come into play. This happens in the form of a $\delta(\phi)$ term in the derivative. When integrating a delta function we use the result from distribution theory that

$$\int f(x)\delta(x - x_0)\mathrm{d}x = f(x_0) = \int f(x_0)\delta(x - x_0)\mathrm{d}x\,. \tag{5.30}$$

We wish to write the integral from Equation (5.15) as an integral of ϕ.

We are only interested in one value of u, and that is the value of u that occurs at $\phi = 0$. At this point, we have that $aH|_{step} = k_{step}$ and so we just have that

$$u = \frac{k}{k_{step}} = \kappa \qquad \text{and} \qquad \frac{\mathrm{d}u}{\mathrm{d}\phi} = \frac{V_0(0)}{V_0'(0)}\kappa. \tag{5.31}$$

This means that the integral becomes

$$\begin{aligned} \textit{Non-slow roll Correction} &= 2\int_0^\infty \mathrm{d}u\, W'(u) \ln\left(\frac{V'}{V'_\star}\right)\Big|_{u=\frac{k}{aH}} \\ &= 2\int_{-\infty}^\infty \mathrm{d}\phi \frac{V_0}{V'_0}\kappa W'(\kappa) \ln\left(\frac{V'}{V'_\star}\right)\Big|_{u=\frac{k}{aH}} . \end{aligned} \quad (5.32)$$

The logarithmic term in this equation can be simplified using the fact that

$$\ln\left(\frac{V'}{V'_\star}\right) \approx \ln\left(\frac{V'_0 + V_0 c\delta(\phi)}{V'_0}\right) \approx \frac{V_0}{V'_0} c\delta(\phi). \quad (5.33)$$

Inserting this result into Equation (5.32) we can evaluate our integral quite simply. We simply evaluate everything inside the integral at the point $\phi = 0$ because of the presence of the delta function to give

$$\textit{Non-slow roll correction} = 2c\left(\frac{V_0}{V'_0}\right)^2 \kappa W'(\kappa). \quad (5.34)$$

This is simply some coefficient $(2c\epsilon_V)$ multiplied by the term $\kappa W'(\kappa)$ which was plotted in Figure 5.1. Hence because $\kappa W'(\kappa)$ tends to $3\cos(2\kappa)$ as κ is greater than 1, our *non-slow roll correction* leads to oscillations in $\mathcal{P}_\mathcal{R}(k)$ of amplitude $6c\epsilon_V$.

We have now described the entire integral in terms of κ and the field ϕ, which we can relate to κ using the Equation (5.25). Using this we can combine all the terms together to get what the power spectrum should look like for a potential given by Equation (5.21),

$$\mathcal{P}_\mathcal{R}(\kappa) = \frac{V_0^3(\phi)}{12\pi^2 V_0'^2(\phi)} \left\{ 1 + \left(3\alpha - \frac{7}{6}\right)\frac{V_0'^2(\phi)}{V_0^2(\phi)} + 2c\left(\frac{V_0(0)}{V'_0(0)}\right)^2 \kappa W'(\kappa) \right\}. \quad (5.35)$$

Using this equation we can calculate the power spectrum for a given background potential V_0, step size c and step position in ϕ and k.

To look at this further we need a form of potential to work as a background for the step. We choose to use the simple potential $V_0(\phi) = 1/2m^2\phi^2$. We set $m = 10^{-5}$ and $\phi_{step} = 2.45M_P$. The amplitude of this (which is related to m^2)

is chosen to give us results for the amplitude of density fluctuations which are consistent with CMB observations. Our value for ϕ is chosen so that the region of density perturbations we are considering corresponds to one that is physically observable. We obtain power spectra as shown in Figure 5.2 for various step sizes.

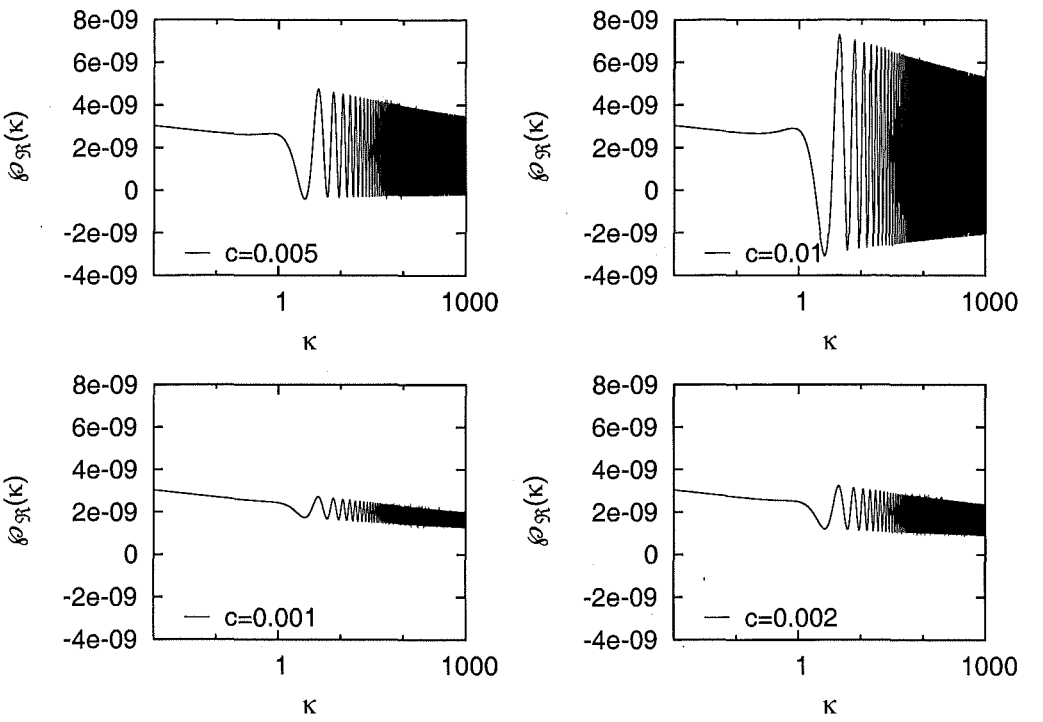

Figure 5.2: Power spectrum from an instantaneous drop in the inflationary effective potential. These plots are for $V_0(\phi) = 1/2m^2\phi^2$, with $m = 10^-5$, $\phi_{step} = 2.45M_P$ for various values of the constant c.

This method of calculating the power spectra has an obvious deficiency, which arises when using our result in cases when the slow roll conditions are not valid. The power spectrum is defined by $\mathcal{P}_{\mathcal{R}} \propto |u_k/z|^2 > 0$ and hence must always be a positive quantity. Any negative values immediately show that the solution is incorrect. The negative values arise from the *non-slow roll correction* term. This is expected to be much less than one based on the slow roll assumptions. If it takes on values of the order of one then it dominates the bracketed part of

Equation (5.15) which the way the formula is derived should be of the form "one plus some small corrections that are much less than one".

We note that in the case of an instantaneous drop in the inflaton potential, the power spectra resulting from this will have oscillations on all scales with $k > k_{step}$. This is because the quantity $xW'(x)$ looks like $3\cos(2x)$ as $x \gg 1$. This corresponds to having oscillations present on all length scales smaller than the size of the horizon at the time of the step in the potential.

We can understand why an instantaneous step generates oscillations on all scales k smaller than k_{step} by looking at Equation (3.30). Because we have an instantaneous step, the term $(k^2 - z''/z)$ at the instant of the step is completely dominated by the z''/z term, which is infinite at the time, regardless of what k value we are looking at. The effect of this is to generate a new set of initial conditions at $\phi = \phi_{step}$ instead of those given by Equation (3.31). These initial conditions are independent of the value of k we are considering, provided we are in the oscillating mode solution regime (with $k \gg z''/z$ around the time at which the step occurs). It is these initial conditions that result in the oscillatory behaviour on all $k > k_{step}$.

The presence of oscillations on all scales does not fit current observational evidence. However, we did not expect an instantaneous step to be physically reasonable. Our motivation for considering a step in the inflaton potential is that we believe there will be phase transitions in fields which interact with the inflaton. This will cause rapid changes in the inflaton potential. We note that from Chapter 4 we do not expect these phase transitions to occur instantaneously, but for them to be spread over some short time, during which time the inflaton potential will change accordingly. The driving term for the oscillations that occurred for the case with an instantaneous step is the z''/z term in Equation (3.30). In the case of a non instantaneous step (which now acts over some small range of ϕ), z''/z takes on very large positive and negative values but will remain finite for the duration of the step. Hence the value of $k - z''/z$ during the step is still influenced by

the value of k and so the new set of initial conditions after the step occurs will be dependent on k. For instance if z''/z briefly becomes 100 times its normal value, this would have little effect on the mode evolution for a mode which would otherwise have had $k = 1000z''/z$ at the time of the step. This mode is well inside the horizon at the time of the step, and so we expect some amount of damping, so that modes near the step are affected but not those much smaller than the horizon at the time of the step.

5.2.2 Continuous drop in potential

The method for generating steps in the inflaton potential which was outlined in Chapter 4 does not predict instantaneous drops in the inflaton potential, but that drops in the potential will occur over some finite range of ϕ. To model this numerically we need to use a function that approximates such a step. We choose here and in the numerical work in Chapter 6 to approximate our step using a $\tanh(\gamma\phi)$ term. This tends to a slightly different form of a step function to a Heaviside Step Function in the limit that γ tends to infinity. As $\gamma\phi \ll 0$, $\tanh(\gamma\phi) \leftarrow -1$, and as $\gamma\phi \gg 0$, $\tanh(\gamma\phi) \leftarrow 1$ as shown in Figure 5.3. We will show later that in the limit that $\gamma \rightarrow \infty$ the solution tends to the solution in the previous section. $\mathrm{Tanh}(\gamma\phi)$ is a convenient function to use as it is smooth and continuous. The results from this are indicative of what we would expect from any other function that approximates a step. The results depend on the derivative of the step, which takes on large positive values regardless of the exact form of the step. The results also depend on the second derivative of the step which will take on very large positive and negative values over the course of any form of step chosen. What specific large values they take on depends on the particular step function used, but the general form is the same for all possible step functions.

For our potential we again choose to insert a step into an otherwise slow roll

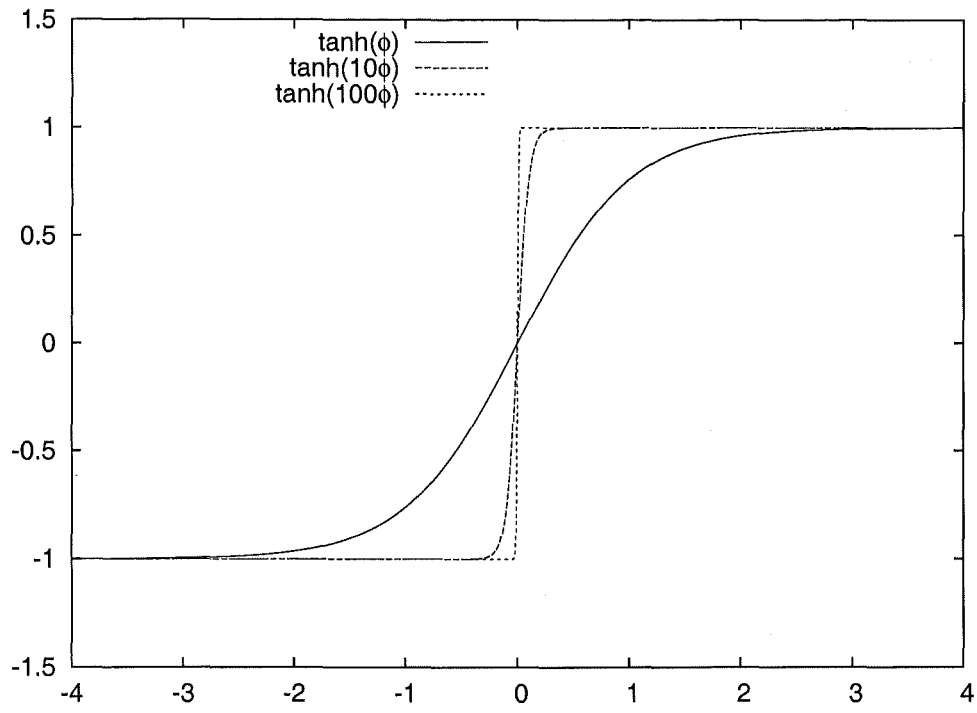

Figure 5.3: The function $\tanh(\gamma\phi)$. We show values of γ of $1, 10$, and 100. We see that for increasing γ the function becomes more and more like an instantaneous step.

potential. We choose to use a potential of the form

$$V(\phi) = V_0(\phi)\,(1 + c\tanh(\gamma\phi)) \tag{5.36}$$

where $V_0(\phi)$ is our underlying slow roll potential function. We require for realistic models that $c \ll 1$ so that we are only dealing with a small jump in the underlying potential. Also in general we want that $\gamma \gg 1$ so that the dip occurs suddenly compared to the slow rolling $V_0(\phi)$.

To solve for this system we insert this potential into Equation (5.15). The first two terms behave in the same way as they did for the instantaneous potential case. The third term again is the one where the step in the potential will have a significant effect, and is where the presence of the tanh function will need to be considered in detail. We again evaluate at the point $x_\star = 1$ and hence $k = aH$ and $\phi_\star = -(V_0'(0)/V_0(0)) \ln \kappa$. Firstly we will simplify the logarithmic part of the

non-slow roll correction for the potential we are considering. We can expand our logarithmic term to first order, bearing in mind that

$$1 \gg \left(\frac{V_0}{V_0'}\frac{c\gamma}{\cosh^2(\gamma\phi)}.\right) \gg c\tanh(\gamma\phi), \tag{5.37}$$

to give

$$\begin{aligned}\ln\left(\frac{V'}{V'_\star}\right)\Big|_{u=\frac{k}{aH}} &= \ln\left(\frac{V_0'(\phi)\left(1+c\tanh(\gamma\phi)+\left(\frac{V_0(\phi)}{V_0'(\phi)}\frac{c\gamma}{\cosh^2(\gamma\phi)}\right)\right)}{V'_{0\star}}\right)\Bigg|_{u=\frac{k}{aH}} \\ &\approx \frac{V_0(0)}{V_0'(0)}\frac{c\gamma}{\cosh^2(\gamma\phi)}\Big|_{u=\frac{k}{aH}}.\end{aligned} \tag{5.38}$$

Here we have made the approximation that because c is small and the field is slowly rolling we can set $V_0'(\phi) \approx V_0'(\phi_\star) \approx V_0'(0)$ especially around the time at which the step is occurring and hence when the $1/\cosh^2$ term is important.

Again we can relate ϕ to u by using

$$\phi|_{aH=k/u} = \frac{V_0'}{V_0}\ln\kappa + \frac{V_0'}{V_0}\ln\left(\frac{k}{aH}\right) = \frac{V_0'}{V_0}\ln\kappa + \frac{V_0'}{V_0}\ln u \tag{5.39}$$

to find that our integral term becomes

$$\begin{aligned}&2\int_0^\infty \mathrm{d}u\, W'(u)\ln\left(\frac{V'}{V'_\star}\right)\Big|_{u=\frac{k}{aH}} \\ =\ &2\int_0^\infty \mathrm{d}u\, W'(u)\,\frac{V_0(0)}{V_0'(0)}\frac{c\gamma}{\cosh^2(\gamma\phi)}\Big|_{u=\frac{k}{aH}} \\ =\ &2\frac{V_0(0)}{V_0'(0)}\gamma c\int_0^\infty \mathrm{d}u\, W'(u)\Big/\left\{\cosh^2\left[\gamma\left(\frac{V_0'(0)}{V_0(0)}\ln\kappa+\frac{V_0'(0)}{V_0(0)}\ln u\right)\right]\right\}.\end{aligned} \tag{5.40}$$

We make the change of variables

$$p = \gamma\left(\frac{V_0'(0)}{V_0(0)}\ln\kappa + \frac{V_0'(0)}{V_0(0)}\right)\ln u \tag{5.41}$$

to get

$$\begin{aligned}&2\frac{V_0(0)}{V_0'(0)}c\gamma\int_0^\infty \mathrm{d}u\, W'(u(p))\frac{1}{\cosh^2(p)} \\ =\ &2\frac{V_0(0)}{V_0'(0)}c\gamma\int_{-\infty}^\infty \mathrm{d}p\,\frac{\kappa V_0(0)}{\gamma V_0'(0)}e^{\frac{V_0(0)p}{\gamma V_0'(0)}}W'\left(\kappa e^{\frac{pV_0(0)}{\gamma V_0'(0)}}\right)\frac{1}{\cosh^2(p)}\end{aligned} \tag{5.42}$$

We can expand W' in terms of sine and cosine terms and making the assumption that $V_0/\gamma V_0'$ is large we find that Equation (5.42) simplifies to

$$2\frac{V_0(0)}{V_0'(0)}c\gamma\frac{V_0(0)}{\gamma V_0'(0)}\int_{-\infty}^{\infty}\mathrm{d}p\left[(k/k_0)W'(k/k_0)\cos\left(\frac{2pV_0(0)}{\gamma V_0'(0)}(k/k_0)\right)\right.$$
$$\left.+3\sin(2(k/k_0))\sin\left(\frac{2pV_0(0)}{\gamma V_0'(0)}\right)\right]\frac{1}{\cosh^2(p)}. \qquad (5.43)$$

Most of this equation is now independent of p and can be taken outside the integral to give

$$2\left(\frac{V_0(0)}{V_0'(0)}\right)^2 c\left[(k/k_0)W'(k/k_0)\int_{-\infty}^{\infty}\mathrm{d}p\cos\left(\frac{2pV_0(0)}{\gamma V_0'(0)}k/k_0\right)\frac{1}{\cosh^2(p)}\right.$$
$$\left.+\,3\sin(2(k/k_0))\int_{-\infty}^{\infty}\mathrm{d}p\sin\left(\frac{2pV_0(0)}{\gamma V_0'(0)}\right)\frac{1}{\cosh^2(p)}\right]. \qquad (5.44)$$

The second of these integrals vanishes as it is an odd function, while first term can be evaluated exactly [30] and is

$$4c\left(\frac{V_0(0)}{V_0'(0)}\right)^2(k/k_0)W'(k/k_0)\left[\frac{(k/k_0)V_0(0)\pi/\gamma V_0'(0)}{\sinh((k/k_0)V_0(0)\pi/\gamma V_0'(0))}\right]. \qquad (5.45)$$

This is the third term in our equation for the power spectrum. This third term can be considered as three distinct parts. Firstly the $4c\left(\frac{V_0(0)}{V_0'(0)}\right)^2$ term is like an amplitude term, saying how big the oscillations are going to be. The second term is of the form $xW'(x)$, an oscillatory term with maximum value 3 and minimum value -3 as shown in Figure 5.1. The third term is a damping term of the form $y/\sinh(y)$ which takes the value 1 when y is small and lowers to 0 as y becomes large. The behaviour of $\sinh(Ay)/(Ay)$ for different values of A is shown in Figure 5.4, where it can be seen the larger the value of A the larger y must be before the damping occurs.

We can now evaluate the whole of Equation (5.15) to find the power spectrum

$$\mathcal{P}_{\mathcal{R}}(k) = \frac{V_0^3(\phi)}{12\pi^2V_0'^2(\phi)}\left\{1+\left(3\alpha-\frac{7}{6}\right)\frac{V_0'^2(\phi)}{V_0^2(\phi)}\right. \qquad (5.46)$$
$$\left.+4\left(\frac{V_0(0)}{V_0'(0)}\right)^2 c(k/k_0)W'(k/k_0)\left[\frac{(k/k_0)V_0(0)\pi/\gamma V_0'(0)}{\sinh((k/k_0)V_0(0)\pi/\gamma V_0'(0))}\right]\right\}.$$

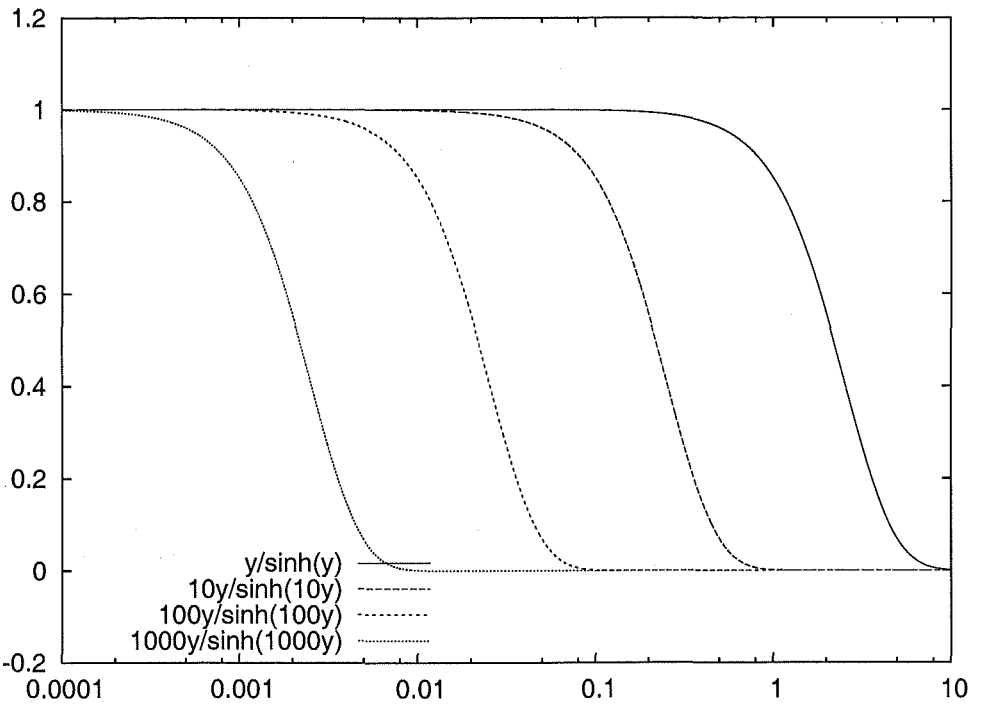

Figure 5.4: The function $Ay/\sinh(Ay)$. We plot this with various values of A. The larger the value of the constant A the larger the value of y required for the function to drop from being ≈ 1 to ≈ 0

One interesting feature in this is that the second term is inversely proportional to the third. The *slow roll correction* dictates what overall slope the power spectrum will have, and the third the amplitude of the oscillations. Hence the smaller the slope of the power spectrum (the closer the power spectrum is to a flat line) the larger the amplitude of any oscillations due to a step in the potential. Because V_0/V_0' also occurs in the $y/\sinh(y)$ term this means that the oscillations will dampen more quickly for a lesser gradient primordial power spectrum. Finally note that the size of the deviation from a potential without a step present has maximum value of (using the facts $-3 \leq xW'(x) \leq 3$ and $x/\sinh(x) \leq 1$)

$$-12c(V_0(0)/V_0'(0))^2 \leq \frac{\mathcal{P}_{\mathcal{R}}(k) - P_R(k)_{\text{no step}}}{\mathcal{P}_{\mathcal{R}}(k)_{\text{no step}}} \leq 12c(V_0(0)/V_0'(0))^2. \qquad (5.47)$$

This can give us an idea of when this solution will become impossible. If we have

$$12c(V_0(0)/V_0'(0))^2 \geq 1 \tag{5.48}$$

then the third term will become larger than the 1 inside the brackets of Equation (5.15) and so the power spectrum will become negative.

Chapter 6

Numerical solution of the perturbation evolution equations

In this chapter we present a technique for solving this system of equations for the power spectrum numerically. We apply this technique to several models of inflation with potentials that obey the slow roll conditions. The resulting power spectra are compared to Equation (3.37), which is an analytic solution for the power spectra under the slow roll approximation. We see that when the slow roll approximation is valid the results are in good agreement. We also look at a potential which has a period where slow roll is violated. For this potential we find the slow roll approximation to disagree with the numerical solution.

6.1 Numerical method

The evolution of perturbations in the inflationary scenario was shown in Chapter 3 to be given by

$$u_k'' + \left(k^2 - \frac{z''}{z}\right) u_k = 0. \tag{6.1}$$

This implies that for a given scale size k, the effect of a step in the potential on u_k will be due to the resulting deviation in the value of the $k^2 - z''/z$ term from its slow roll value. We can write z''/z as a function of the slow roll parameters

$$\frac{z''}{z} = 2a^2H^2(1 + \epsilon - \frac{3}{2}\eta + \epsilon^2 - 2\epsilon\eta + \frac{\eta^2}{2} + \xi^2), \tag{6.2}$$

where

$$\xi^2 \equiv \frac{M_P^2}{4\pi}\frac{H_{,\phi\phi\phi}H_{,\phi}}{H}. \tag{6.3}$$

Here and throughout this chapter subscripts after commas are used to denote derivatives. While this equation (6.2) looks like it is only written to second order in the slow roll parameters, this is in fact an exact expression.

To look at this system in further detail we solve the background evolution of the scale factor $a(t)$ and inflaton field ϕ numerically. These equations mentioned in chapter (2) are

$$H^2 = \frac{8\pi G}{3}\left(\frac{1}{2}\dot{\phi}^2 + V(\phi)\right), \tag{6.4}$$

$$\frac{\ddot{a}}{a} = \frac{8\pi G}{3}(V(\phi) - \dot{\phi}^2), \tag{6.5}$$

and

$$\ddot{\phi} + 3H\dot{\phi} + V'(\phi) = 0. \tag{6.6}$$

Using this background solution we numerically solve equation (6.1) for the perturbations, which then gives us the resulting power spectrum. To achieve this we first parameterize the equations in terms of one variable. The intrinsic time scale of the dynamics is not constant in conformal time so we change the independent variable of the equations to $\alpha = \log(a)$. Derivatives can be rewritten in terms of α by making use of the relations

$$\frac{\mathrm{d}t}{\mathrm{d}\alpha} = \frac{1}{H} \qquad \text{and} \qquad \frac{\mathrm{d}\tau}{\mathrm{d}\alpha} = \frac{1}{He^{\alpha}}. \tag{6.7}$$

One can then recast the above equations in terms of α, which then allows the equations to be solved numerically for different values of k. The equations of motion of the field become

$$\phi_{,\alpha\alpha} + \left(\frac{H_{,\alpha}}{H} + 3\right)\phi_{,\alpha} + \frac{1}{H^2}V_{,\phi} = 0, \tag{6.8}$$

and

$$H_{,\alpha} = \frac{-4\pi}{M_p^2}H\phi_{,\alpha}^2, \tag{6.9}$$

We can also write the slow roll parameters of equations (2.11,2.12) in terms involving derivatives with respect to α to get

$$\epsilon = \frac{\dot{\phi}}{H} = \phi_{,\alpha} \tag{6.10}$$

$$\eta = \frac{\ddot{\phi}}{H\dot{\phi}} = \frac{\phi_{,\alpha\alpha}}{\phi_{,\alpha}} + \frac{H_{,\alpha}}{H}. \tag{6.11}$$

6.1.1 Scalar Modes

The equation for the evolution of the density perturbations (equation (3.30)) is then given by

$$\begin{aligned} 0 \;=\; & u_{k,\alpha\alpha} + \left(\frac{H_{,\alpha}}{H} + 1\right) u_{k,\alpha} + \\ & \left[\frac{k^2}{e^{2\alpha}H^2} - \left(2 - \frac{4H_{,\alpha}}{H}\frac{\phi_{,\alpha\alpha}}{\phi_{,\alpha}} - 2\left(\frac{H_{,\alpha}}{H}\right)^2 - \frac{5H_{,\alpha}}{H} - \frac{1}{H^2}V_{,\phi\phi}\right)\right] u_k. \end{aligned} \tag{6.12}$$

Being a second order differential equation, this has two independent solutions. We restrain the solution using the initial conditions for the mode when it is oscillating well inside the horizon. We set $\tau = 0$ in Equation (3.31) to give the initial conditions on u_k,

$$\begin{aligned} u_k|_{\tau=0} &= \frac{1}{\sqrt{2k}} \qquad \text{and} \\ \left.\frac{\mathrm{d}u_k}{\mathrm{d}\alpha}\right|_{\tau=0} &= \left.-i\sqrt{\frac{k}{2}}\frac{1}{e^{\alpha}H}\right|_{\tau=0}. \end{aligned} \tag{6.13}$$

We choose two orthogonal solutions to evolve,

$$\begin{aligned} u_k^1|_{\tau=0} &= 1, \\ \left.\frac{\mathrm{d}u_k^1}{\mathrm{d}\alpha}\right|_{\tau=0} &= 0 \qquad \text{and} \\ u_k^2|_{\tau=0} &= 0, \\ \left.\frac{\mathrm{d}u_k^2}{\mathrm{d}\alpha}\right|_{\tau=0} &= 1 \end{aligned} \tag{6.14}$$

and combine these in accordance with the conditions for each u_k at $\tau = 0$ to get the combined mode evolution

$$u_k = \frac{1}{\sqrt{2k}} u_k^1 - i\sqrt{\frac{k}{2}} \frac{1}{e^\alpha H}\bigg|_{\tau=0} u_k^2. \tag{6.15}$$

Our numerical method calculates the perturbation spectrum given a particular inflaton potential $V(\phi)$ and the first and second derivatives of the potential with respect to ϕ. This calculation is done using the Bulirsch-Stoer algorithm [53]. For each value of k, we first evolve the background equations (6.7,6.8,6.9) until the evolution of the background has settled but the mode is still well inside the horizon. We then evolve the perturbation equation with the background until the perturbation passes well outside the horizon. Initially with the mode well inside the horizon we observe the two modes u_k^1 and u_k^2 oscillating. These oscillations are orthogonal, which leads to the combined amplitude of the oscillations being constant. When the size of the mode inflates to be outside the horizon the modes cease their oscillations and grow proportional to z. This means that the curvature perturbation, which was found to be the ratio of u_k to z, is constant once the mode passes outside the horizon. The evolution of the individual modes and their combined amplitude is shown in figure (6.1).

The calculation is found to be independent of the point at which the evolution of the perturbations is started and finished, so long as their evolution is begun well inside the horizon and finished well outside. This confirms the convergence of the modes. We repeat the numerical solution for multiple k values to give the power spectrum. We compare the output from this to the slow roll approximation results in section (6.2).

6.1.2 Tensor Modes

The treatment of the tensor modes is similar to that of the scalar modes. The evolution of the background is the same as in the scalar mode case, governed by

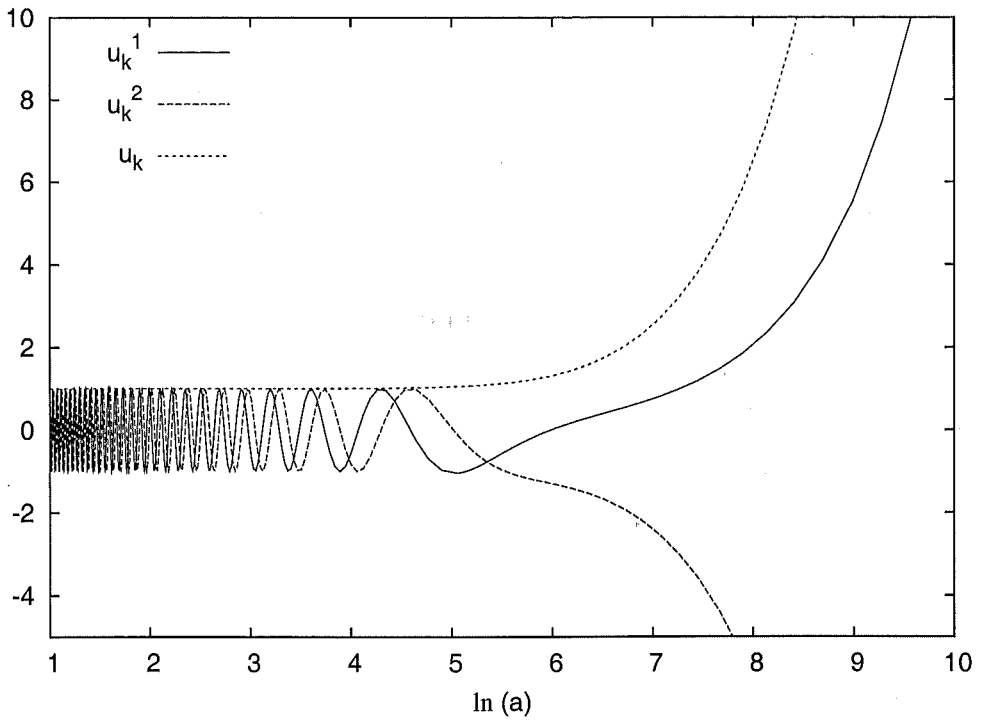

Figure 6.1: Here we show how the modes u_k^1, u_k^2 and the combined mode amplitude vary with the scale factor. We can see that as the mode passes outside the horizon the oscillations of the individual modes cease and the combined mode just grows exponentially

equations (6.8, 6.9). The mode evolution equation was given in chapter (3) to be

$$v_k'' + \left(k^2 - \frac{a''}{a}\right) v_k = 0. \tag{6.16}$$

Unlike the scalar mode case this does not have the same complication of having to convert z into a function of α. Hence the form of the equation when written in terms of α is the much more compact

$$0 = v_{k,\alpha\alpha} + \left(\frac{H_{,\alpha}}{H} + 1\right) v_{k,\alpha} + \left[\frac{k^2}{e^{2\alpha}H^2} - \left(\frac{H_{,\alpha}}{H} + 2\right)\right] v_k. \tag{6.17}$$

The numerical code we use to generate the tensor perturbation spectrum is therefore very similar to the one used in the case of the scalar modes. Modes are again seen to oscillate while inside the horizon. Once they grow to larger than horizon size they grow linearly with a to give a constant amplitude for the density perturbation $\mathcal{P}_\psi$.

6.2 Comparison between numerical solution and known slow roll inflation solutions

Here we consider forms of the inflationary potential that obey the slow roll conditions. We compare the primordial power spectrum given by the slow roll approximation with that resulting from the numerical solution of the perturbation and background equations. We do this for examples of both chaotic potentials (such as when the potential is a numerical constant multiplying the field to the power of some positive integer) as well as for a natural inflation potential where ϕ increases away from zero instead of evolving towards zero like in the chaotic potential case.

6.2.1 ϕ^2 Potential

This is an example of a chaotic inflationary potential. This potential is commonly used as it arises naturally in the Lagrangian of a scalar field as a mass term. We compare the output of the numerical code with that from slow roll. We use the slow roll result of Liddle and Lyth that the power spectrum is given by

$$\mathcal{P}_{\mathcal{R}}(k) = \frac{V^3}{12\pi^2 V'^2}\left[1 + \left(2\alpha - \frac{1}{6}\right)\epsilon_V + \left(-\alpha + \frac{1}{3}\right)\eta_V + \mathcal{O}(\epsilon_V^2, \eta_V^2)\right], \quad (6.18)$$

where $\alpha = 2 - \ln 2 - b \approx 0.7296$. We plot this prediction for the power spectrum against the numerical code in figure (6.2). We find that the difference between the slow roll result and the numerical result is less than 0.1%. The slow roll parameters in this case both have values of $\epsilon_V = \eta_V = 2/\phi^2$. We have chosen ϕ to be around $2.5M_P \approx 12.3$, which means our slow roll parameters will be less than 0.014. Given that we anticipate errors of the order of the slow roll parameters squared this leads to an error between the actual solution and the slow roll approximation of 0.02%.

One can easily extend this to look at any potential of the form ϕ^n, for n a

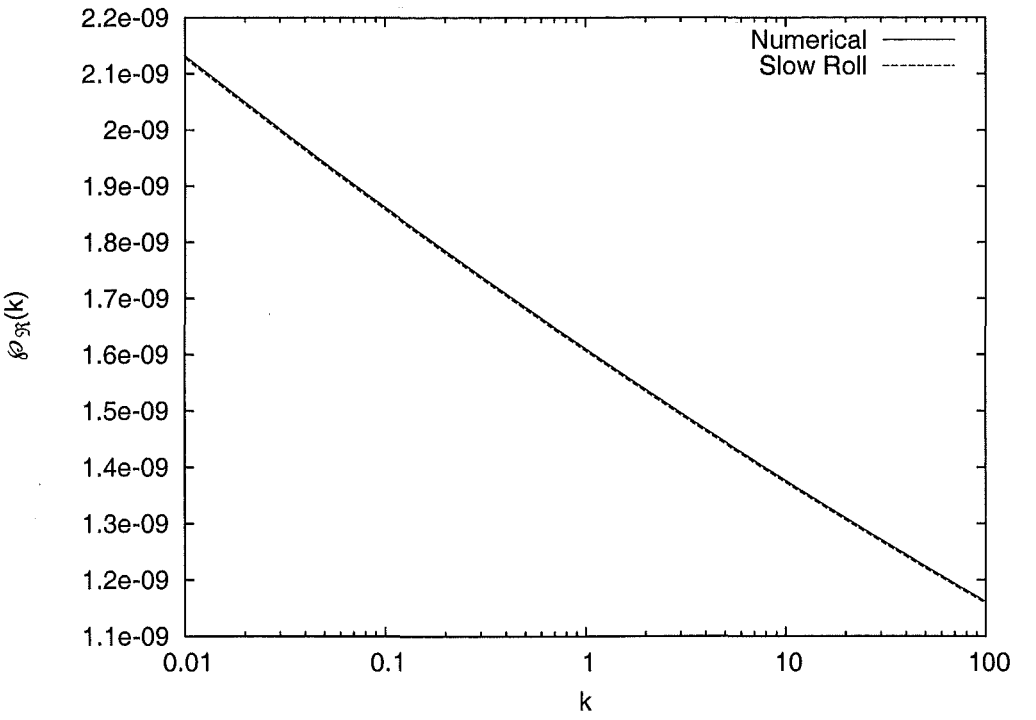

Figure 6.2: Here we plot the primordial power spectrum calculated numerically as well as that from the slow roll approximation given in equation 6.18.

positive integer. We can also apply our numerical technique to any other one field slow roll potential. We have also looked at the natural inflation model described by equation (2.23), for which we had similar agreement between the numerical code and the slow roll approximation.

6.2.2 $(1 + \phi^4)$ Potential

This potential, a false vacuum quartic potential was first suggested in 1995 by Roberts et al. [55]. The potential effectively has two variables, an overall amplitude and a relative amplitude of the ϕ^4 term to the constant term.

$$V(\phi) = A(1 + B\phi^4) \tag{6.19}$$

The perturbation spectrum was looked at by Leach and Liddle [38] because it offers slow roll inflation in two distinct regions, separated by a period that is not slow roll. This can be understood by looking at the slow roll parameters and how they vary with ϕ. We consider here the slow roll parameters as functions of the potential as in equations (2.18). These take the values for this potential of

$$\epsilon_V \equiv \frac{1}{2}\left(\frac{V'}{V}\right)^2 = \left(\frac{4B\phi^3}{1+B\phi^4}\right)^2 \tag{6.20}$$

and

$$\eta_V \equiv \frac{V''}{V} = \frac{12B\phi^2}{1+B\phi^4}. \tag{6.21}$$

This leads to the power spectrum having two roughly scale invariant periods.

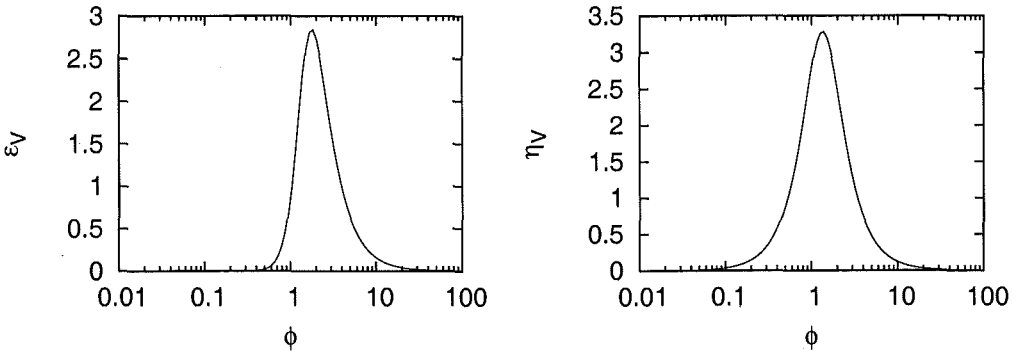

Figure 6.3: Here we show how the slow roll parameters vary with ϕ for a potential of the form $1+0.3\phi^4$. As you can see for ϕ above and below certain values we have slow roll but there is a range of ϕ for which slow roll cannot be assumed.

The amplitudes of these two regions can be estimated in terms of the slow roll approximation, recalling that

$$\mathcal{P}_{\mathcal{R}}(k) \approx \frac{V(\phi)^3}{12\pi^2 V'^2(\phi)} = \frac{A^3(1+B\phi^4)^3}{12\pi^2(4AB\phi^3)^2}. \tag{6.22}$$

These periods of slow roll are separated by a region in which the power spectrum undergoes highly scale-dependent behaviour. We plot the power spectrum for this potential in figure 6.4. The main feature of this potential is a sharp dip at the point where slow roll is violated, and then a rise from this point to where

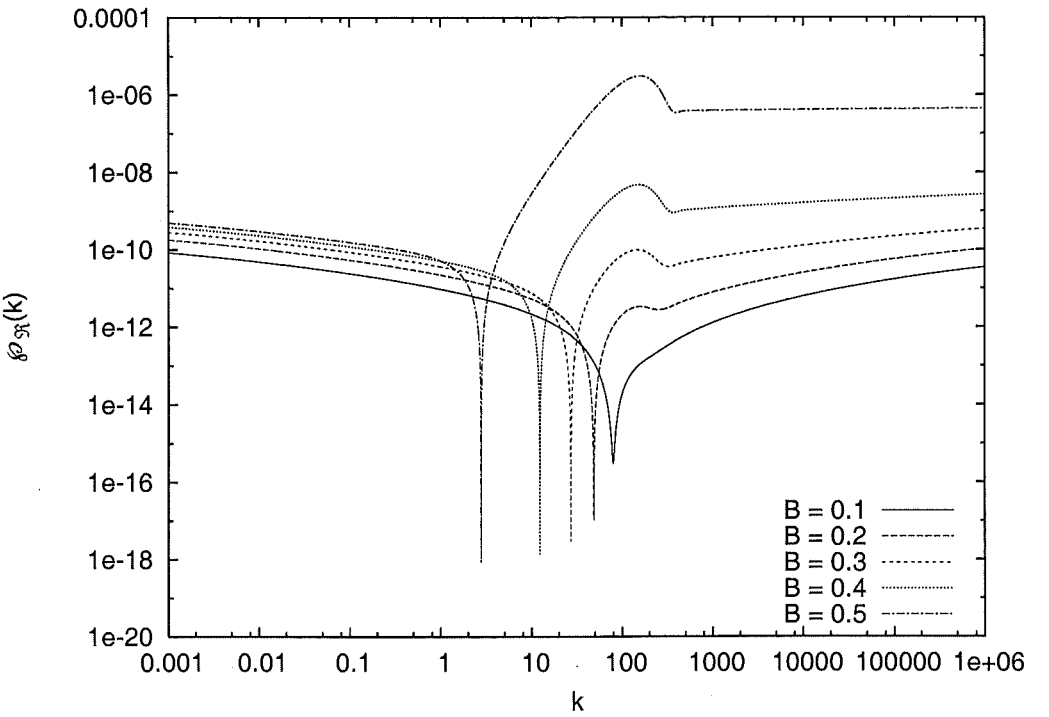

Figure 6.4: We can see here the resulting power spectrum from an $A(1+B\phi^4)$ type potential. Specifically here we choose $A = 10^{-12}$ and vary B as shown in the graph.

the potential settles into a new slow roll regime. The amplitudes of the power spectrum before and after the non-slow roll period are equal to their slow roll values. This can be seen in figure (6.5) where we have plotted for a particular value of B the slow roll approximations in terms of the hubble parameter ϵ and η and in terms of the potential, ϵ_V and η_V. We see that the two different slow roll approximations have different behaviours when slow roll cannot be applied. Both predict a dip in the power spectrum much later than is observed in the numerical case, and the formulation in terms of the hubble parameter has an extra dip in the power spectrum.

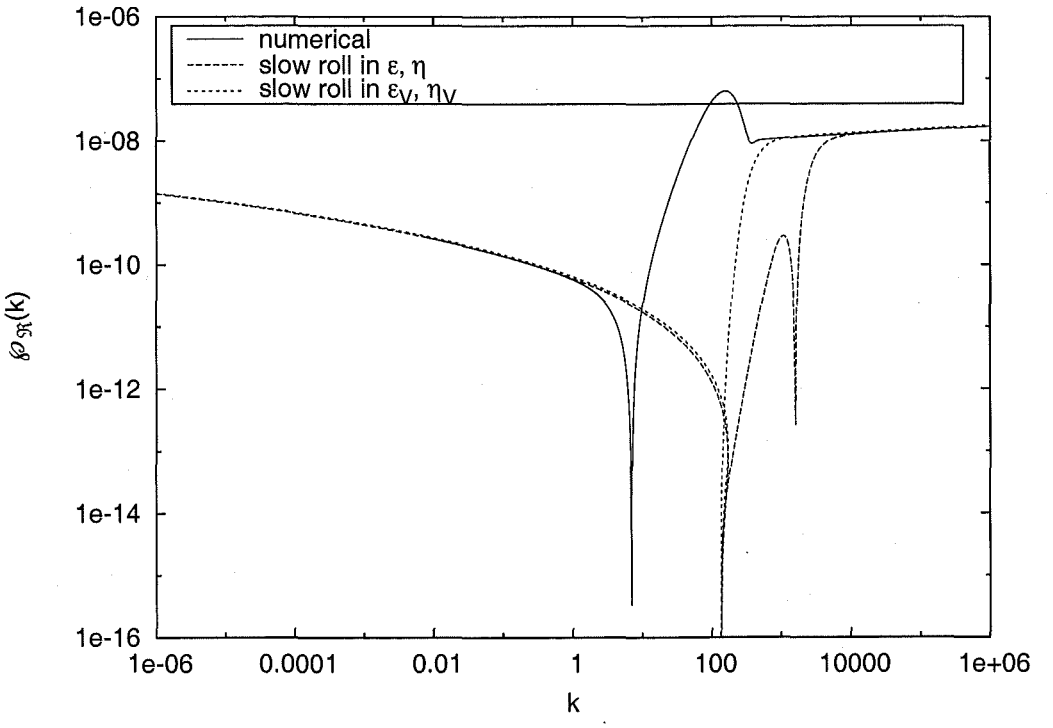

Figure 6.5: Here we plot the numerical solution for the power spectrum for a potential of the form $1 + 0.45\phi^4$ against the two slow roll solutions formulated in terms of ϵ, η and ϵ_V, η_V respectively.

Chapter 7

Numerical solution for an Inflationary step potential

We mentioned the possibility of having a sudden change in the inflaton potential in Chapter 4. This was based on the idea that a phase transition in a field coupled to the inflaton would cause a sudden change in the constants present in the Lagrangian of the inflaton. In Chapter 5 we determined the primordial power spectrum for an inflaton potential with a sudden step making some assumptions about the potential. We found this lead to some cases with negative power spectra and so the results had limited applicability. In this chapter we are going to use the numerical method developed in Chapter 6 to find the power spectrum resulting from a sudden drop in the inflaton potential. Physically this drop would not occur instantaneously but instead over some small range of ϕ.

We approximate the step in the inflaton potential by addition of a term involving $\tanh\gamma(\phi - \phi_{step})$ of a function of the field. $\tanh(\gamma x)$ is a continuous differentiable function that approximates a step from -1 to 1 in the limit that γ approaches infinity. The function tanh is not special in this regard and any differentiable function with the desired properties could have been chosen to approximate a step in the potential.

We choose a quadratic potential because a quadratic term appears very naturally as a mass term in the scalar field Lagrangian. It is also a mathematically simple potential to use. The form of the potential to which we add the step is

not qualitatively important as long as it approximates a slow roll potential. We shall detail later just what effect the form of the underlying potential has on the perturbed power spectrum. Far away from the presence of the step the effective potential looks as though it were slow roll, and just leads to a power spectrum with spectral index given by Equation (3.36). Into this potential we add a step term to get a potential of the form

$$V(\phi) = \frac{1}{2}m^2\phi^2\left[1 + c\tanh\left(\gamma(\phi - \phi_{step})\right)\right]. \tag{7.1}$$

Here the parameter ϕ_{step} dictates the position of the step in the potential function, c specifies the size of the step and γ the sharpness of the step. γ acts so that an *increase* in γ leads to a *more sudden* change in the value of the potential, that is a steeper step. This is exactly the potential we looked at in Chapter 5 when we were considering a continuous step in the field.

Figure 7.1 shows the power spectrum from the numerical code for the potential of Equation (7.1), for parameter values $\phi_{step} = 2.45M_p$ (M_p is the Planck mass), $c = 0.002$ (for 0.4% change in the value of the potential), and $\gamma = 1000$. Here it can clearly be seen that the presence of the step causes scale dependent oscillatory behaviour. The oscillation in k can be seen for an order of magnitude larger than the k value at which the step occurs (and so an order of magnitude smaller in size). There is an increase of a factor of 3 from the original power spectrum amplitude. We show the scale dependent oscillations in further detail in Figure 7.2 for several different values of c and γ and in all cases we see similar oscillatory behaviour in the power spectrum. Also we note that if we compare the oscillations on a linear k scale like in Figure 7.3 we find that the oscillations have approximately constant period and that the period of the oscillations is independent of the values of c and γ, but does depend on the k value at which $\phi = \phi_{step}$ occurs.

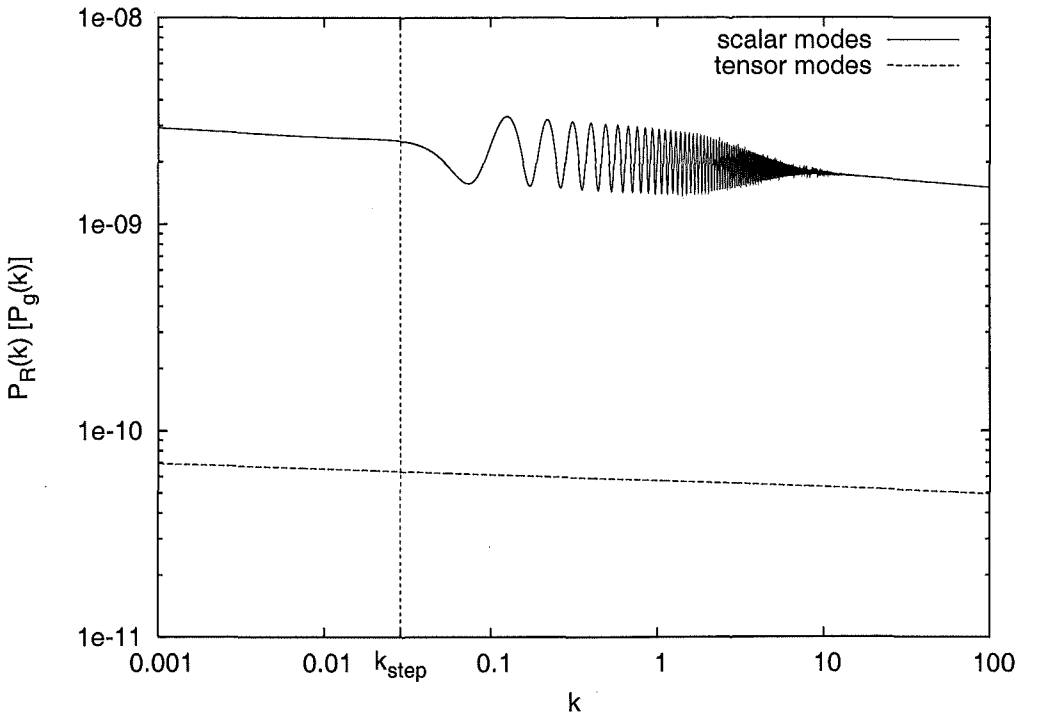

Figure 7.1: The scalar and tensor power spectra for a potential containing a step. The step size is only 0.4% but has a large effect on the resulting power spectrum (parameters are $c = 0.002$, $\gamma = 1000$). The tensor modes are also shown to be almost entirely unaffected by the presence of the step.

7.1 Slow roll violation

The slow roll parameters were defined by Equations (2.11), (2.12) and (2.18). We recall that there were two definitions, one in terms of the Hubble parameter and the time derivatives of the field ϕ, and the other in terms of the potential. Looking at the slow roll parameters written in terms of the potential $V(\phi)$, we find that for our particular step potential involving a tanh function that

$$\epsilon_V = \frac{1}{2}\left(\frac{V'}{V}\right)^2 = \frac{1}{2}\left(\frac{m^2\phi + \frac{1}{2}m^2\phi^2 c\gamma/\cosh^2(\gamma\phi)}{\frac{1}{2}m^2\phi^2\left[1 + c\tanh\left(\gamma(\phi - \phi_{step})\right)\right]}\right)^2 \tag{7.2}$$

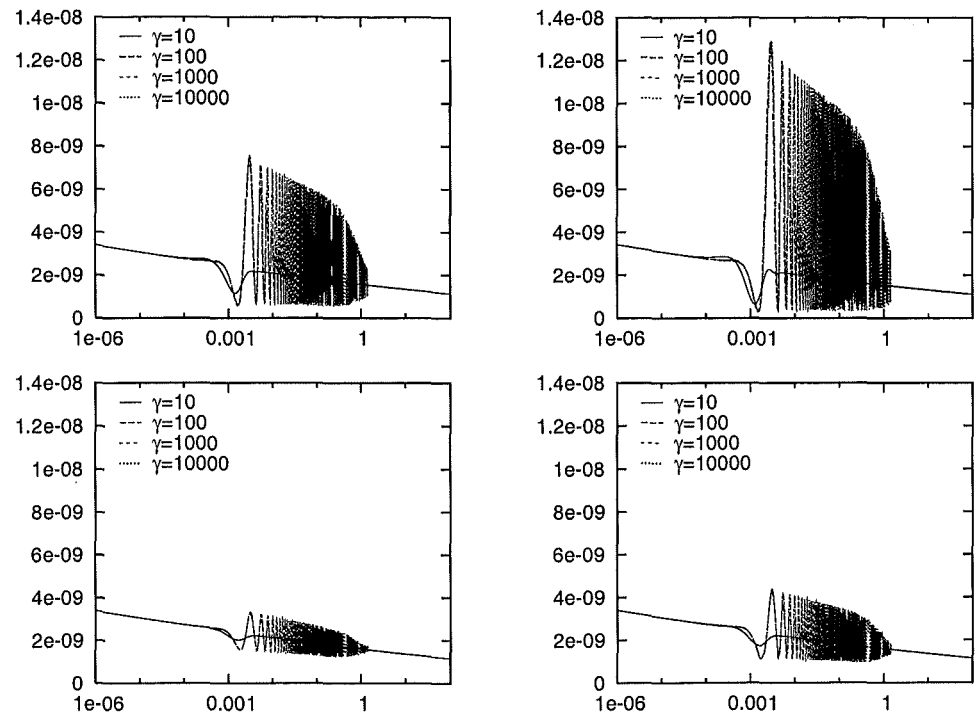

Figure 7.2: The variation in the power spectrum as the step parameters c and γ are varied. The number of coherent oscillations is shown to increase with γ but not depend on c. The size of the deviation from scale invariance increases with increasing c, and is unaffected by changing γ.

and

$$\eta_V = \left(\frac{V''}{V}\right) = \frac{\left[m^2 + 2m^2\phi c\gamma/\cosh^2(\gamma\phi) + \frac{1}{2}m^2\phi^2 c\gamma^2 \frac{\tanh(\gamma(\phi-\phi_{step}))}{\cosh^2(\gamma(\phi-\phi_{step}))}\right]}{\frac{1}{2}m^2\phi^2\left[1 + c\tanh\left(\gamma(\phi-\phi_{step})\right)\right]}. \quad (7.3)$$

This means that the slow roll parameters have maximum values that are approximately given by (looking only at the largest term in each equation)

$$\epsilon_{V\mathbf{MAX}} \approx \frac{1}{2}c^2\gamma^2 \qquad \text{and} \qquad \eta_{V\mathbf{MAX}} \approx c\gamma^2 \quad (7.4)$$

We plot the evolution of the slow roll parameters in Figure 7.4 for a step potential with $c = 0.001, \gamma = 1000$ and $\phi_{step} = 2.45M_{PL} \approx 12.28$. All the parameters are seen to deviate from the condition $\epsilon, \eta \ll 1$. This deviation lasts for less than one e-fold of inflation. Also the two definitions of the slow roll parameters have very

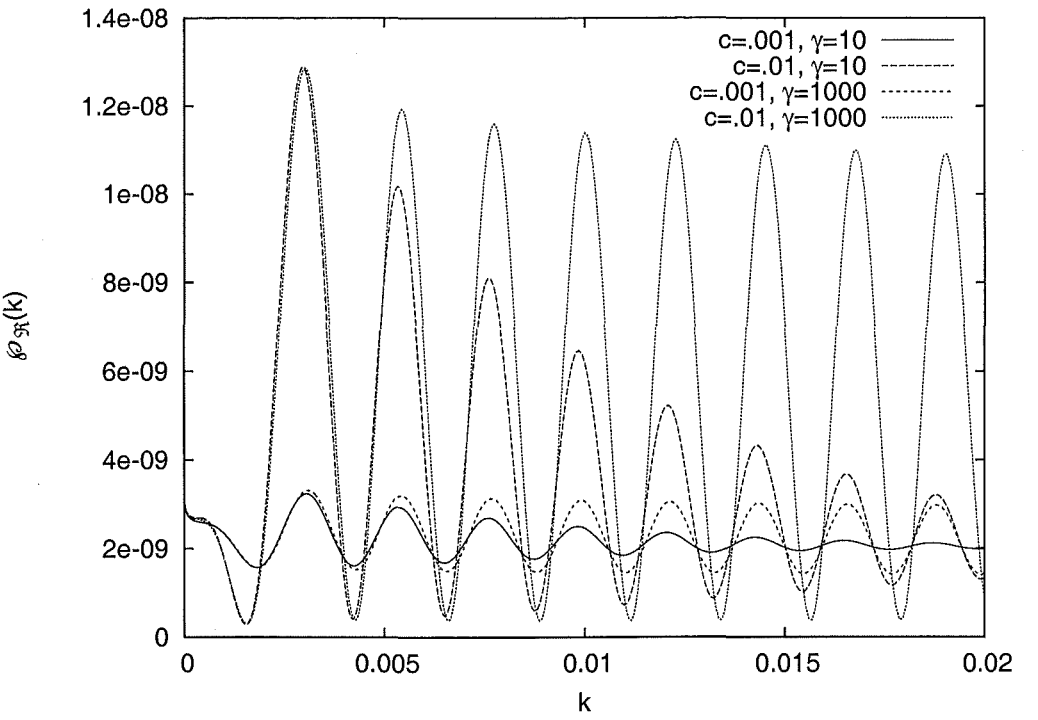

Figure 7.3: The power spectrum for different values of c and γ plotted on a linear scale with k. This shows that the scale dependent oscillations in each case have the same period independent of the values of c and γ.

different behaviour in the presence of a step. This is very different from during slow roll, when the two different definitions were seen to be simple multiples of one another.

7.2 The z''/z parameter

The presence of a step in the potential has a large impact on the value of the term z''/z in Equation (3.30). It is through this term that we can understand what is generating the oscillations in the power spectrum, and how the damping is dependent on the parameters c and γ that we have used to describe the size

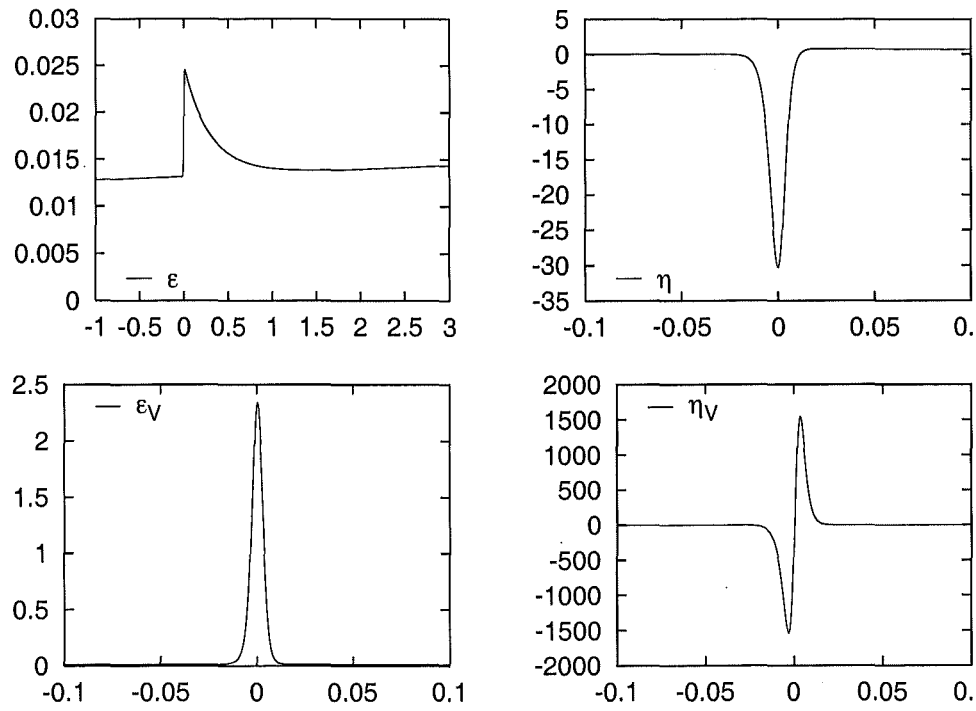

Figure 7.4: The evolution of the various forms of the slow roll parameters for an inflationary potential with a step, as a function of the number of e-folds from the position of the step. The behaviours are all markedly different from each other, as are the scales of their maxima/minima. We can still obey the slow roll condition $\epsilon \ll 1$ but have other slow roll parameters take on values much greater than 1.

and width of our potential step. We see from Equation (6.12) that

$$\begin{aligned}\frac{z''}{z}\frac{1}{2a^2H^2} &= \left(1-\frac{2H_{,\alpha}}{H}\frac{\phi_{,\alpha\alpha}}{\phi_{,\alpha}}-\left(\frac{H_{,\alpha}}{H}\right)^2-\frac{5H_{,\alpha}}{2H}-\frac{1}{2H^2}V_{,\phi\phi}(\phi)\right)\\ &= 1-2\epsilon\eta-\frac{5}{2}\epsilon^2-\frac{1}{2H^2}V_{,\phi\phi}. \end{aligned} \tag{7.5}$$

The last term in this equation can be related to the slow roll parameter involving the second derivative of the potential $V_{,\phi\phi}(\phi)/(2H^2) \approx 3\eta_V$ We can see in Figure 7.4 that when we have a step in the potential then $\eta_V \gg \epsilon\eta$, ϵ^2. Using this we can simplify Equation (7.5) at the time of the step to give

$$\frac{z''}{z}\frac{1}{2a^2H^2} \approx \frac{1}{2H^2}V_{,\phi\phi} \approx -3\eta_V. \tag{7.6}$$

We can see that the plot of η_V in Figure 7.4 has the same shape as the plot of $z''/z \times 1/2a^2H^2$ in Figure 7.5.

From this, considering only the largest term in $V_{,\phi\phi}(\phi)$ we see that for our step potential we can approximate z''/z by

$$\frac{z''}{z}\frac{1}{2a^2H^2} \simeq -\frac{m^2\phi^2c\gamma^2}{2H^2}\frac{\sinh\left(\gamma(\phi-\phi_{step})\right)}{\cosh^3\left(\gamma(\phi-\phi_{step})\right)}. \tag{7.7}$$

7.3 Uninterrupted accelerating expansion

Unlike other scenarios where features in the primordial power spectrum arise [38, 39], inflation is not halted by a step in the inflaton potential of the size we are considering here. Given that we define inflation in Chapter 2 as occurring when $\ddot{a} > 0$ it takes a much larger value of c than the values we have considered so far to halt inflation even momentarily. We can understand this by looking at the energies involved. Energy conservation requires the change in the inflaton kinetic energy can not exceed the change in the potential energy, which is given by $\Delta V(\phi)$ (this is done for a general potential step of size $V_i(\phi) - V_f(\phi) = \Delta V(\phi)$ (defined to be a positive quantity)). If we assume that during the step the Hubble

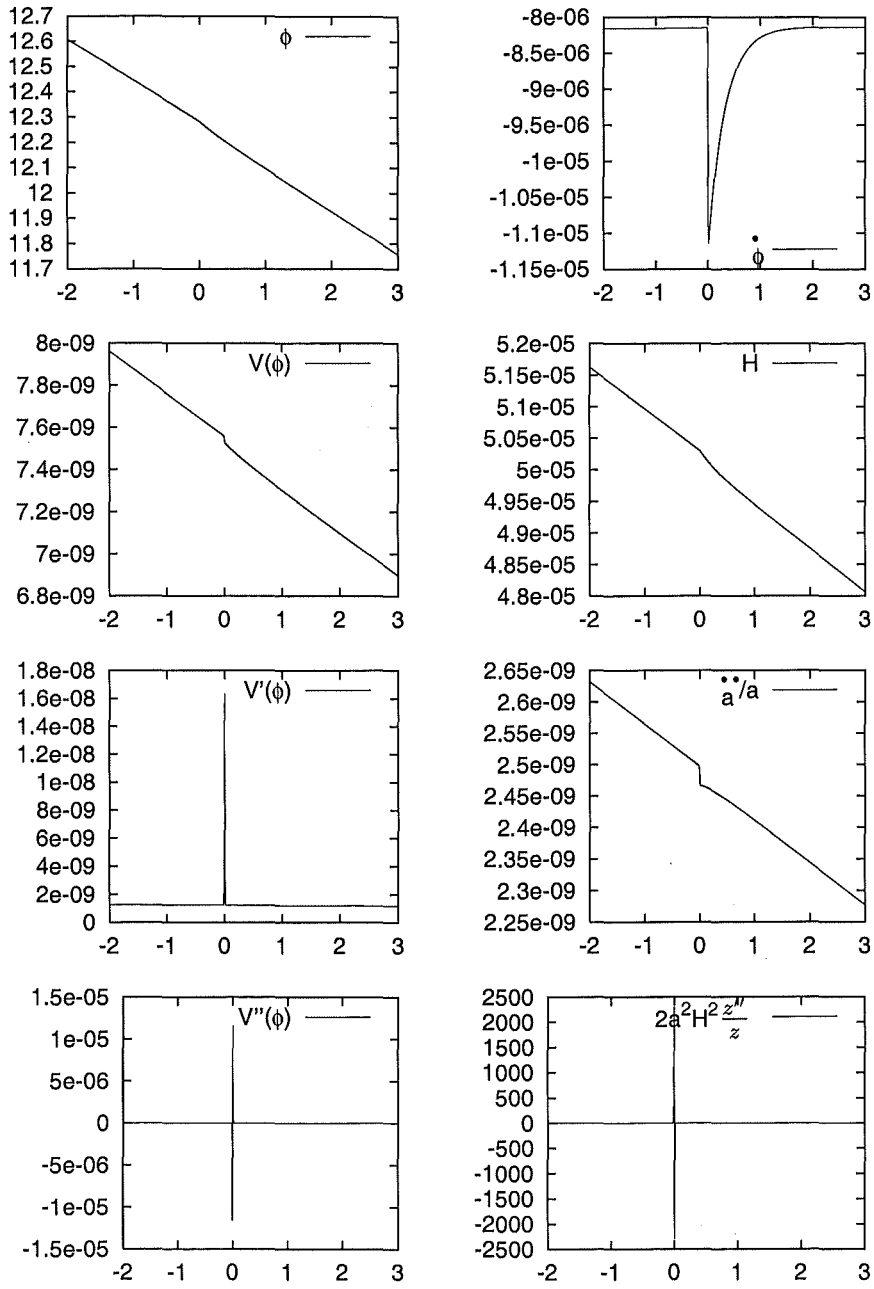

Figure 7.5: The evolution of some of the background parameters during a step in the inflaton potential. We show how these vary with the number of efolds from the position of the step. On the left hand side going down we plot $\phi, V(\phi), V'(\phi)$ and $V''(\phi)$, and on the right hand side we have from top to bottom $\dot{\phi}, H, \ddot{a}/a$ and $2a^2H^2(z''/z)$.

parameter H is constant then from Equation (2.5)), concerning the energy of the system, the quantity $\frac{1}{2}\dot{\phi}^2 + V(\phi)$ is constant. So if $V(\phi)$ falls by $\Delta V(\phi)$ then $\dot{\phi}^2$ increases by $2\Delta V(\phi)$. Inflation ends if the value of $\ddot{a}$ becomes negative, which we

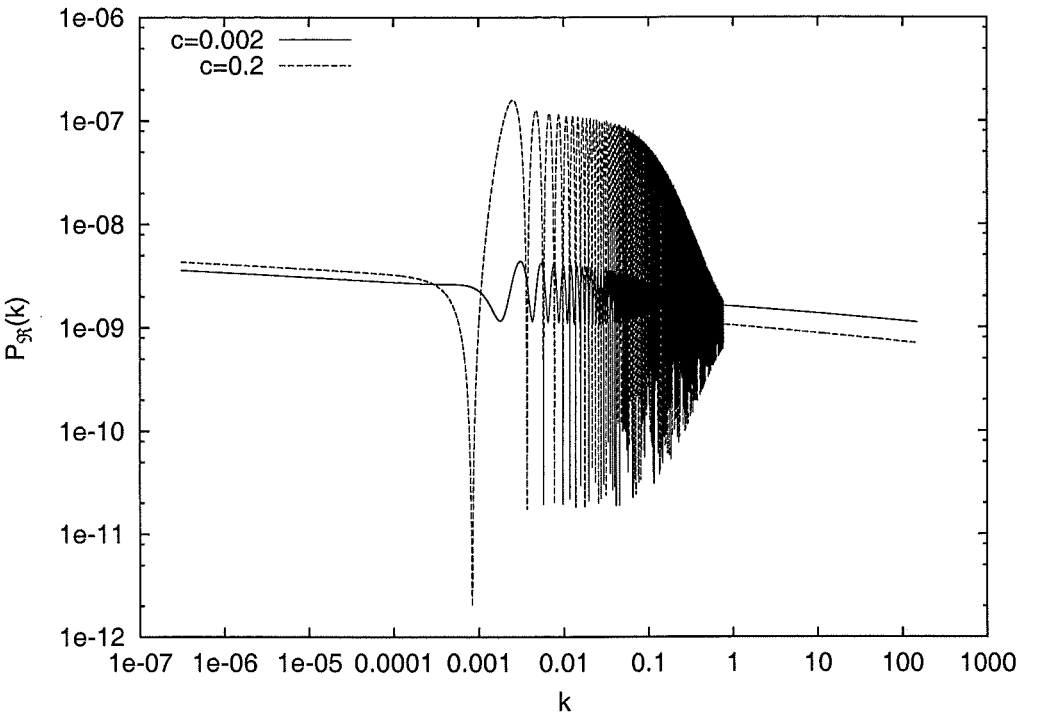

Figure 7.6: The change in the power spectrum required for a step in the potential to halt inflation. Here we have increased the value of c by a factor of 100 to $c = 0.2$, which leads to a 100 fold increase in the power spectrum.

can see from Equation (2.6) occurs if

$$\frac{\ddot{a}}{a} = \frac{8\pi G}{3}\left(V(\phi) - \dot{\phi}^2\right) < 0 \quad \Rightarrow \quad V(\phi) < \dot{\phi}^2. \tag{7.8}$$

We can make the assumption that

$$\dot{\phi}_i \ll \dot{\phi}_f. \tag{7.9}$$

This assumption follows from the fact that before the step in the potential we have slow roll. This means that because we assume the Hubble parameter is constant we have

$$\dot{\phi}_f \simeq 2\Delta V(\phi). \tag{7.10}$$

Using this in Equation (7.8) we find that inflation ends if

$$V_f(\phi) \leq 2\Delta V(\phi). \tag{7.11}$$

This result for a step ending inflation is model independent. It is true for any reasonably sudden step regardless of the particular form of the step or the background potential, making the assumptions that the background potential is slow roll, and the step rapid.

For our model with a tanh step we have

$$\begin{aligned} V_i(\phi) = &\quad (1+c)m^2\phi^2/2, \\ V_f(\phi) = &\quad (1-c)m^2\phi^2/2 \qquad \text{and} \\ \Delta V(\phi) = &\quad cm^2\phi^2. \end{aligned} \tag{7.12}$$

For inflation to end we require $c \geq 0.2$. Even such a large change in the potential is seen to halt inflation for a short time period (approximately 1/10 of an e-fold). The power spectrum resulting from such a potential is plotted in Figure 7.3. Were such a change present in the observable region of the inflaton potential, we would see huge features in the CMB power spectrum, and in the galaxy power spectrum. Such features have not been observed.

7.4 Source of coherent oscillations

Let us consider the origin of the oscillatory behaviour. To find the origin of the oscillations we consider the individual modes u_k^1 and u_k^2 separately. We look at the effect a step has on the evolution of each mode. For a given k without any step in the potential the modes are observed to oscillate orthogonally from their beginning. Once they reach the point where they cross outside the horizon (that is when $k = aH$) the modes go from oscillatory behaviour to exponentially growing behaviour, with this exponential growth being proportional to z. The amplitude each mode has during the exponential growth behaviour relative to z depends on

the point in their evolution they are at when $k = aH$. The orthogonal modes are out of phase when they begin growing and so their growth with z from this time is just related to their amplitude at the time that the mode passes outside the horizon. The combined amplitude is independent of the particular phase of each, and is constant during the oscillatory phase. This amplitude then grows proportional to z outside the horizon.

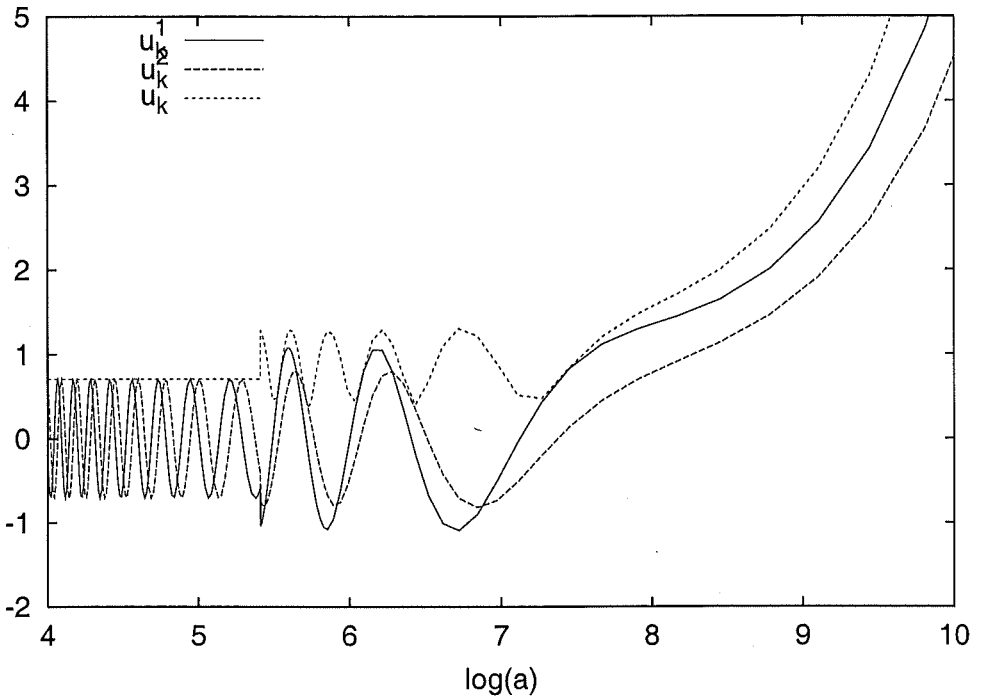

Figure 7.7: The evolution of the two modes u_k^1 and u_k^2, as well as the combined mode amplitude u_k, with number of e-folds of inflation. The two modes are initially orthogonal, but at the point of the step their amplitudes are altered so as to increase the combined amplitude, which then oscillates. It can be seen here that both individual modes are amplified, and that their phases are also altered by the presence of the step in the potential. This mode is seen to oscillate three times before entering the growing mode regime at a local maximum (both this and the following figure are for parameter values $m = 10^-5$, $\gamma = 0.0001$, $c = 0.005$, $\phi_{step} = 2.45 M_{pl}$ and $k = 8k_{step}$).

Now consider the case when a step is introduced in the potential. First we shall consider having a step after the mode has crossed outside the horizon. The mode is in the regime where it is evolving proportional to $|z|$, and hence the

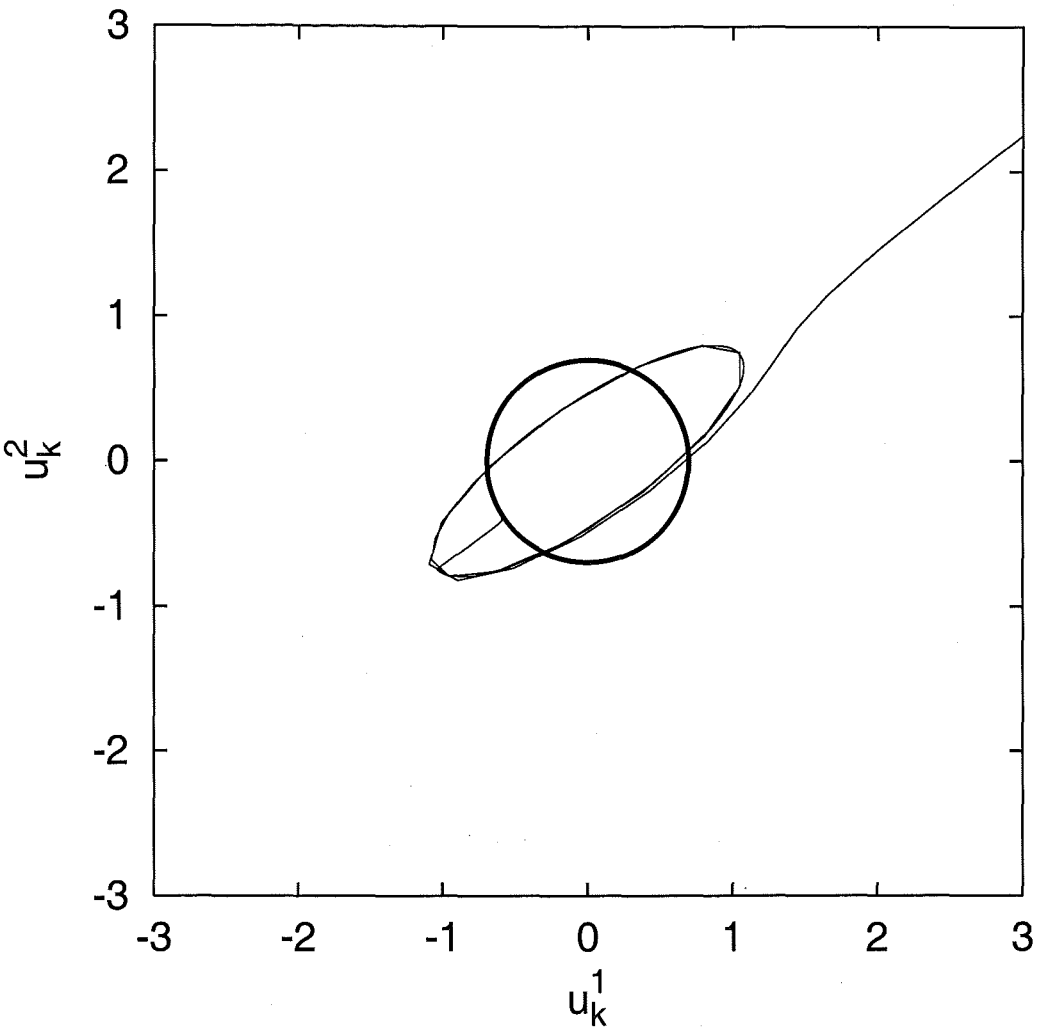

Figure 7.8: The evolution of the two modes u_k^1 and u_k^2 for a particular scale. The solution to the Equation (3.30) in the small z''/z limit is elliptical in general. The step in the potential perturbs the initially circular solution, resulting in elliptical evolution of the two modes. The phase of ellipse at which the two modes move into the regime where they are proportional to z will give the phase of oscillation in the power spectrum. This particular mode corresponds to a peak in the power spectrum as it leaves the elliptical regime at a maximum.

mode simply continues this proportionality. We have $|z| = |a\dot{\phi}/H|$ which means $|u_k|$ increases in the same way that $\dot{\phi}$ increases (as shown in Figure 7.5) but then returns to its slow roll value as though the step had not occurred, just as $\dot{\phi}$ does.

For larger k, so that $k > aH|_{step}$ the modes are oscillating when the step occurs. An increase in the z''/z term causes an immediate increase in u_k, the size of the increase being dependent on the relative sizes of k^2 and z''/z. This increase is independent of the relative phases of u_k^1 and u_k^2, but each mode is amplified or diminished to result in a net increase to u_k. This amounts to a new set of initial conditions for the two modes which are no longer necessarily orthogonal, and may have different amplitudes. We have plotted the evolution of the individual modes and their combined amplitude in Figure 7.7.

We can consider Equation (3.30) in terms of the elliptical nature of its solutions. Our solution is initially circular (having constant amplitude inside the horizon) but the step in the potential has the effect of immediately boosting the amplitude while not boosting the derivative term, which leads to oscillations of amplitude. This is shown in Figure 7.8. For very large values of z''/z relative to k the modes are so amplified that their phases after the step occurs coincide. The change in phase and amplitudes leads to the combined mode u_k oscillating. The phase of this oscillation at the point where the mode begins a growing solution will result in the corresponding phase in the power spectrum.

Knowing this we are able to calculate the period of mode oscillation in the power spectrum. The proper time interval between the step and the mode exiting the horizon is given by

$$\Delta\tau \sim 1/aH|_{\text{step}} - 1/aH|_{\text{exit}} = 1/k_{\text{low}} - 1/k, \tag{7.13}$$

during which time the amplitude of the mode will have undergone $1/\pi(k/k_{\text{low}} - 1)$ oscillations. Hence the period of variations in the power spectrum is given by approximately πk_{low}.

7.5 Decay of oscillations

We can determine approximately how the number of oscillations that occur depends on the values of c and γ. It can be seen in Figure 7.5 that the feature in z''/z has some finite width. This width is related to the rate of change of the field $\dot{\phi}$ and the width of the step in the potential, which is over some range $\Delta\phi$. This range $\Delta\phi$ is proportional to the parameter we use to describe how sharply the step occurs γ, and is independent of the size of our step, c. In the specific example of when we are dealing with a tanh step, we can see from Equation (7.7) that the width of the effect comes from the $\sinh / \cosh^3$ term. Now ϕ and $\alpha = \ln a$ are linearly related (approximately) and so the width is given by $A\gamma$ (A is some constant related to the definition of the width of the z''/z feature and the linear relation between ϕ and α). Looking at the form of Equation (6.12), the oscillation length of a particular mode u_k is given by $2\pi e^{\alpha} H/k$. So when this oscillation length is smaller than the length of the feature z''/z in α, the feature will have less effect because there will be cancellation of phase of the mode. So the number of oscillations is proportional to γ. This result can be seen in Figure 7.2 where the damping is independent of the value of c and is similar in all four cases in its dependence on the value of γ.

The relationship between the duration of the effect in k space and the parameter c is more complex. The assumption above that ϕ varies linearly with α is only valid for small step sizes. Given a very large step in the potential, by conservation of energy arguments we find that there is also a large increase in $\dot{\phi}$. Hence the linear relationship between ϕ and α can no longer be assumed during the phase in which the feature occurs. The number of oscillations present in the power spectrum is primarily related to changes in γ, and dependence on c is secondary to this.

7.6 Tensor modes

We now turn our attention from the scalar modes to the tensor or gravitational wave modes. The results from solving Equation (3.41) numerically for the step potential which we have been considering is shown in Figure 7.9. We can see that there is very little change in the tensor mode spectrum, even for a step which was seen to have a very significant effect on the scalar power spectrum.

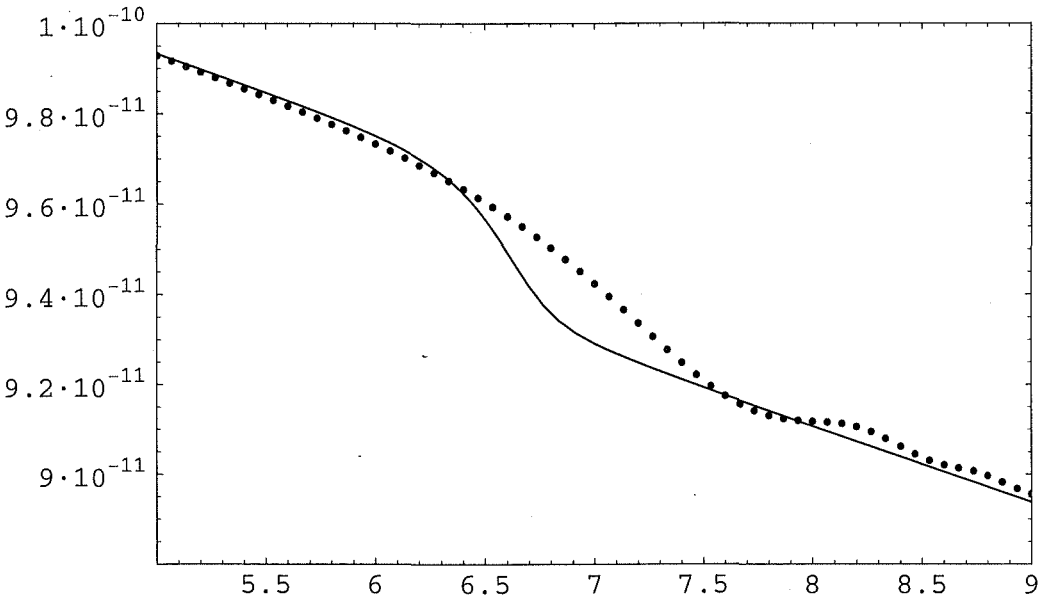

Figure 7.9: The tensorial power spectrum. We show both the analytic solution assuming the parameter ϵ is constant (solid line), and the numerical solution of the differential equations that we have been examining (dotted line). This is for a much larger step than any of the power spectrum shown and is ruled out by current observations.

This can be understood because unlike u_k which is dependent on $k^2 - z''/z$ and is hence altered by the change in the $\dot{\phi}$ term, v_k grows proportional to $k^2 - a''/a$. This term is largely unaffected by the presence of our step in the potential. This is shown in Figure 7.5 where we plotted the evolution of many of the physical variables over the course of a particular step in the potential, including both a'' and z''.

Chapter 8

Comparison between Numerical and Analytic Solutions for Inflation with a step potential

In this chapter we are going to compare the results from the numerical method for finding the power spectrum discussed in Chapter 6 with the method of Chapter 5 where we assume a slow roll inflaton potential.

There are two areas where the agreement between numerical and slow roll are very good. The first of these is the damping of the oscillations. This was accounted for in the slow roll solution by a $x/\sinh(x)$ term. This is seen to be in very good agreement with the damping observed in the numerical code. The agreement is particularly good for larger values of γ, as with small values of γ there are not enough oscillations for the damping to be determined solely by the $x/\sinh(x)$ term. We can see this looking at Figure 8.1, where we plot the different solution for varying values of the parameters c and γ.

c	γ	ϕ_{step}	$\Delta\mathcal{P}_{\mathcal{R}max}$	$\Delta\mathcal{P}_{\mathcal{R}min}$	$12c(V_0/V_0')^2$
1×10^{-5}	1000	$2.45M_P$	-0.0047369	0.0045275	0.0045258
2×10^{-5}	1000	$2.45M_P$	-0.0094335	0.0090580	0.0090516
4×10^{-5}	1000	$2.45M_P$	-0.018701	0.018116	0.01810

Table 8.1: Here we compare the Numerical results for the maximum and minimum variation of the power spectrum with the expected deviation based on the Oscillatory Slow Roll results for a ϕ^2 potential. Here we have varied c, γ and ϕ_{step} in turn while keeping the other two constant.

In Table 8 we tabulate the maximum and minimum variation from the step

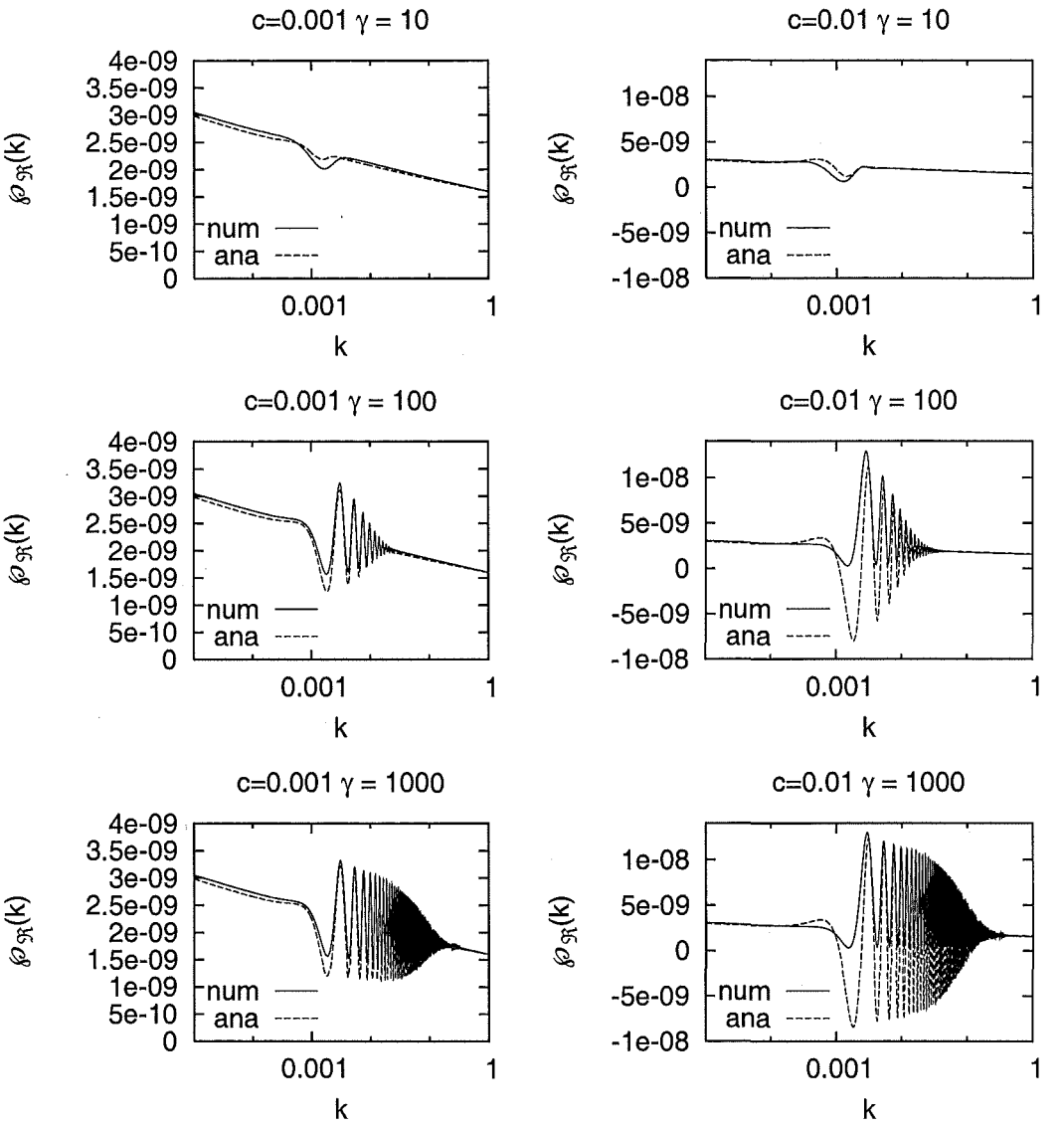

Figure 8.1: Numerical and analytic spectra for a step in the inflaton potential. We plot this for the parameter values $c = 0.001, 0.01$ and $\gamma = 10, 100, 1000$.

free case, defined as

$$\Delta\mathcal{P}_{\mathcal{R}}(k)|_{\text{max, min}} = \left.\frac{\mathcal{P}_{\mathcal{R}}(k) - \mathcal{P}_{\mathcal{R}\text{no step}}(k)}{\mathcal{P}_{\mathcal{R}\text{no step}}(k)}\right|_{\text{max, min}} . \tag{8.1}$$

We do this for the numerical solution and for the predicted value from Equation (5.47) of $12c(V_0/V_0')^2$, which uses the slow roll result. We do this for several values

c	γ	ϕ_{step}	$\Delta\mathcal{P}_{\mathcal{R}max}$	$\Delta\mathcal{P}_{\mathcal{R}min}$	$12c(V_0/V_0')^2$
0.0001	1000	3 M_P	-0.03085	0.03002	0.03016
0.001	1000	3 M_P	-0.2456	0.3009	0.3016
0.01	1000	3 M_P	-0.8032	3.045	3.016
0.001	10	3 M_P	-0.2454	0.3006	0.3016
0.001	100	3 M_P	-0.2456	0.3009	0.3016

Table 8.2: Here we compare the Numerical results for the maximum and minimum variation of the power spectrum with the expected deviation based on the Oscillatory Slow Roll results for a ϕ^3 potential. Here we have varied c, γ and the value of ϕ_{step} in turn, holding the other two constant.

of the parameters c, γ and ϕ_{step}. We also consider the case of the a ϕ^3 potential in Table 8. Looking at these tables we see that the maximum value predicted for $\Delta\mathcal{P}_{\mathcal{R}}$ shows good agreement between the numerical and slow roll case when we are considering values of γ above 1000, for all values of the parameters c and ϕ_{step}, in both the quadratic and cubic potential case. The predictions for when the power spectrum is less than the power spectrum without a step present are not so accurate. The numerical code respects the fact that the power spectrum is the square of the amplitude of the mode, and hence there is no way it can become negative. This fact is not incorporated into the size of the slow roll solution which is modelled upon the idea that the deviation from scale invariance is much smaller than the power spectrum. We note that the numerical and slow roll result for the lower bound agree well when c is small and hence our perturbation can be considered to be much less than the power spectrum, ie when $\Delta\mathcal{P}_{\mathcal{R}} \ll 1$.

The other problem with the Oscillatory Slow Roll solution is that the hump at the initial point of the step (before the first dip) is larger than seen in the numerical solution. This is because the assumption of linearity between the change in $\ln k$ the change in ϕ is not valid.

Chapter 9

Comparison with CMB observations

In this chapter we will discuss the CMB anisotropy spectrum, and how features in the primordial power spectrum manifest themselves in the CMB anisotropy spectrum. We then consider two CMB anisotropy data sets. The first is a compilation of the data from many CMB experiments developed by Wang *et. al.* [67]. The other data set we will consider is the recently released WMAP data. We compare these two sets of observations to the theoretical CMB anisotropy spectrum for the inflationary potential with a step we have discussed earlier.

9.1 Acoustic Peaks

We recall from Section 1.3 that the cosmic microwave background is formed when electrons and atomic nuclei (primarily hydrogen) combine to form neutral atoms. This means that there are no longer free electrons present to Compton scatter the photons.

At the time of recombination, any perturbations that have passed inside the horizon distance will have been able to evolve for the length of time they have been inside the horizon. This time they are inside the horizon will be inversely proportional to how large the modes are (smaller length scales will have been inside the horizon for longer).

Recall that the inhomogeneities were frozen in as they crossed outside the horizon and are no longer evolved. This is the primordial power spectrum we have been calculating from our inflationary models. However as the modes later re-enter the horizon they are again free to interact. The perturbations are then influenced by two main forces. The first is the gravitational attraction which causes overdense regions to contract, and increase in density. This acts to increase the amplitude of perturbations. The second force is the radiation pressure which causes overdense regions to expand. These two forces combine to generate oscillations. These oscillations mean that photons are observed at different energies (or temperatures) depending on whether they were emitted from an underdense or overdense region at the time of decoupling. These oscillations occur on each particular length scale independent of the behaviour of other length scales due to the fact that the perturbations remain small, and are therefore still in the linear regime.

There are three different influences on the CMB photons around the time of decoupling, which affect the temperature of the CMB as we observe it.

- Gravity: the gravitational field causes red or blue shifting of photons as they come from overdense or underdense regions, respectively.
- Density: compression heating and rarefaction cooling effects mean the energies of photons leaving overdense regions is higher than that of photons leaving underdense regions.
- Velocity: photons last emitted by moving particles will have their energies Doppler shifted.

For analysis, we decompose the CMB anisotropies into spherical harmonics. This is convenient because each length scale is evolving independently. So we have

$$\frac{\Delta T(\mathbf{x})}{T_0} = \sum_{l=2}^{\infty} \sum_{m=-l}^{l} a_l^m Y_l^m(\mathbf{x}). \tag{9.1}$$

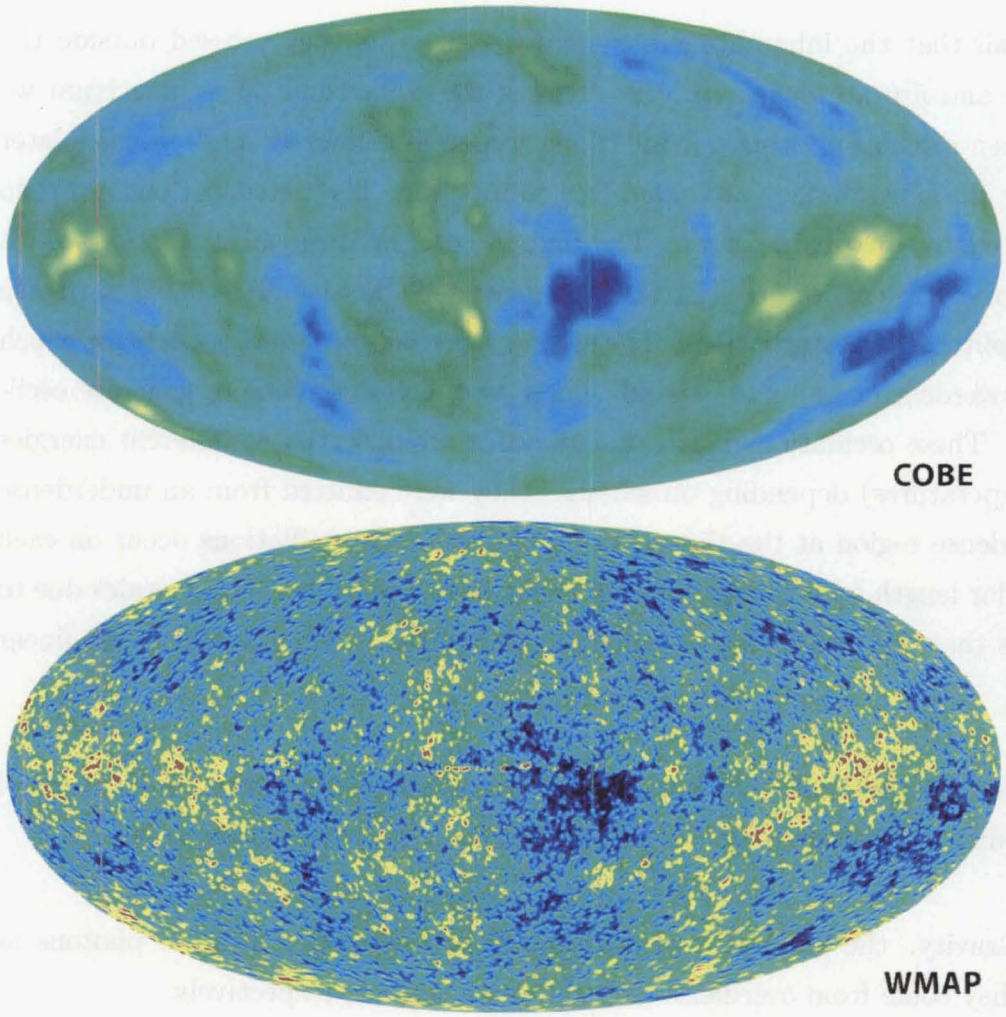

Figure 9.1: Variations in the CMB across the night sky. Included are both those first observed by COBE, as well as the latest pictures obtained from the WMAP satellite. Our thanks to the WMAP team for providing this image [32]

From this we get the power spectrum as the sum of the squares of the coefficients

$$C_l = \frac{1}{2l+1} \sum_{m=-l}^{l} (a_l^m)^2. \tag{9.2}$$

Note here that we have chosen the convention of normalizing the temperature anisotropies by dividing by the average CMB temperature.

The resulting CMB decomposition can be separated into three distinct ar-

eas. The first corresponds to scales which were super horizon sized at the time of decoupling. These scales are unable to evolve after inflation, because they have expanded to outside the horizon during inflation and frozen in as metric perturbations, and have not been able to evolve between then and decoupling (this corresponds to angular scales of roughly 1 degree or larger). The second section corresponds to angular sizes which were inside the horizon at the time of decoupling. These modes had time to oscillate between the time they entered the horizon and the time of decoupling and hence it is on these scale sizes we are able to see the acoustic peaks. On even smaller scale sizes (less than 0.1 degree) the finite thickness of the surface of last scattering, and the diffusion of photons (photons diffusing out of small scale fluctuations) causes acoustic peaks to be suppressed.

9.2 CMB Experiments

Recently there has been interest in the observed inhomogeneities in the CMB, and how these inhomogeneities vary on angular distance scales. Experiments in the last 5 years have revealed the nature of the inhomogeneities with much higher precision that was previously possible. Much analysis has gone into these results, and how cosmological parameters can be extrapolated from the data. The data seems to support the inflationary hypothesis with acoustic peaks observed in line with the predictions of inflation. There has also been a dramatic increase in the amount of data supporting the flatness of the universe, with estimates for Ω going from $\Omega = 0.1 - 1.2$ in 1998 [9] to $\Omega = 1.00 \pm 0.02$ from the latest WMAP data in 2003 [17]. An inflationary phase transition affects on these observations if the transition occurs a certain number of e-folds before the end of the inflationary period.

I will now survey the three main types of CMB anisotropy experiments. These are ground based, balloon based and satellite based, and each method

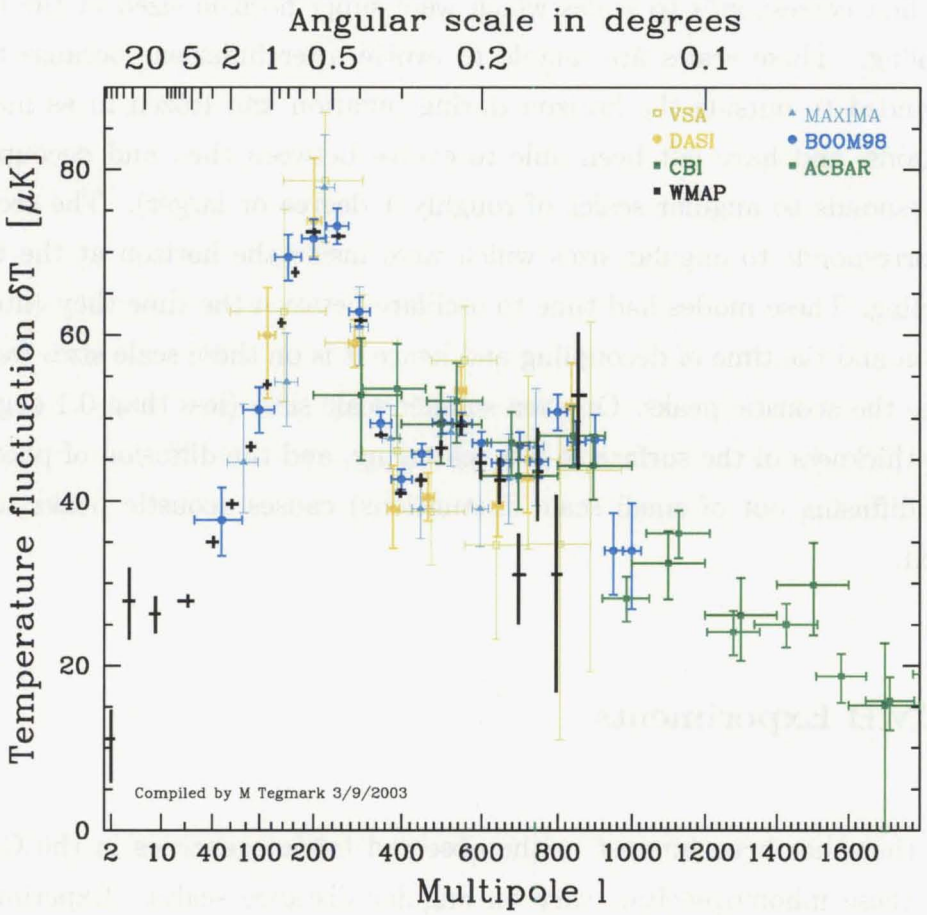

Figure 9.2: CMB data as measured by several CMB Experiments. This figure is taken directly from Tegmark [33], and includes the data from selected CMB experiments.

has advantages and disadvantages over the others.

9.2.1 Ground Based

There are many ground based arrays. The Very Small Array (VSA) is a radio telescope (operating between 26-36 GHz) based in Tenerife. They released data in

December 2002 up to a scale of $l = 1400$ [15, 24]. There are two Antarctic based ground detectors. The Degree Angular Scale Interferometry (DASI) experiment [26] which has measured up to $l = 800$. The Arcminute Cosmology Bolometer Array Receiver (ACBAR), also operates out of Antarctica [18, 23]. Acbar consists of an array of 16 detectors sensing radio frequencies between 29-50 GHz and has generated results out to l values of 3000. Finally the Cosmic Background Imager (CBI) [16, 27] is located at an altitude of 5080 m (16,700 feet) in the Chilean Andes. It has measured the anisotropy out to values of l of 3500. This ability to measure to small angular scales is the main advantage of the ground based detectors, due to the ease of updating the hardware and software, and lengthy observing times they are able to get results on smaller length scales than is possible in the case of the balloon and space based detectors.

9.2.2 Balloon based

There are two notable balloon based detectors. These are the Boomerang [8, 14] and Maxima [22, 13] projects. The two experiments are very similar and rely on high balloon flights with CMB measurements made over the duration of the flight. Due to the better atmospheric conditions these experiments are very good at gathering intermediate scale results. However they have limited data gathering for $l > 1500$ due to the short flight duration. It is fair to say that at the time of publication the data from BOOMERanG and MAXIMA were the most accurate sets available, however with the introduction of the space based detectors they have largely been superseded on scales $l < 900$.

9.2.3 Wilkinson Microwave Anisotropy Probe

The first satellite to look at the CMB in detail was the COBE satellite. This had multiple detectors; however its primary purpose was to verify that the CMB was indeed a black body spectrum. The instrument achieved this with great

accuracy and also made measurements of the anisotropy on larger angular scales (for small l values). The Wilkinson Microwave Anisotropy Probe (WMAP) is a satellite based CMB detector launched by NASA in 2001. It is located some 1.5 million kilometers from the Earth at the second Lagrange point of the orbit of the earth and the sun. This second Lagrange point is one of five points where a small body can maintain a stable orbit under the gravitational attraction of two much more massive bodies. Due to both its location where it has an almost completely unobstructed view of then entire sky, and the fact it is designed solely to look at CMB anisotropies, WMAP has been able to probe the CMB anisotropy spectrum with unparalleled precision from scales of $l = 1$ to $l = 900$. We show the observations of the anisotropy spectrum from the WMAP satellite in Figure 9.3.

9.3 CMBFAST

The CMBFAST numerical package [59] is one of the standard computational packages used for calculating CMB anisotropy spectra. It takes into account a number of effects on the photon light path the details of which are not important here. It calculates the anisotropy spectrum by integration over all sources on the photon past light cone. All work here is based on version 4.0 of the program, which is the same version used by the WMAP team in their recent data release.

9.3.1 Alterations to the CMBFAST code

To test our nonstandard primordial power spectrum, we must alter the CMBFAST program to call data from our code for calculating the primordial power spectrum. The default CMBFAST program just considers a primordial power spectrum with a potentially non-zero slope to the power spectrum set by the user. The first way we altered this was to just write into the code where the primordial

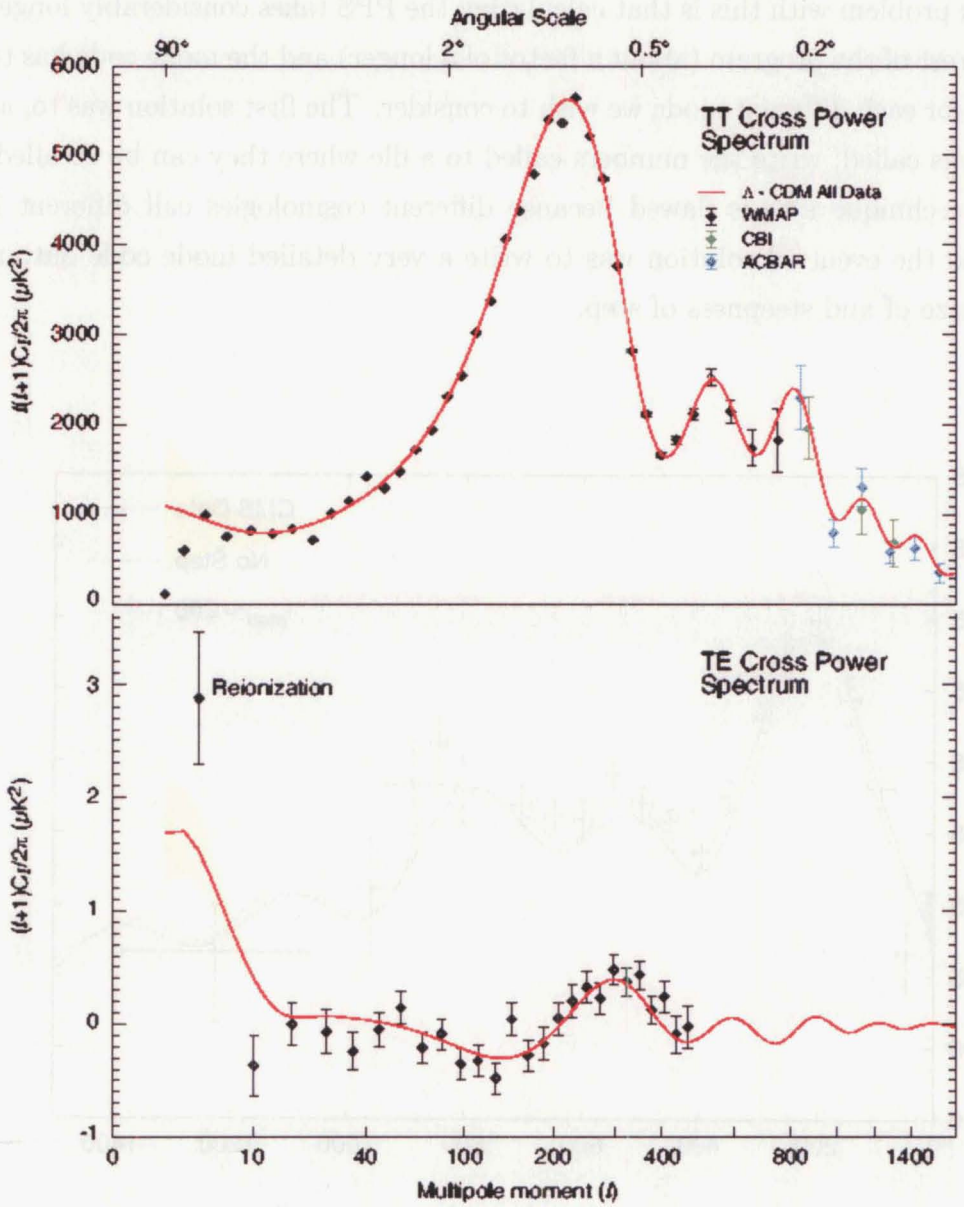

Figure 9.3: Binned WMAP data for the CMB anisotropy spectrum. We show the best fit line for this data as calculated by CMBFAST. The binning of this data is done corresponding to the best fit line shown. This figure provided by the WMAP Legacy Archive [32].

power spectrum (PPS) is generated a subroutine which calls the code we have written to generate the PPS. This technique was not ideal for several reasons. The main problem with this is that calculating the PPS takes considerably longer than the rest of the program (about a factor of 5 longer) and the mode code has to be called for each different mode we wish to consider. The first solution was to, as the mode is called, write the numbers called to a file where they can be recalled, but this technique also is flawed because different cosmologies call different k values. So the eventual solution was to write a very detailed mode code output for each size of and steepness of step.

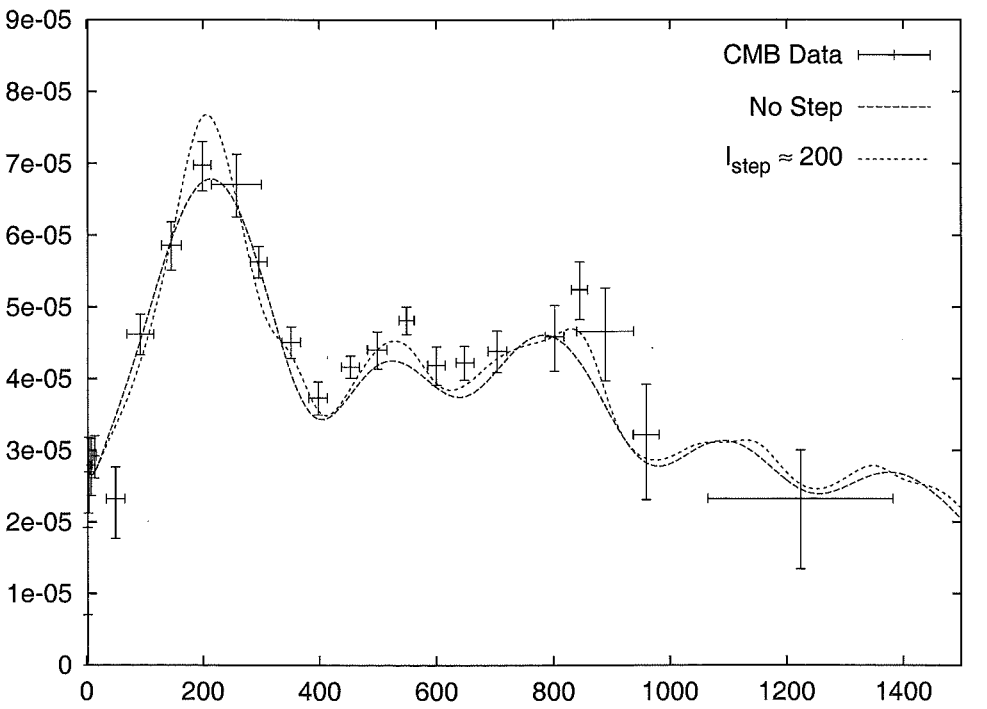

Figure 9.4: CMB anisotropy spectra with and without a step in the inflaton potential. We can see that there is a step in the potential at around $l = 200$, and that this causes a significant deviation from the anisotropy spectrum without a step.

9.4 CMB Observations

9.4.1 Compilation of CMB Data

We want to incorporate as much of the available CMB data as possible. We do this by using the data from a technique suggested by Wang *et al* [67]. In doing this we exclude the WMAP data which we shall consider separately later.

The method involves filtering the existing CMB measurements to make them more workable. Firstly the existing experiments are written as a vector $\mathbf{y}$. Then we can write

$$\mathbf{y} = W\mathbf{x} + \mathbf{n} \tag{9.3}$$

where $\mathbf{x}$ is a vector containing the true power spectrum coefficients, W is a matrix containing the relevant experimental window functions (rows of W being normalized to unity), and $\mathbf{n}$ is a vector which represents the experimental uncertainties for each data point. We assume that the errors are random, with zero mean. Then we can decompose the covariance matrix $N \equiv \langle \mathbf{n}\mathbf{n}^t \rangle$ that is the sum of four terms, basic measurement errors, source calibration errors, instrumental calibration errors and beam errors. These individual errors can be calculated explicitly and so N can, in the limit that the errors are small, be calculated independently of $\mathbf{x}$.

We can invert Equation (9.3) to calculate the actual power spectrum $\mathbf{x}$. We find that

$$\tilde{\mathbf{x}} \equiv [W^t N^{-1} W]^{-1} W^t N^{-1} \mathbf{y} \tag{9.4}$$

can be shown to be unbiased, to minimize the *rms* noise in each power band, and if the noise properties are Gaussian, to retain all information about the true power spectrum $\mathbf{x}$ from the original data $\mathbf{y}$ [64]). From this technique the data from Table 9.1 is obtained. This data has been checked for internal consistency to assure that no one experimental data set significantly alters the combined data.

Point	l Mid	l Range	$\delta T^2[\mu K^2]$	Uncertainty
1	2.02207	1.70658 - 2.33755	48.645146	309.81249
2	4.38515	3.26886 - 6.90321	876.542873	308.41444
3	8.32762	6.47599 - 11.19266	782.432119	218.28001
4	15.86700	11.68231 - 24.67657	831.506959	150.96813
5	39.66270	29.56841 - 49.53998	1112.662689	244.37413
6	60.36304	47.28106 - 74.40646	1119.901879	254.79077
7	86.78309	74.42739 - 96.82825	2138.846781	279.08362
8	109.50461	92.65733 - 120.88309	2766.524367	340.36785
9	134.92816	121.15929 - 147.36297	3460.591017	442.70796
10	160.59932	137.61756 - 181.78508	4122.154551	529.13258
11	196.09337	162.29245 - 220.51347	4899.728226	410.06064
12	246.13680	201.98817 - 269.02271	5078.754028	440.51099
13	296.88466	269.28084 - 320.81458	3164.114409	359.26684
14	348.35768	325.02673 - 369.89785	1892.017032	265.30611
15	398.18217	375.98281 - 418.49576	1468.002700	212.90651
16	449.58482	427.42155 - 470.47754	1793.261880	218.51371
17	499.39098	477.80171 - 520.12977	2037.427127	256.62371
18	549.00511	526.36786 - 570.16406	2306.290817	267.87662
19	599.51799	577.85713 - 620.21579	1931.599358	266.57652
20	649.00530	627.03945 - 669.73165	1789.632527	259.27809
21	699.51426	678.38950 - 719.56254	1948.345293	293.34968
22	749.33873	726.82318 - 771.69965	1428.093513	334.28814
23	801.21322	778.28218 - 824.51262	2321.982645	437.59452
24	887.73587	842.15324 - 940.01104	2066.656294	260.72431
25	1093.04791	1028.48398 - 1149.17073	952.526315	299.76908
26	1298.52121	1243.06030 - 1352.40230	637.589700	291.22329
27	1500.72347	1445.79175 - 1554.33150	923.555555	368.25555
28	1699.90414	1646.43385 - 1751.30778	188.838831	273.38091

Table 9.1: This set of 28 points combines all the data from the 105 CMB data points. The first column gives the range of l values considered, the second the average and *rms* widths of the window functions, and the third column the squared temperature fluctuations.

For details readers are referred to Wang *et al* [67].

9.4.2 χ^2 testing of Compiled data

We begin by considering a grid of points in the three dimensional space spanned by the parameters of the potential: c, which is the size of the potential step; γ, the gradient of the potential step; and k_{step}, the scale the step occurs. We use the numerical package CMBFAST to calculate the CMB anisotropy spectrum which would result from this choice of the parameter values. This is then compared to the observed CMB anisotropy spectrum. We use the data listed in Table 9.1 which contains 24 data points, which means acceptable χ^2 results will be around 21, given three degrees of freedom corresponding to our three variables.

The package, CMBFAST already has 11 free parameters which can be tuned to give a good fit to the observational data. So by enlarging the parameter space to include c, d, and k_{step} we may be able to be more flexible in the other allowed parameter values. Also we should be able to exclude some solutions to very high probability.

For our χ^2 method we follow the formalism of Lineweaver *et al* [46]. We convolve each model with the experimental window functions and fit this result to the experimental data as follows. The χ^2 value is given by

$$\chi^2(c, d, k_{\text{step}}) = \sum_{N=1}^{N} \left(\frac{\delta T_{l_{eff}}^{\text{data}}(N) - \delta T_{l_{eff}}^{\text{model}}(N, c, d, k_{\text{step}})}{\sigma^{\text{data}}} \right)^2 . \tag{9.5}$$

Here, $\delta T_{l_{eff}}^{\text{data}}(N)$ represents the convolved temperature fluctuations from each of the N experiments being compared to the theoretical models, with σ^{data} the corresponding errors. $\delta T_{l_{eff}}^{\text{model}}(N, c, d, k_{\text{step}})$ represents the temperature fluctuations from the model being considered. These terms have been convolved using the experimental specific window functions $W_l(N)$, and the logarithmic integrals of the window functions defined by

$$I(W_l) = 2\pi \sum_{l=2}^{l_{max}} \frac{(2l+1)}{4\pi} \frac{W_l}{l(l+1)}. \tag{9.6}$$

Using this the convolved temperatures are given by

$$T_{l_{eff}}^{\text{data}}(N) = \frac{\delta T_{rms}^{obs}(N)}{\sqrt{I(W_l(N))}}, \tag{9.7}$$

$$T_{l_{eff}}^{\text{model}}(N, c, d, k_{\text{step}}) = \frac{\delta T_{rms}^{model}(N, c, d, k_{\text{step}})}{\sqrt{I(W_l(N))}}. \tag{9.8}$$

The Nth experiment then probes the angular scale

$$l_{eff}(N) = \frac{I(lW_l(N))}{I(W_l(N))}. \tag{9.9}$$

We use for our N experiments the data from the paper by Wang *et al* [67].

9.4.3 WMAP Data

The data from WMAP must be looked at in terms of the likelihood function. We do this by using a numerical code freely available from the WMAP data website [32] to calculate the likelihood from the covariance matrix. We are forced to do this instead of the approach of previous work because the WMAP covariance matrix has non-trivial off diagonal elements.

Using the WMAP data we can place a lot of constraints on the values of free parameters in the universe [20]. Some of these results from the WMAP data are shown in Table 9.2. We show the mean and uncertainty for each result as well as the value that is found to give the maximal likelihood and hence lowest χ^2 value.

9.5 Results for Step Potential model

Firstly we consider the step potential case. We consider several different possibilities. We consider one of the parameters c and γ at a time, while also varying the parameter k_{step}. Throughout this we use a fixed cosmology, for which we use the

Parameter		Mean and 68% confidence level	Maximum Likelihood
Baryon Density	$\Omega_b h^2$	0.024 ± 0.001	0.023
Matter Density	$\Omega_m h^2$	0.14 ± 0.02	0.15
Hubble Constant	h	0.72 ± 0.05	0.68
Amplitude	A	0.9 ± 0.1	0.80
Optical Depth	τ	$0.166^{+0.076}_{-0.071}$	0.11
Spectral Index	n_s	0.99 ± 0.04	0.97

Table 9.2: Here we can see the various values that are estimated from WMAP, along with their uncertainty and best fit value. The maximum likelihood model is found to have a χ^2 of 1431 for 1342 degrees of freedom.

best fit WMAP model as detailed in Table 9.2. We also investigate the results from varying the cosmology. We compare these theoretical CMB power spectra firstly to the CMB data compilation of [67] using the χ^2 to evaluate goodness of fit. We then compare to the WMAP data using the likelihood code provided by the WMAP team [32].

The WMAP team, in an article about the implications of their data for the inflationary paradigm [21], mention the idea of a step in the inflaton potential. They refer to our method for modelling a step in the potential we published in 2001 [2] as we detail in Chapter 7. They use a Monte Carlo analysis and they find a fit for a step in the inflaton potential which decreases the combined $\chi^2/d.o.f.$ from 1432/1342 to 1422/1339.

9.5.1 Changing the step parameters

The presence of a step in the primordial power spectrum will cause changes in the CMB anisotropy spectrum. These changes in the CMB anisotropy spectrum will depend on the size of the step c, the sharpness of the step γ and the position of the step in k. Figure 9.4 shows for a particular size and slope of step how

the position of the step affects the CMB anisotropy spectrum. When varying k, differences in the CMB anisotropy spectrum leads to a large variation of χ^2. The variation in the resulting χ^2 fit is shown in Figure 9.5.

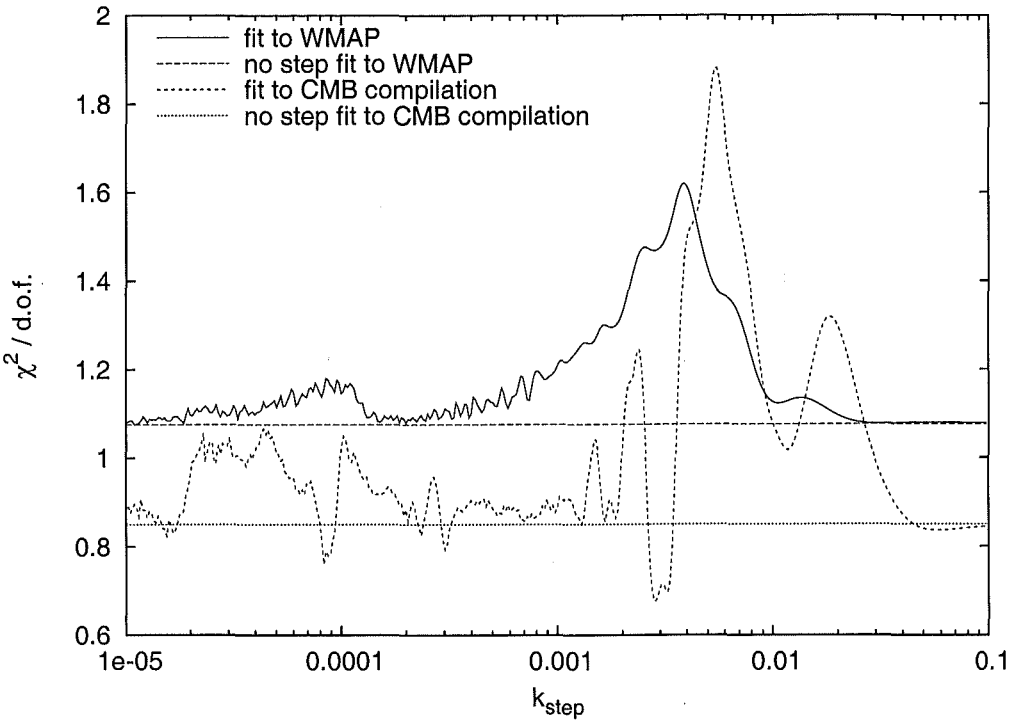

Figure 9.5: The value of χ^2 for a particular step as the position of the step is changed. Here we have used $\gamma = 10000$ and $c = 0.0005$. The step occurs at $\phi = 2.45 M_P$. Shown is the fit of both the CMB compilation, which has 25 degrees of freedom, and the WMAP data which has 1339 degrees of freedom.

For relatively high k_{step} values (only just inside observational bounds), only the initial dip in the perturbation spectrum is relevant, and the result is a lower spectrum at high k (and hence l) values. As the step position is moved to lower k values, the peak after the initial dip becomes relevant, which means that the spectrum displays a lowering and raising relative to a CMB anisotropy spectrum generated by a flat potential. As the step position lowers further more and more of the anisotropy spectrum is affected.

This initial lowering of the potential does not depend on the gradient term γ. The value of γ has more effect on the number of oscillations observed in k before the effect of the step is damped out. This can be seen in Figure 9.6. The higher the value of γ, the greater the width of k values effected by the feature in the power spectrum. So for lower k_{step} values the χ^2 levels off when γ is small whereas if γ is large the χ^2 value is still being affected by the step.

The step size term, c, only affects the magnitude of the power spectrum change from the scale invariant case. This is shown in Figure 9.6 where the higher c values lead to worse fits to the data, and hence higher χ^2 values for almost all k_{step} values. The best value of χ^2 we obtained was 1433 for 1339 d.o.f, which is a better fit to the data than the χ^2 of 1441 for 1342 d.o.f. in the case of no step. This was in the case that $\gamma = 10000$ and $c = 0.0002$, at a k_{step} position of 3.3×10^{-5}. This improvement is of similar magnitude to the one mentioned earlier that was found by the WMAP team. Their base χ^2 value was 1432 and their improvement was by 10, whereas our base value was 1441 with an improvement of 8 with a step.

9.5.2 Changing the background cosmology

Here we will consider how the fit to the data with a step change if we change some of the cosmological parameters. Specifically we try two different values of both Ω_Λ and H_0, one higher and one lower than the best fit values of 0.6756 and 0.68 respectively. We find that the behaviour is qualitatively similar, though some cases have considerably better χ^2 values with the introduction of a step.

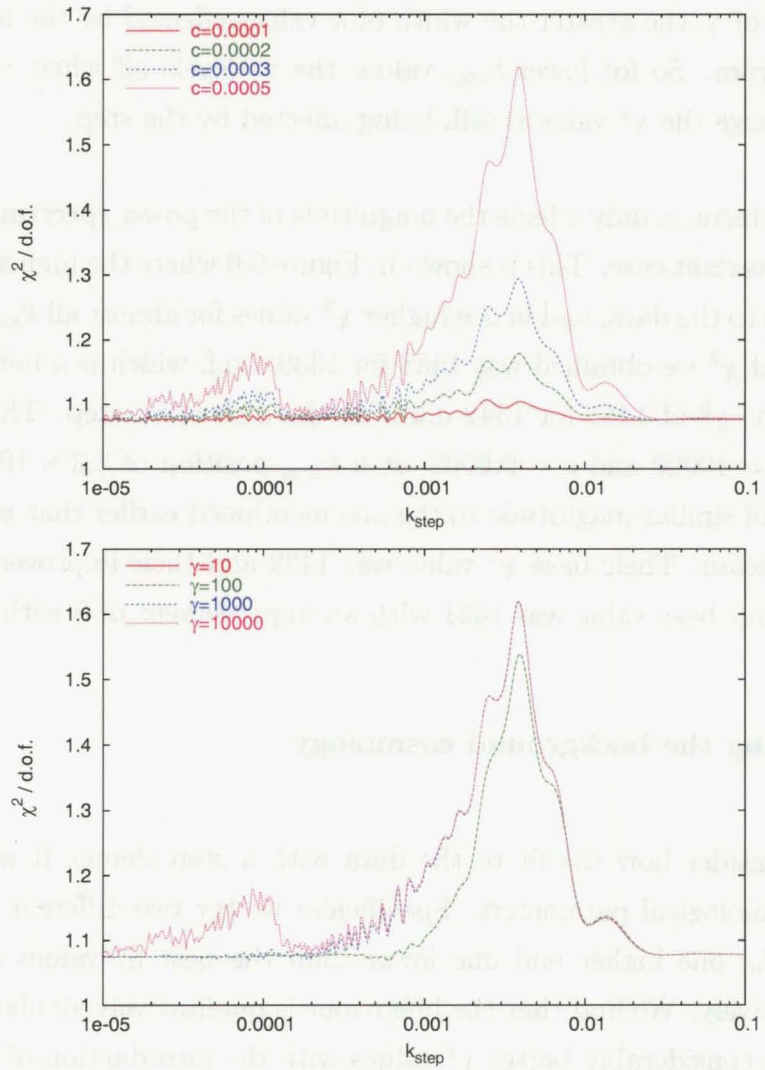

Figure 9.6: χ^2 fit to the WMAP data for changing parameters c and γ. In the first plot we keep the slope parameter constant at $\gamma = 1000$ and vary the size of the step c. In the second plot we have kept the step size constant $c = 0.0005$ and have varied the size of the slope parameter γ.

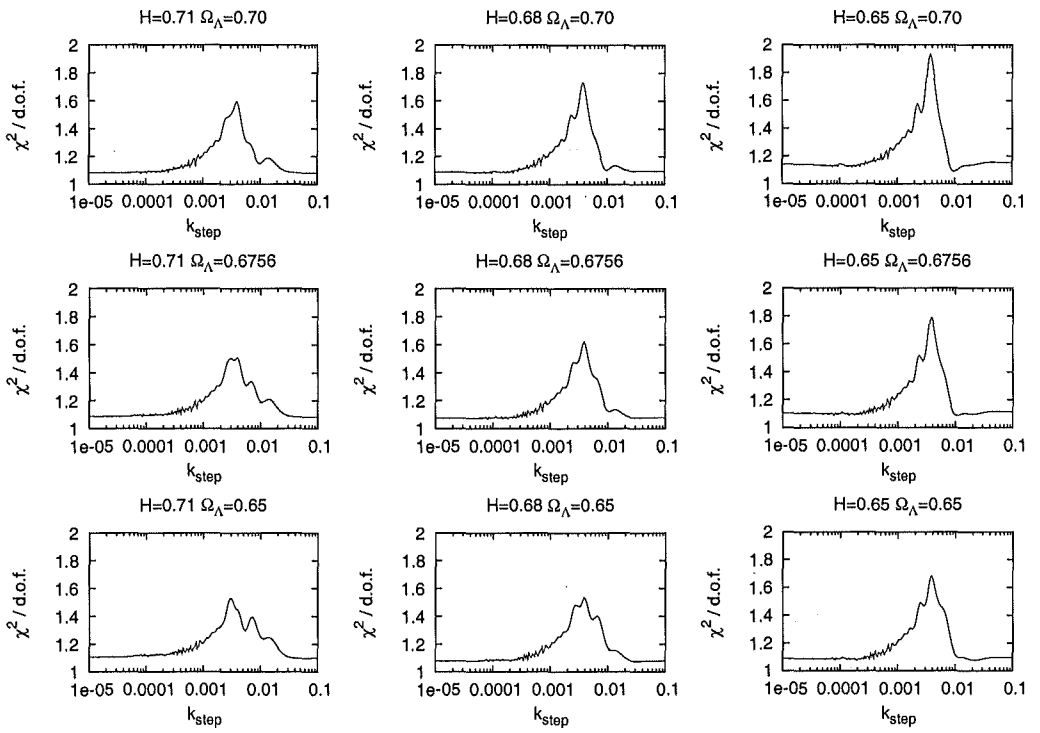

Figure 9.7: χ^2 fit to the WMAP data for different cosmologies. We fix the step size at $c = 0.0005$ and slope parameter $\gamma = 1000$, and vary the position of the step in the potential. We try values of Hubble parameter $H = 0.65$, 0.68 and 0.71, and cosmological constant $\Omega_\Lambda = 0.65$, 0.6756 and 0.70.

Chapter 10

Broken Scale Invariance

In this section we consider a different form of potential that could result from a phase transition. Instead of having a jump in the inflaton potential, we have a jump in the first derivative of the potential. This model was first suggested in 1992 by Starobinski [60], and has been studied extensively [36, 41, 42]. The simplest form of this model is to choose the specific case of a linear potential, where we have two constant sloped regions of potential with differing slopes joined continuously to one another, that is

$$V(\phi) = \begin{cases} V_0 + A_+(\phi - \phi_{step}) & \phi > \phi_{step} \\ V_0 + A_-(\phi - \phi_{step}) & \phi \leq \phi_{step} \end{cases} . \tag{10.1}$$

We can choose either one of two situations, a decrease in slope ($A_+ > A_- > 0$) or an increase in slope ($A_- > A_+ > 0$).

This model is referred to as Broken Scale Invariance (BSI). This is because the two constant slope regions lead to two scale invariant sections of the primordial power spectrum. These two regions are separated by features in the power spectrum resulting from the change in slope of the potential.

10.1 Exact Solution

There exists a well known analytic solution for a BSI potential, introduced by Starobinski when he first suggested the potential [60]. This result makes the

assumption that around the time of the change in slope of the potential, this slope change is the significant factor in determining the power spectrum.

This analytic solution is different to the step case as under the condition that the transition occurs reasonably sharply then there is no dependence on just how sharp the change is. The transition is assumed to occur instantaneously in this case. The result is that the power spectrum is given by

$$P_{\mathcal{R}}(\kappa) = \frac{V_0^3}{12\pi^2 A_-^2} S(\kappa, p) \tag{10.2}$$

where $p = A_-/A_+$, and the function $S(\kappa, p)$ is

$$\begin{aligned} S(\kappa, p) \quad &= 1 - \frac{3(p-1)}{\kappa}\left(\left(1 - \frac{1}{\kappa^2}\right)\sin(2\kappa) + \frac{2}{\kappa}\cos(2\kappa)\right) + \\ &\frac{9(p-1)^2}{2\kappa^2} f(\kappa)\left[f(\kappa) + \left(1 - \frac{1}{\kappa^2}\right)(\kappa)\cos(2\kappa) - \frac{2}{\kappa}\sin(2\kappa)\right] \end{aligned} \tag{10.3}$$

Here $\kappa = k/k_{step}$ and $f(\kappa) = 1 + 1/\kappa^2$. Note there is the same periodicity with terms involving $\sin(2\kappa)$ and $\cos(2\kappa)$ as seen in the step case. In fact the second term in this expression is exactly $W(\kappa)$ as defined in Equation (5.16), multiplied by the change in slope $(p-1)$. The nature of the oscillations present here is different to that in the step case. The oscillations present here damp with factors of $1/\kappa$ and $1/\kappa^2$ and so the periodicity is only present for a limited range of k modes.

As $\kappa \to 0$ we find that $S(k, p) \to p^2$ and as $\kappa \to \infty$ we find that $S(k, p) \to 1$. This means that in the limits of $\kappa \ll 1$ and $\kappa \gg 1$ we get the power spectrum we would expect based on a slow rolling potential with slopes A_+ and A_- respectively.

One can attempt to solve for the power spectrum from Equation (5.16) as done in Chapter 5. Doing this one arrives at a similar expression to Equation (10.2). However this method only obtains the first two of the three terms in $S(\kappa, p)$, and so the limit as $\kappa \gg 1$ is not consistent with what would be expected. This difference arises because Equation (5.16) does not allow for terms of more than first order in the slow roll parameters.

10.2 Numerical Solution

We now apply our numerical method from Chapter 6 to the BSI potential. This allows us to compare between the numerical and analytic solutions. The use of the numerical method is also helpful in that looking at the evolution of the individual parameters provides us with an explanation for the oscillatory behaviour in the power spectrum. This potential contains a singular point where the second derivative of this potential is discontinuous. So following our approach for the case of a step in the potential we approximate this potential with a potential that tends to an instantaneous slope change in the limit that a parameter γ tends to infinity. Again this is done using the tanh function this time with

$$\begin{aligned} V(\phi) &= V_0 + \left\{ \frac{A_+}{2} \left[1 + \tanh\left(\gamma\phi\right)\right] \right. \\ &+ \left. \frac{A_-}{2} \left[1 - \tanh\left(\gamma\phi\right)\right] \right\} \phi. \end{aligned} \tag{10.4}$$

The term in the first set of square brackets disappears for $\phi \gg 0$, and the term in the second set of square brackets disappears when $\phi \ll 0$.

The power spectrum we obtain from numerical solution of Equation (3.30) is shown in Figure 10.1. As we would expect considering the analytic expression of Equation (10.2), number of features from this potential are similar to those from the step potential. Scale dependent oscillations are observed, which die down to leave a flat power spectrum of differing amplitude to the flat power spectrum we had before the slope change occurred. This is a direct result of this change in slope. It can be shown that the amplitudes of the power spectrum well before and well after the change in slope are exactly what are expected from the slow roll solution for the power spectrum.

To explain what is happening with this potential we again look at the parameter z''/z. This can be approximated as in the case with the step potential (from

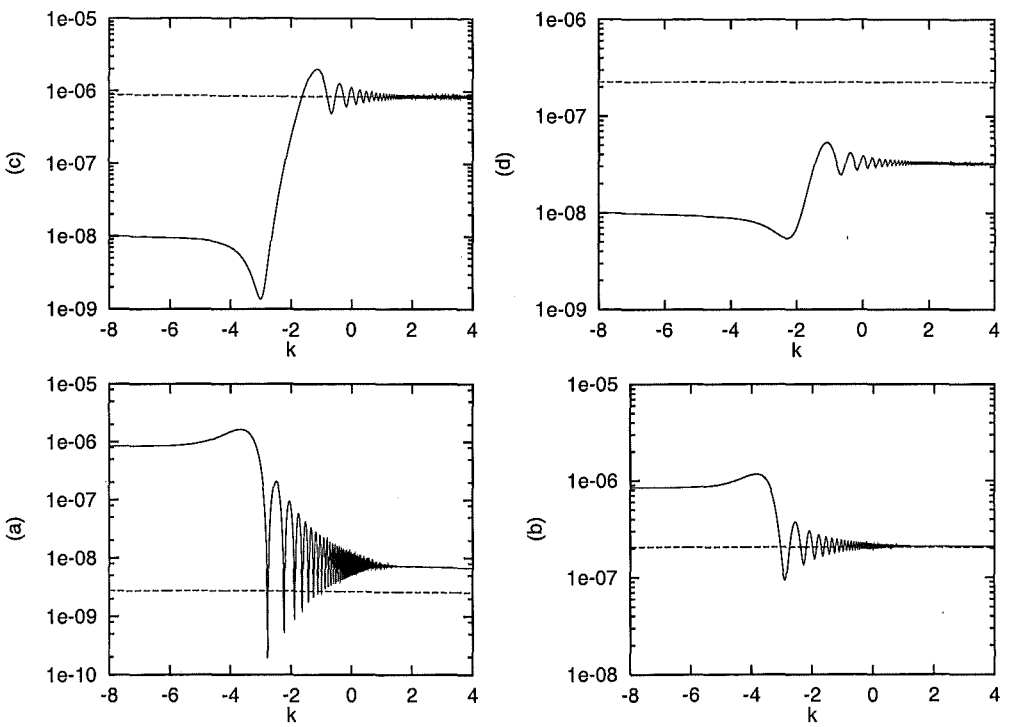

Figure 10.1: BSI power spectra for various values of change in slope. We plot for slopes after the time of slope change taking the values (a) $A_+ = 10A_-$, (b) $A_+ = 2A_-$, (c) $A_- = 10A_+$ and (d) $A_- = 2A_+$. The straight dotted line in each plot is the tensor modes. It can be seen that in each case there is an increase or decrease in the asymptotic value of the power spectrum, and that there are coherent oscillations between the end of the first asymptotic region and the second.

Equation (7.5)) by

$$\frac{z''}{z}\frac{1}{2a^2H^2} \simeq \frac{\gamma(A_+ - A_-)\left(\gamma\phi\tanh\left(\gamma\phi\right) - 1\right)}{\cosh^2\left(\gamma\phi\right)}. \tag{10.5}$$

This compares well with the result from the numerical code, and takes the form of a delta function as $\gamma \to \infty$. Making the assumption this is a delta function in Equation (3.30) gives that u_k'' also takes the form of a delta function. This means that u_k' has a sudden change in value. This can be seen looking at Figure 10.2 which plots the evolution of u_k^1 against u_k^2, normalized by multiplication by $\sqrt{2k}$ so they all inscribe a circle of radius 1 when well inside the horizon. This circular motion normally continues until the mode reaches the horizon size, at which time the mode grows with z. If we introduce a change in potential slope, this causes a

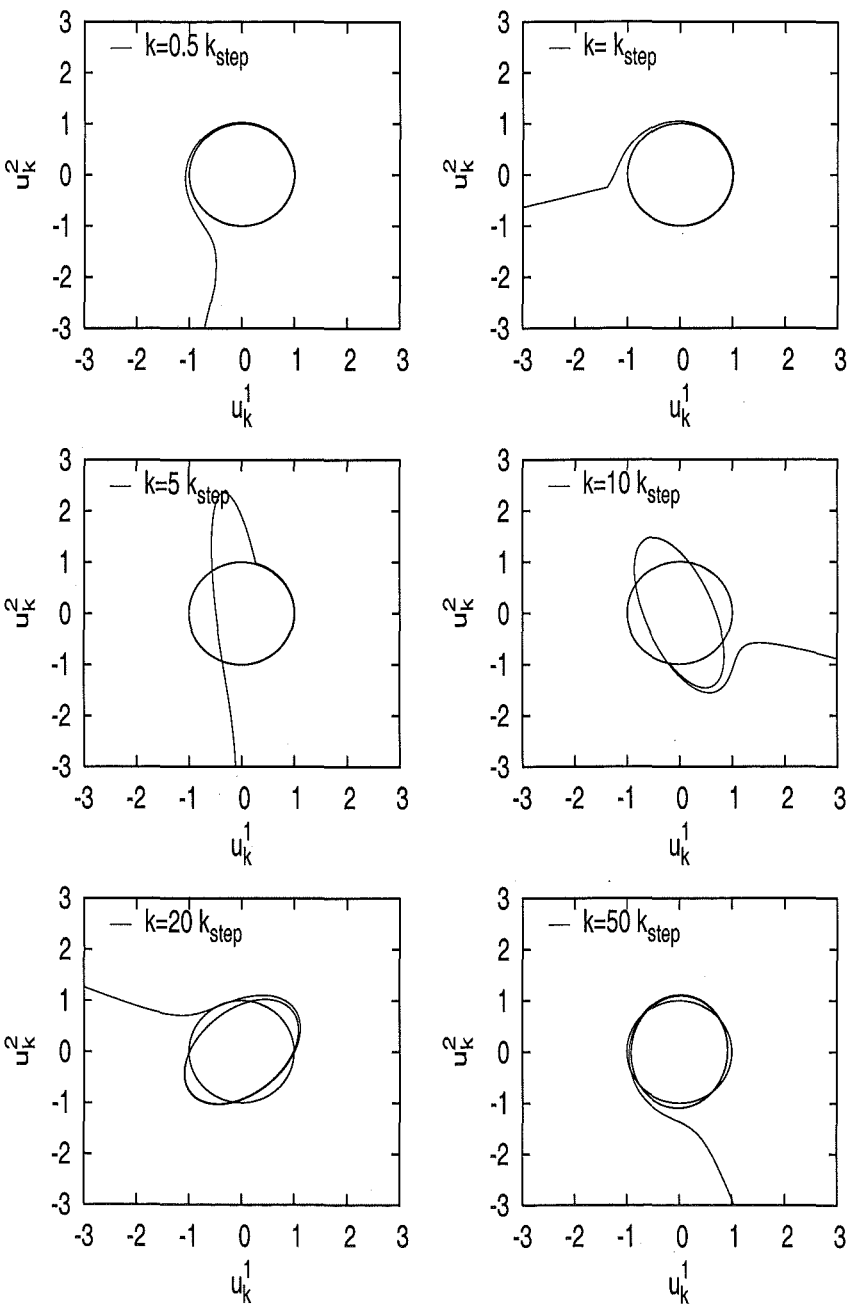

Figure 10.2: Evolution of individual modes for several different values of k/k_{step} in the case of a BSI potential. The mode is initially of constant amplitude, and is then perturbed by the change in slope to take on an elliptical type motion, so having varying amplitude. The eccentricity of the resulting ellipse depends on how close to the mode exiting the horizon the change in potential occurs.

sudden change in u'_k and so the solution is perturbed from being a circle to being elliptical. The phase of this ellipse at the time the mode leaves the horizon then dictates the phase of oscillation of the mode.

The size of the perturbation to the circle that describes u_k depends on the size of the delta-like function that occurs in z''/z. This means there is a proportionality to $(A_+ - A_-)$ as would be expected. There is also a dependence on how far inside the horizon the mode is when the change occurs ie k/k_{change}. This can be understood by considering the value of $|u_k|$, which well inside the horizon before the occurrence of the change in slope is given by $|u_k| = 1/\sqrt{2k}$ from Equation (6.13). This means that $|u'_k| = \sqrt{k/2}$. Hence as k/k_{change} increases the value of $|u'_k|$ increases. This means the relative effect of a perturbation in $|u'_k|$, which has constant amplitude, decreases as k/k_{change} increases.

One interesting difference between the BSI potential case and that of a step in the inflaton potential is the lack of dependence on the value of the parameter γ. Above a certain size, the value of γ has no effect on the resultant power spectrum. One can see this by looking at the damping of oscillations with k/k_{change}. If the change in potential occurs rapidly enough that then any damping will be due to k/k_{change}. In the step potential case there was no other means for the oscillations to damp besides the size of γ and so the value of γ was seen to be very important. Here the relative size of increase in $|u'_k|$ is also dependent on k/k_{change}.

Unlike the step potential case a potential with a change in slope cannot cause a halt to inflation, because the value of $\ddot{a}$ remains greater than zero throughout the change in slope in the potential.

Another difference in a potential with a slope change is the behaviour of the tensor modes. This differs to the step potential case as the slope before the feature is different to the slope after the feature. This causes the slope of the tensor modes spectrum to also change. Again the oscillatory bahaviour observed for the scalar modes is not observed for the tensor modes.

10.3 Comparison between Exact and Numerical solutions

Here we will compare the numerical solution for the BSI spectrum to the exact solution of Equation (10.2). We choose particular values for the parameters in the potential

$$V(\phi) = \begin{cases} 10^{-10} + 10^{-12}\phi & \phi > 0 \\ 10^{-10} + 10^{-12}\phi p & \phi \leq 0. \end{cases} \tag{10.6}$$

The parameter p is used to describe the change in slope of the inflaton potential, with $p = 1$ corresponding to no slope change, $p < 1$ corresponding to decreasing slope and $p > 1$ corresponding to increasing the slope of the potential.

We see extremely good agreement between the numerical solution and that from Equation (10.2). We plot the two solutions in Figure 10.3. From Equation (3.37) we find, for potential we are considering, the power spectrum for modes which left the horizon well before the change in slope to have value $V^3/(12\pi^2 V'^2) \approx 8.44 \times 10^{-9}$. For modes well inside the horizon at the time of the change in potential, the power spectrum will be $1/p^2$ times the power spectrum for modes that left well before the change occurred. This is exactly what is observed.

The agreement between numerical and exact solution is aided by the fact that both ϵ and η are very small for the particular potential we have chosen. We find for this potential that outside the region of the step

$$\epsilon = \frac{1}{2}\left(\frac{V'}{V}\right)^2 = \begin{cases} 5 \times 10^{-5} & \phi \gg 0 \\ 5p^2 \times 10^{-5} & \phi \ll 0 \end{cases} \qquad \text{and} \qquad \eta = 0. \tag{10.7}$$

These values are very small, which means that ϕ is changing extremely slowly with k. This leads to the regions well before and well after the slope change being flat. The exact solution assumes this flatness. If we use a different potential, for instance $V_0 = 10^{-10} + 10^{-11}\phi$ then we would expect a significant slope to the power spectrum away from the change in slope and so there would be disagreement between the exact solution and the numerical solution. This disagreement could

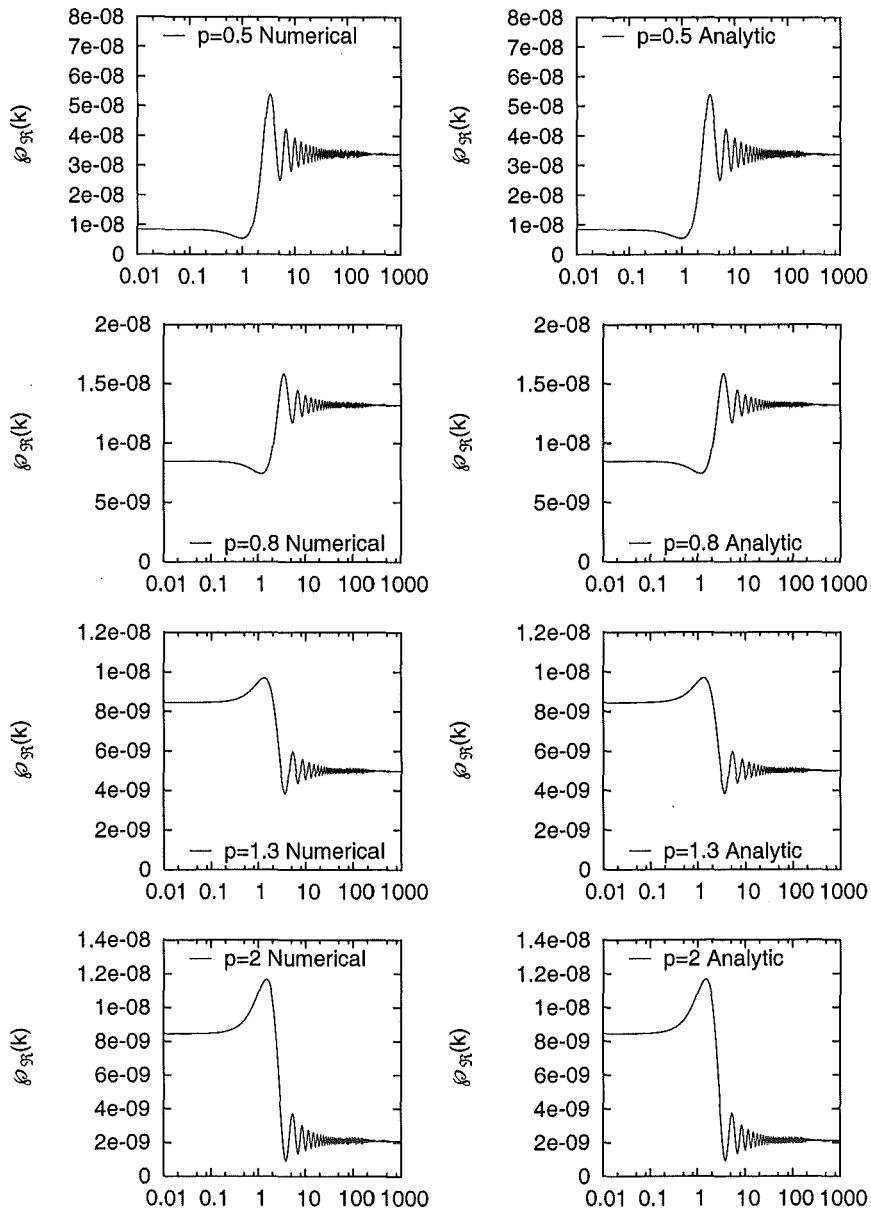

Figure 10.3: Primordial power spectra for a BSI type power spectrum. We show both numerical and analytic spectra plotted for several values of $p = A_+/A_-$. In both cases we choose to position the change in slope at $k = 1$.

easily be accounted for in the exact solution by introducing a slope term in Equation (10.2).

10.4 Fit to CMB Anisotropy data

10.4.1 Fit for altering only position and size of slope change

We will now try to fit the CMB anisotropy spectrum, resulting from the BSI primordial power spectrum, to the CMB data. We look at the χ^2 values for both the combined CMB data and the WMAP data. As shown in Section 10.1, a BSI potential can be parameterized in terms of two variables, the position of the change in slope k_{step} and the amount of slope change A_+/A_-. This is assuming the change in slope is sudden enough, ie the value of γ is large enough that it does not affect the shape of the potential. Then we can vary (for $V(\phi_0)$ and A_+ constant) the value of A_-, and the k scale on which the slope change occurs. The value of A_+ is chosen to be the value seen to best fit the WMAP data in the case without any change present.

The χ^2 results are plotted in Figure 10.4. We can see from here that the χ^2 value varies considerably depending on the position and magnitude of the slope change. The position of the lowest χ^2 value is near but not at the line of $A_+ = A_-$ (the actual location is at $A_+/A- = 1.025$, and $k_{step} = 0.0038$). This χ^2 value of 1437.6 compared to 1441 for modes with $A_+ = A-$ is not a significantly better fit to the data as two extra degrees of freedom have been introduced into the system to get this χ^2 value.

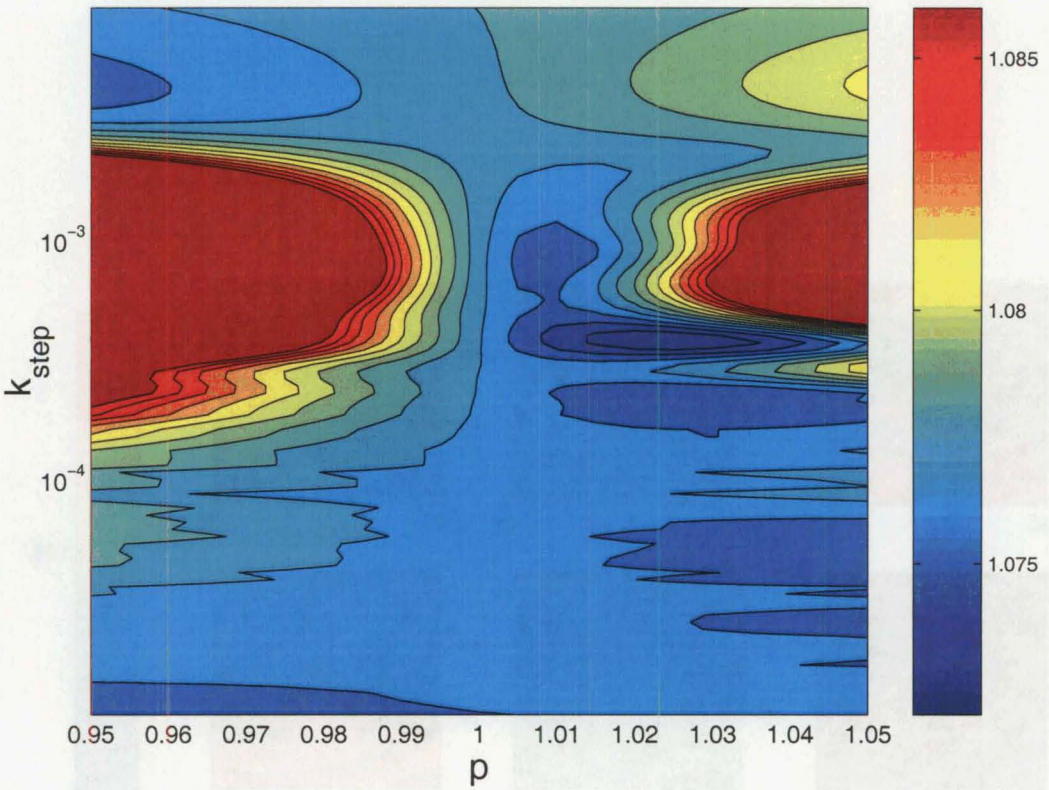

Figure 10.4: χ^2 for a BSI type potential. We plot $\log(\chi^2)$ as a function of two variables, the position of slope change and amplitude of slope after change.

10.4.2 Fit for altering background cosmology

Here we choose to alter the background cosmology as well as the position of and magnitude of the change in slope of the inflaton potential. We show this in Figure 10.5. It can be seen from this figure that no other cosmologies are significantly favoured by a model including a slope change in the inflationary potential. The alterations to the χ^2 that do occur due to the presence of a change in inflaton potential slope are generally to make the fit worse.

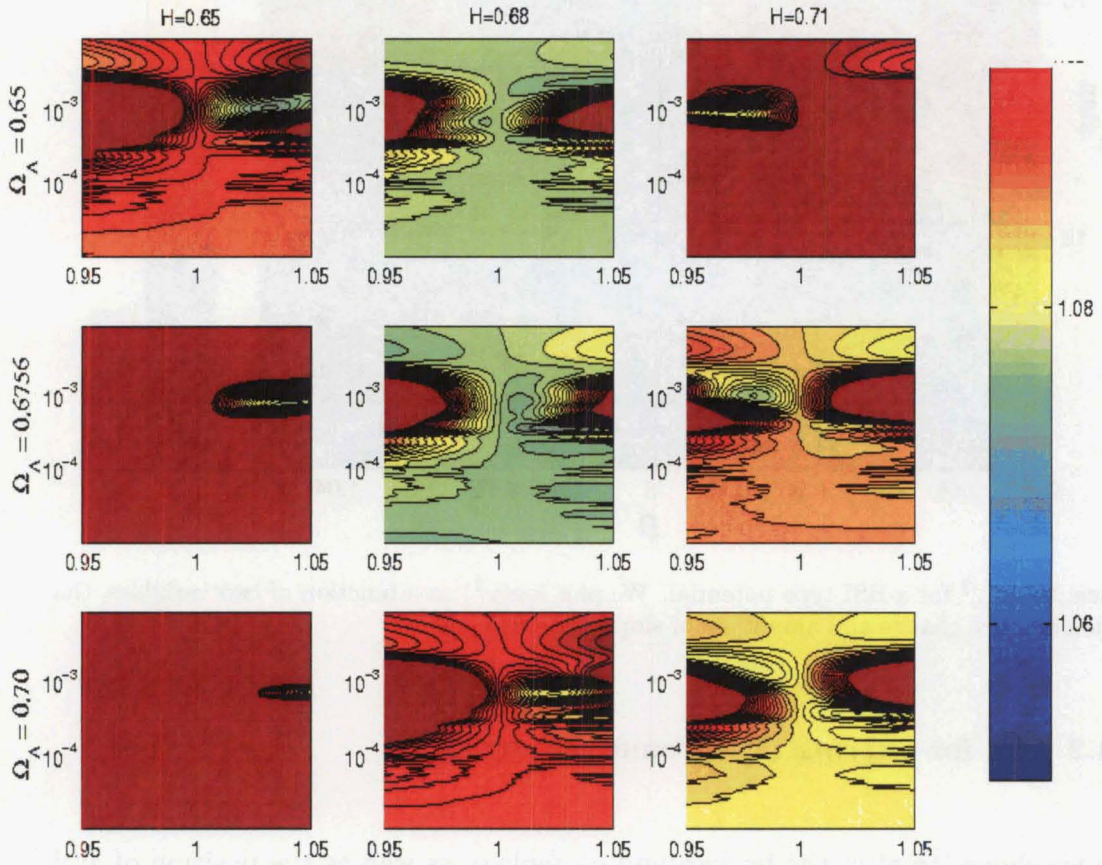

Figure 10.5: Fit of BSI spectra with a slope change in the inflaton potential to the WMAP data, for varying cosmologies. We plot the variable $\log(\chi^2)$ as a function of position of slope change, and amplitude of slope after change. This is done for cosmologies with Hubble parameter $H = 0.65$, 0.68 and 0.71, and cosmological constant $\Omega_\Lambda = 0.65$, 0.6756 and 0.70.

Chapter 11

Conclusion

We have looked at several different ways of modelling the effect an early universe phase transition would have on the inflationary potential. We have investigated how this affects the primordial power spectrum, as well as how these changes in the primordial power spectrum would alter the CMB anisotropy spectrum.

The main feature in the case of a step in the inflaton potential was the presence of scale dependent oscillations as a result of a step. This was seen as a step generates a new set of initial conditions for the quantum fluctuation. If the step occurs when the quantum fluctuations are in the growing mode regime this new set of initial conditions has no effect on the power spectrum because both degrees of freedom (d.o.f.) of the mode are growing independently. If however the step occurs in the oscillatory phase then the two modes get different amplitude shifts, and the phase of these shifts relative to the phase at which the mode exits the horizon will dictate the final amplitude of the power spectrum. It is this effect which leads to oscillations. In the case of an instantaneous step the oscillations are observed for any mode with $k > k_{step}$. However if the step takes place over some range of ϕ (as modelled in most of this work by a tanh function) then the oscillations damp and so are only present for some finite range of k values greater than k_{step}. This damping is shown to depend linearly with the sharpness of the step, as well as the slope of the background potential, and inversely proportional to the amplitude of the background potential.

We then evolved the primordial power spectrum to give the theoretical CMB anisotropy spectrum. Comparing this to observation we find that there are values of step size and position for which we have improved χ^2 values compared to that of a primordial power spectrum without a step. The best value of χ^2 we obtained was 1433 for 1339 d.o.f, which compares well to 1441 for 1342 d.o.f. in the case of no step. Most steps however were found to fit the data worse than in the case with no step present.

In the case of a sudden change in the slope of the potential (BSI) we find the existing exact solution of Starobinski agrees well with our numerical solution. The change in the spectrum is again the result of a change in the initial conditions of the evolution of the mode u_k. This change in initial conditions is in the first derivative of the mode whereas in the step potential case the change was in the mode amplitude. This leads to the oscillations in the primordial power spectrum in the BSI case being rapidly damped. The amplitude of perturbations changes for modes well inside the horizon at the time of slope change compared to modes well outside as the perturbation amplitude depends on the slope of the potential, which has changed in this case.

When comparing the theoretical CMB anisotropy spectrum including a slope change to the observed CMB anisotropies, we find there is little to no improvement to the χ^2 fit. For most magnitudes of slope change, and scale sizes at which the change occurs, the χ^2 fit to the data is worse than in the case when there is no slope change. We find the best χ^2 value of 1437, compared to 1441 for without a change in slope. Given we have removed two degrees of freedom from 1342 to 1340, our improvement in χ^2/d.o.f. is very small.

We have found that even tiny sudden changes in the magnitude or slope of the inflaton potential can have a large impact on the resulting primordial power spectrum and correspondingly on the CMB anisotropy spectrum. As cosmological observations increase in precision this will become more and more important, as evidence for or against such changes in the inflaton potential will have an effect

both on how we model the universe, and our model of particle physics at the time of inflation.

11.1 Potential for further work

There are several directions in which this research could be continued in the future. Given the recent release of the WMAP data this is a very topical area of research at the moment. One could do further fitting of the WMAP data to cosmological models involving a step in the inflaton potential. The best way to do this would be using a Monte Carlo approach to the fitting, gradually moving around the 11 dimensional parameter space until the best fit is found. Such a technique could in future be applied to the Planck satellite data which would provide an even more accurate picture as to the possibility of a step in the inflaton potential.

The other way in which the research could be furthered is by taking a more theoretical approach, considering particular models of supersymmetry and making predictions from these as to what form of step could be expected in the inflaton potential. This could easily then be compared to the data, giving a validation or negation of the theory.

Appendix A

Glossary of terms and symbols used

Broken Scale Invariance (BSI) A model of inflation where there is a change in the slope of the effective potential, which results in a deviation from scale invariance of the primordial power spectrum.

Causal contact Two objects are said to be in causal contact if they are able to have an effect on each other under Einstein's theory of relativity.

Chi squared (χ^2) A method of fitting a theoretical curve to data with known uncertainties. One expects with such a fit to get a value equal to the number of degrees of freedom of the system.

Cosmic Microwave Background (CMB) The relic radiation left over from the time of matter-radiation decoupling. This is present as a blackbody spectrum of temperature 2.7 K.

CMB anisotropy spectrum The temperature fluctuations observed in the CMB, decomposed into spherical harmonics. The initial temperature map is normalized to remove any dependence on our motion relative to the background.

Energy density The amount of energy associated with any given point in space.

Inflation Defined strictly as a period of accelerating expansion of the universe. This means the scale factor has the property $\ddot{a} > 0$.

Inflaton (ϕ) The field, usually a scalar field, which drives inflation.

Large scale structure Structure in the universe on the scale of galaxies and clusters of galaxies.

Omega (Ω) The ratio of the density of the universe to the critical density required to close the universe.

Perturbation The deviation from the average value of a particular parameter.

Perturbation spectrum A measure of how perturbations are present on different scales, calculated by considering spherical harmonics.

Primordial power spectrum The perturbation spectrum present as a classical metric perturbation outside the horizon, after inflation has occurred but before the perturbation has been able to re-enter the horizon and evolve further.

Relic particles Particles generated in the early on in the universe when the temperature was much higher.

Scalar field A scalar field is a field in which every point in space has an associated scalar value. Inflation is usually formulated in terms of a scalar field with a large energy density.

Scale factor $a(t)$ A term representing the scale size of the universe. In this thesis we normalize $a(t)$ so that it currently has a value of 1.

Scale invariant A flat power spectrum, which means that the amplitude of perturbations is not dependent on the scale size of the perturbation.

Supersymmetry A symmetry involving an operator which acts on bosonic particles to make fermionic particles and vice versa. Supersymmetry requires every standard model particle to have a supersymmetric partner with the same mass. Thus if it is a symmetry realised in nature, the supersymmetry must currently be broken as these supersymmetric partners are not observed.

Tensorial modes Perturbations of a tensorial nature. These can be treated independently of the more commonly considered scalar perturbations.

References

[1] J. A. Adams, G. G. Ross, and S. Sarkar. Multiple inflation. *Nucl. Phys.*, B503, 1997.

[2] Jennifer Adams, Bevan Cresswell, and Richard Easther. Inflationary perturbations from a potential with a step. *Phys. Rev. D*, 64, 2001.

[3] J. Bardeen. Gauge-invariant cosmological perturbations. *Phys. Rev. D*, 22:1882–1905, 1980.

[4] J. Barriga, E. Gaztañaga, M. G. Santos, and S. Sarkar. On the APM power spectrum and the CMB anisotropy: Evidence for a phase transition during inflation? *Mon. Not. Roy. Astro. Soc.*, 324:977, 2001.

[5] S. Basilakos and M Plionis. Modelling the two point correlation function of galaxy clusters in the sloan digital sky survey. *astro-ph/0304551*, 2003.

[6] T. Broadhurst, R. Ellis, D. Koo, and A. Szalay. Large scale distribution of galaxies at the galactic poles. *Nature*, 343:726, 1990.

[7] M. Colless. Measuring and modeling the universe. *astro-ph/0305051*, 2003.

[8] P. de Bernardis *et. al.* A flat universe from high-resolution maps of the cosmic microwave background radiation. *Nature*, 404:955, 2000.

[9] N. A. Doughty. Cosmology, 1998.

[10] Richard Easther, Brian R. Greene, William H. Kinney, and Gary Shiu. A generic estimate of trans-planckian modifications to the primordial power spectrum in inflation. *Phys. Rev. D*, D66:023518, 2002.

[11] Richard Easther, Brian R. Greene, William H. Kinney, and Gary Shiu. Inflation as a probe of short distance physics. *Phys. Rev. D*, D64:103502, 2001.

[12] J. Einasto. A 120-mpc periodicity in the three-dimensional distribution of galaxy superclusters. *Nature*, 385:139–141, 1997.

[13] A. Balbi *et. al.* Constraints on cosmological parameters from MAXIMA-1. *astro-ph/0005124*, 2000.

[14] A. E. Lange *et. al.* First estimations of cosmological parameters from BOOMERanG. *astro-ph/0005004*, 2000.

[15] Anze Slosar *et. al.* Cosmological parameter estimation and Bayesian model comparison using VSA data. *MNRAS*, 341:L29, 2003.

[16] B. S. Mason *et. al.* The anisotropy of the microwave background to l=3500: Deep field observations with the cosmic background imager. *Astrophys. J.*, 591:540–555, 2003.

[17] C. L. Bennett *et. al.* First year Wilkinson Microwave Anisotropy Probe (WMAP) observations : Preliminary maps and basic results. *Astrophys.J.Suppl.*, 148:1, 2003.

[18] C. L. Kou *et. al.* High resolution observations of the cmb power spectrum with acbar. *astro-ph/0212289*, 2002.

[19] D. G. York *et. al.* The sloan digital sky survey: Technical summary. *Astron. J.*, 120:1579–1587, 2000.

[20] D. N. Spergel *et. al.* First year wilkinson microwave anisotropy probe (wmap) observations: Determination of cosmological parameters. *Astrophys.J.Suppl.*, 148:175, 2003.

[21] H. V. Peiris *et. al.* First year Wilkinson Microwave Anisotropy Probe (WMAP) observations: Implications for inflation. *Astrophys.J.Suppl.*, 148:213, 2003.

[22] Hanany S *et. al.* MAXIMA-1:A measurement of the cosmic microwave anisotropy on angular scales of 10 arcminutes to 5 degrees. *astro-ph/0005123*, 2000.

[23] J. H. Goldstein *et. al.* Estimates of cosmological parameters using the cmb angular power spectrum of acbar. *astro-ph/0212517*, 2002.

[24] Keith Griange *et. al.* The cmb power spectrum out to l=1400 measured by the VSA. *MNRAS*, 341:L23, 2003.

[25] M. A. Strauss *et. al.* Spectroscopic target selection in the sloan digital sky survey: The main galaxy sample. *Astron. J.*, 124:1810, 2002.

[26] N. W. Halverson *et. al.* DASI first results: A measurement of the cosmic microwave background angular power spectrum. *Astrophys. J.*, 568:38–45, 2002.

[27] T. J. Pearson *et. al.* The anisotropy of the microwave background to l=3500: Mosaic observations with the cosmic background imager. *Astrophys. J.*, 591:556–574, 2003.

[28] A. Friedmann. On the curvature of space. *Z. Phys.*, 10:377–386, 1922.

[29] G. Gamow. Expanding universe and the origin of the elements. *Physics Review*, 70:572L–573L, 1946.

[30] I. S. Gradshteyn and I. M. Ryzhik. *Table of Integrals, Series and Products.* Academic Press, 4th edition, 1980.

[31] A. H. Guth. Inflationary universe : A possible solution to the horizon and flatness problems. *Physical Review D*, 23(2), 1981.

[32] http://lambda.gsfc.nasa.gov/. The legacy archive for microwave background data analysis, 2003. We acknowledge the use of the Legacy Archive for Microwave Background Data Analysis (LAMBDA). Support for LAMBDA is provided by the NASA Office of Space Science.

[33] http://www.hep.upenn.edu/ max/. Max Tegmark's CMB analysis center, 2003. We gratefully acknowledge Max Tegmark for providing this image, and highly informative web site.

[34] E. Hubble. A relation between distance and radial velocity among extragalactic nebula. *Proc. Nat. Acad. Sci.*, 15:169–173, 1929.

[35] J. Jeans. The stability of spherical nebula. *Phil. Trans. Roy. Soc.*, 199:1–53, 1902.

[36] J.Lesgourgues, D.Polarski, and A.A.Starobinsky. CDM models with a BSI steplike primordial spectrum and a cosmological constant. *Mon.Not.Roy.Astron.Soc.*, 297:769–776, 1998.

[37] E. W. Kolb and M. Turner. *The early universe.* Addison Wesley, 1990.

[38] S. M. Leach and A. R. Liddle. Inflationary perturbations near horizon crossing. *astro-ph/0010082*, 2000.

[39] S. M. Leech, M. Sasaki, D. Wands, and A. R. Liddle. Enhancement of superhorizon scale inflationary curvature perturbations. *astro-ph/0101406*, 2001.

[40] G Lemaître. A homogeneous universe of constant mass and increasing radius accounting fir the radial velocity of extragalactic nebulae. *Ann. Soc. Sci. Bruxelles*, 47A:49–59, 1927.

[41] J. Lesgourgues, D. Polarski, and A. A. Starobinsky. Large primordial gravitational wave background in a class of BSI Lambda-CDM models. *Mon.Not.Roy.Astron.Soc.*, 308:281–288, 1999.

[42] J. Lesgourgues, S. Prunet, and D. Polarski. Parameter extraction by Planck for a CDM model with broken scale invariance and cosmological constant. *Mon.Not.Roy.Astron.Soc.*, 303:45–49, 1999.

[43] A. R. Liddle and D. H. Lyth. The cold dark matter density perturbation. *Phys. Rep.*, 231:1–105, 1993.

[44] J. E. Lidsey, A. R. Liddle, E. W. Kolb, E. J. Copeland, T. Barreiro, and M. Abney. Reconstructing the inflaton potential — an overview. *Rev. Mod. Phys.*, 69:373, 1997.

[45] A. D. Linde. Hybrid inflation. *Phys. Rev. D*, 49:748–757, 1994.

[46] C. H. Lineweaver, D. Barbosa, A. Blanchard, and J. G. Bartlett. Constraints on h, ω_b and λ_0 from cosmic microwave background observations. *astro-ph/9610133*, 1996.

[47] A. H. Maller, D. H. McIntosh, N. Katz, and M. D. Weinberg. The galaxy angular correlation functions and power spectrum from the two micron all sky survey. *astro-ph/0304005*, 2003.

[48] Jèrôme Martin and Christophe Ringeval. Superimposd oscillations in the WMAP data. *astro-ph/0310382*, 2003.

[49] V. Mukhanov, H. Feldman, and R. Brandenberger. Theory of cosmological perturbations. *Phys. Rep.*, 215:203–333, 1992.

[50] J. A. Peacock. The emergence of cosmic structure. *astro-ph/0301042*, 2003.

[51] A. A. Penzias and R. W. Wilson. A measurement of excess antenna temperature at 4080 *mc/s*. *Astrophysical Journal*, 142:419–421, 1965.

[52] J. P. Preskill. Cosmological production of superheavy magnetic monopoles. *Phys. Rev. Lett.*, 43:1365–1368, 1979.

[53] W. H. Press, S. A. Teukolsky, W. T. Vettering, and B. P. Flannery. *Numerical Recipes in Fortran*. Cambridge University Press, 2nd edition, 1992.

[54] J. Retzlaff, S. Borgani, S. Gottlober, A. Klypin, and V. Muller. Constraining cosmological models with cluster power spectra. *New Astron.*, 3:631, 1998.

[55] D. Roberts, A. R. Liddle, and D. H. Lyth. False vacuum Inflation with a quartic potential. *Phys. Rev. D*, 51:4122, 1995.

[56] H. P. Robertson. Kinematics and world structure. *Astrophysical Journal*, 1935.

[57] H. P. Robertson. Kinematics and world structure. *Astrophysical Journal*, 83, 1935.

[58] M. Roos and S. M. Harun-or-Rashid. The flatness of the universe is robust. *astro-ph/0005541*, 2000.

[59] U. Seljak and M. Zaldarriaga. A line of sight approach to cosmic microwave background anisotropies. *Astrophys. J.*, 469:437–444, 1996.

[60] A. A. Starobinsky. Spectrum of adiabatic perturbations in the universe when there are singularities in the inflation potential. *JETP*, 55, 1992.

[61] E. D. Stewart. The spectrum of density perturbations produced during inflation to leading order in a general slow-roll approximation. *Phys. Rev. D*, 65, 2002.

[62] E. D. Stewart and Gong Jin-Ook. The density perturbation power spectrum to second-order corrections in the slow-roll expansion. *Phys. Lett.*, B510:1–9, 2001.

[63] E. D. Stewart and D. H. Lyth. A more accurate analytic calculation of the spectrum of cosmological perturbations produced during inflation. *Physics Letters B*, 302:171–175, 1993.

[64] M. Tegmark. How to make maps from cmb data without losing information. *ApJ Let*, 480:L87–90, 1997.

[65] Shinji Tsujikawa. Introductory review of cosmic inflation. *astro-ph/0304257*, 2003.

[66] A. G. Walker. On Milne's theory of world structure. *Proc. London Math. Soc.*, 42, 1936.

[67] X. Wang, M. Tegmark, and M. Zaldarriaga. Is cosmology consistent? *astro-ph/0105091*, 2001.

[68] Y. B. Zeldovich and M. Y. Khlopov. On the concentration of relic magnetic monopoles in the universe. *Phys. Lett.*, 79B:239–241, 1978.